AMERICAN UNIVERSITY OF BEIRUT

METHODOLOGIES OF GROUNDWATER VULNERABILITY ASSESSMENT AND SPATIAL ANALYSIS OF GROUNDWATER QUALITY: COMPARISON OF METHODS UNDER URBANIZATION STRESS

by
NANOR AVEDIS MOMEJIAN

A thesis
submitted in partial fulfillment of the requirements
for the degree of Master of Science in Environmental Sciences
to the Interfaculty Graduate Environmental Science Program
Environmental Technology
the Faculty of Engineering and Architecture
at the American University of Beirut

Beirut, Lebanon
September, 2014

AMERICAN UNIVERSITY OF BEIRUT

METHODOLOGIES OF GROUNDWATER VULNERABILITY ASSESSMENT AND SPATIAL ANALYSIS OF GROUNDWATER QUALITY: COMPARISON OF METHODS UNDER URBANIZATION STRESS

by
NANOR AVEDIS MOMJIAN

Approved by:

Dr. Majdi Abou Najm, Assistant Professor Department of Civil and Environmental Engineering	Advisor
Dr, Ibrahim Alameddine, Assistant Professor Department of Civil and Environmental Engineering	Co-Advisor
Dr. Mutasem El Fadel, Professor Department of Civil and Environmental Engineering	Co-Advisor

Date of thesis/dissertation defense: September 29, 2014

AMERICAN UNIVERSITY OF BEIRUT

THESIS, DISSERTATION, PROJECT RELEASE FORM

Student Name: Momejian Nanor Avedis

● Master's Thesis ○ Master's Project ○ Doctoral Dissertation

☐ I authorize the American University of Beirut to: (a) reproduce hard or electronic copies of my thesis, dissertation, or project; (b) include such copies in the archives and digital repositories of the University; and (c) make freely available such copies to third parties for research or educational purposes.

☐ I authorize the American University of Beirut, **three years after the date of submitting my thesis, dissertation, or project,** to: (a) reproduce hard or electronic copies of it; (b) include such copies in the archives and digital repositories of the University; and (c) make freely available such copies to third parties for research or educational purposes.

______________________________ 18/February/2015

ACKNOWLEDGMENTS

First of all, I would like to acknowledge my family's patience with my endless crave for learning and education, and I would thank them for not giving up on asking "So, when will you finish?" question, which reminded me of my target every time I was about to give up.

I would also like to thank Issam Bou Jaoude for creating my passion for groundwater and hydrogeology, and Dr. Mutasem el Fadel for discovering this passion and wanting to move me from category of people “who know, and don’t know that they know” to “who know, and know that they know”. I would like to thank my Adviser, Dr. Majdi Abou Najm, for gearing my passion into practical and academic use, while believing in my ability to finish this work, when I was in denial and about to give up several times. I thank Dr. Ibrahim Alameddine, who helped overcome my fear of the word “statistics”, when my failures with this struggle were “statistically significant”.

I thank Grace and Rania, and all IDRC team who helped my work in the lab and the field.

I also thank my friends near or abroad, specifically Khajag, Basma, Rena, because every time I had my panic attacks (and they were too many), they helped me overcome it and managed to survive with me and stay my friends.

I would like to thank Dr. Kamal Azar who was the first to introduce me to GIS, and created an interest, which I pursued and built on. This interest eventually helped me in my thesis work and diversified my career options.

I thank my BGR colleagues, with whom I spent three beautiful years, full of great memories and rewarding outcomes.

AN ABSTRACT OF THE THESIS OF

Nanor Avedis Momejian for Master of Science
Major: Environmental Technology

Title: Methodologies of Groundwater Vulnerability assessment and Spatial Analysis of Groundwater Quality: Comparison of methods under urbanization stress

This study is divided into two parts. The first part is titled “Assessment of methodologies for groundwater vulnerability to seawater intrusion along coastal and urban Areas”. It evaluates the performance of DRASTIC and EPIK, two commonly used groundwater vulnerability assessment models, using groundwater quality data by establishing water quality categories and cross-checking field measurements to that of simulated vulnerability levels. The results of this study show that the vulnerability levels in outcropping Karstic formations in Mount Lebanon and Anti Lebanon to be of high vulnerability with both used models. The extent of accuracy of the evaluation criteria for the water vulnerability assessment was limited by the accuracy of experimental measurements, the choice of analyzed parameters and model assumptions.

The second Part is titled “Variation of the Spatial distribution of Groundwater Quality in Karstic aquifers under urbanization stress”. It evaluates the ability of different spatial interpolation methods to produce accurate groundwater quality maps using interpolation schemes. This study uses three different interpolation methods (IDW, Kriging, and Co-Kriging) with combinations of different semivariogram models and data transformation, producing 380 different combinations/scenarios. The study evaluated the accuracy of these scenarios using three validation approaches, (1) statistical indicators by Leave-One-Out cross validation method; (2) matching the results of measured and interpolated values based on established water quality categories, and (3) evaluating the accuracy relying on the results of groundwater vulnerability assessment (GVA). The results varied between cities and to the values of the measured parameters, and it also showed the different function of the two methods, which could not be used interchangeably.

Keywords: Groundwater Quality Assessment, Groundwater Vulnerability Assessment, Evaluation, Validation, Accuracy Check

ILLUSTRATIONS

Figure 3-1: (a) Geological formations of the Northern Coast of Lebanon with the focus study areas and the wells' locations for the three areas of study (b) Tripoli (c) Jal el Dib (d) Beirut ... 10

Figure 3-2: Diagram showing the parameters of the analysis of DRASTIC and the weights and ranks for each parameter NOTE: SS is Sandstone, LS is Limestone, weathrd is weathered, Meta. & metamor. is metamorphic, ign. is igneous 14

Figure 3-3: Diagram showing the parameters of the analysis of EPIK and the vulnerability zones based on the Protection Factor (F) calculation 16

Figure 3-4: Diagram showing the work flow for this study.. 21

Figure 4-1: Map of showing the Groundwater Vulnerbaility of Lebanon based on DRASTIC Pollution Protection values (redrawn after M. Metni, et al., 2004) 24

Figure 4-2: Map of showing the Groundwater Vulnerability of Lebanon based on EPIK Protection Factor as defined in Version 1... 28

Figure 4-3: Map of showing the Groundwater Vulnerability of Lebanon based on EPIK Protection Factor as defined in Version 2... 30

Figure 4-4: Map of showing the Groundwater Vulnerability of Lebanon based on EPIK Protection Factor as defined in Version 3... 31

Figure 4-5: Comparing the three versions of EPIK 32

Figure 4-6: Comparison between EPIK and DRASTIC 35

Figure 1-1: Steps to follow when conducting a spatial groundwater quality assessment............. 41

Figure 2-1: Diagram showing the work flow for this study... 46

Figure 2-2: (a) Geological formations of the Northern Coast of Lebanon with the focus study areas and the wells' locations for the three areas of study (b) Tripoli (c) Jal el Dib (d) Beirut ... 49

Figure 3-1: Examples of error maps of Tripoli 52

Figure 3-2: Example of Error map in Beirut round 1 sampling, for IDW with Cl^- 53

Figure 3-3 : Examples on error distribution of Jal el Dib 55

Figure 3-4: Comparing the Interpolation results with Vulnerability assessment results 61

Figure 5-1: Formulas for different variogram models 125

Figure 5-2: General representations of variograms of the three models (Delbari, et al., 2013; Smith, 2014)... 126

TABLES

Table 1-1: Comparison of commonly used intrinsic vulnerability assessment methods with corresponding parameter 5

Table 2-1: Summary of intrinsic Vulnerability Assessment Methods applied in various study areas 7

Table 3-1: Different versions of EPIK methodology with corresponding definition (the main variation is the variation of the urban areas factor) NOTE: The buffer around the coast is not dynamic, it uses a fixed value without taking topography into consideration (For more details per version see section 5.1 – Annex 1) 18

Table 3-2: Water Quality categories and their equalivalent PP and PF ranges 22

Table 4-1: Field measured Chloride levels (WQ_{Field})and Metni, 2002 DRASTIC ranges for Round 1 Beirut matching with DRASTIC Pollution Protection (PP) ranges($WQ_{DRASTIC}$)........ 26

Table 4-2: Percent of match for the DRASTIC methodology Validation (the highlighted blue are when the 50 percentile is crossed) 27

Table 4-3: Field measured TDS (WQ_{Field}) and EPIK version 3 ranges for Round 2 Tripoli matching with EPIK Protection Factor (PF) ranges (WQ_{EPIK}) 33

Table 4-4: Percent of match for the EPIK Version 1 methodology Validation (the highlighted blue are when the 50 percentile is crossed) 33

Table 4-5: Percent of match for the EPIK Version 2 methodology Validation (the highlighted blue are when the 50 percentile is crossed) 34

Table 4-6: Percent of match for the EPIK Version 3 methodology Validation (the highlighted blue are when the 50 percentile is crossed) 34

Table 1-1: Some of the references reviewed in this study that used interpolation models in various study areas (N/A: not applicatble and (-) means not found), WL: water Level) 43

Table 3-1: The 8 chosen scenarios for City of Tripoli Round 1 (Blue highlighted cells are the statistical indicators that indicate most accurate interpolation) (The red box is the chosen interpolation to show the error map).. 51

Table 3-2: The 8 chosen scenarios for City of Tripoli Round 2 (Blue highlighted cells are the statistical indicators that indicate most accurate interpolation) (The red box is the chosen interpolation to show the error map).. 52

Table 3-3: The 8 chosen scenarios for City of Beirut Round 1 (the highlighted blue cells are the statistical indicators that indicate most accurate interpolation) (The red box is the chosen interpolation to show the error map).. 53

Table 3-4: The 14 chosen scenarios for Jal el Dib Round 3 (Blue highlighted cells are the statistical indicators that indicate most accurate interpolation) (The red box is the chosen interpolation to show the error map).. 54

Table 3-5: The 14 chosen scenarios for Jal el Dib Round 7 (the highlighted blue cells are the statistical indicators that indicate most accurate interpolation) (The red box is the chosen interpolation to show the error map).. 55

Table 3-6: Water Quality categories and their equalivalent PP and PF ranges 56

Table 3-7: Water Quality ranges based on Chloride concentration the field measured (WQ_{Field}) versus the interpolated value (WQ_{Cl^-}) 57

Table 3-8: Water Quality ranges based on Chloride concentration the field measured (WQ_{Field}) versus the interpolated value (WQ_{TDS}) 57

Table 3-9: Cumulative per cent match results for 10 scenarios using interpolation method Kriging (the highlighted blue cells are when the 50 percentile is crossed) 58

Table 3-10: Cumulative per cent match results for 10 scenarios using interpolation method IDW (the highlighted blue cells are when the 50 percentile is crossed)... 59

Table 3-11: Cumulative per cent match results for 10 scenarios using interpolation method Co-Kriging with distance of well from shoreline, transmissivity of the tapped aquifer and well depth (the highlighted blue cells are when the 50 percentile is crossed)... 59

Table 3-12: Cumulative per cent water category matching result for EPIK (EP), DRASTIC (DR) and the interpolation results (Kr, IDW, CK) for Jal el Dib Round 3 (January 2013) (the highlighted blue are when the 50 percentile is crossed) 62

Table 3-13: Cumulative percent water category matching result for EPIK (EP), DRASTIC (DR) and the interpolation results (Kr, IDW, CK) for Jal el Dib Round 7 (October 2013) (the highlighted blue are when the 50 percentile is crossed) 63

Table 3-14: Cumulative percent water category matching result for EPIK (EP), DRASTIC (DR) and the interpolation results (Kr, IDW, CK) for Beirut Round 1 (May, June 2013) (the highlighted blue are when the 50 percentile is crossed) 64

Table 3-15: Percent water category matching result for EPIK (EP), DRASTIC (DR) and the interpolation results (Kr, IDW, CK) for Tripoli Round 1 (July 2007) (the highlighted blue are when the 50 percentile is crossed) 65

Table 3-16: Cumulative percent water category matching result for EPIK (EP), DRASTIC (DR) and the interpolation results (Kr, IDW, CK) for Tripoli Round 2 (September 2006) (the highlighted blue are when the 50 percentile is crossed) 65

Table 5-1: Field measured Chloride levels (WQ_{Field}) matching with Metni, 2002 DRASTIC Pollution Protection (PP) ranges ($WQ_{DRASTIC}$) for Round 1 Beirut for Chloride 81

Table 5-2: Field measured Chloride levels (WQ_{Field}) matching with Metni, 2002 DRASTIC Pollution Protection (PP) ranges ($WQ_{DRASTIC}$) for Round 1 Beirut for TDS................................ 81

Table 5-3: Field measured Chloride levels (WQ_{Field}) matching with Metni, 2002 DRASTIC Pollution Protection (PP) ranges ($WQ_{DRASTIC}$) for Round 3 Jal el Dib for Chloride.................... 82

Table 5-4: Field measured Chloride levels (WQ_{Field}) matching with Metni, 2002 DRASTIC Pollution Protection (PP) ranges ($WQ_{DRASTIC}$) for Round 3 Jal el Dib for TDS 82

Table 5-5: Field measured Chloride levels (WQ_{Field}) matching with Metni, 2002 DRASTIC Pollution Protection (PP) ranges ($WQ_{DRASTIC}$) for Round 7 Jal el Dib for Chloride 83

Table 5-6: Field measured Chloride levels (WQ_{Field}) matching with Metni, 2002 DRASTIC Pollution Protection (PP) ranges ($WQ_{DRASTIC}$) for Round 7 Jal el Dib for TDS 83

Table 5-7: Field measured Chloride levels (WQ_{Field}) matching with Metni, 2002 DRASTIC Pollution Protection (PP) ranges ($WQ_{DRASTIC}$) for Round 1 Tripoli for Chloride 84

Table 5-8: Field measured Chloride levels (WQ_{Field}) matching with Metni, 2002 DRASTIC Pollution Protection (PP) ranges ($WQ_{DRASTIC}$) for Round 1 Tripoli for TDS 84

Table 5-9: Field measured Chloride levels (WQ_{Field}) matching with Metni, 2002 DRASTIC Pollution Protection (PP) ranges ($WQ_{DRASTIC}$) for Round 2 Tripoli for Chloride 85

Table 5-10: Field measured Chloride levels (WQ_{Field}) matching with Metni, 2002 DRASTIC Pollution Protection (PP) ranges ($WQ_{DRASTIC}$) for Round 2 Tripoli for TDS 85

Table 5-11: Jal el Dib R3 Chloride measurements with the ±3% error margin 86

Table 5-12: Jal el Dib R3 TDS measurements with the ±3% error margin 86

Table 5-13: Jal el Dib R7 Chloride measurements with the ±3% error margin 87

Table 5-14: Jal el Dib R7 TDS measurements with the ±3% error margin 88

Table 5-15: Beirut R1 Cl^- measurements with the ±3% error margin 89

Table 5-16: Beirut R1 TDS measurements with the ±3% error margin 93

Table 5-17: Tripoli R1 Cl^- measurements with the ±3% error margin 97

Table 5-18: Tripoli R1 TDS measurements with the ±3% error margin 99

Table 5-19: Tripoli R2 Cl^- measurements with the ±3% error margin 100

Table 5-20: Tripoli R2 TDS measurements with the ±3% error margin 102

Table 5-21: Field measurements (WQ_{Field}) matching with EPIK Protection Factor (WQ_{EPIK}) ranges Version 1 produced by this study for Round 1 Beirut for Chloride 104

Table 5-22: Field measurements (WQ_{Field}) matching with EPIK Protection Factor (WQ_{EPIK}) ranges Version 1 produced by this study for Round 1 Beirut for TDS....................................... 104

Table 5-23: Field measurements (WQ_{Field}) matching with EPIK Protection Factor (WQ_{EPIK}) ranges Version 1 produced by this study for Round 3 Jal el Dib for Chloride........................... 105

Table 5-24: Field measurements (WQ_{Field}) matching with EPIK Protection Factor (WQ_{EPIK}) ranges Version 1 produced by this study for Round 3 Jal el Dib for TDS 105

Table 5-25: Field measurements (WQ_{Field}) matching with EPIK Protection Factor (WQ_{EPIK}) ranges Version 1 produced by this study for Round 7 Jal el Dib for Chloride........................... 106

Table 5-26: Field measurements (WQ_{Field}) matching with EPIK Protection Factor (WQ_{EPIK}) ranges Version 1 produced by this study for Round 7 Jal el Dib for TDS 106

Table 5-27: Field measurements (WQ_{Field}) matching with EPIK Protection Factor (WQ_{EPIK}) ranges Version 1 produced by this study for Round 1 Tripoli for Chloride 107

Table 5-28: Field measurements (WQ_{Field}) matching with EPIK Protection Factor (WQ_{EPIK}) ranges Version 1 produced by this study for Round 1 Tripoli for TDS 107

Table 5-29: Field measurements (WQ_{Field}) matching with EPIK Protection Factor (WQ_{EPIK}) ranges Version 1 produced by this study for Round 2 Tripoli for Chloride 108

Table 5-30: Field measurements (WQ_{Field}) matching with EPIK Protection Factor (WQ_{EPIK}) ranges Version 1 produced by this study for Round 2 Tripoli for TDS 108

Table 5-31: Field measurements (WQ_{Field}) matching with EPIK Protection Factor (WQ_{EPIK}) ranges Version 2 produced by this study for Round 1 Beirut for Chloride 109

Table 5-32: Field measurements (WQ_{Field}) matching with EPIK Protection Factor (WQ_{EPIK}) ranges Version 2 produced by this study for Round 1 Beirut for TDS...................................... 110

Table 5-33: Field measurements (WQ_{Field}) matching with EPIK Protection Factor (WQ_{EPIK}) ranges Version 2 produced by this study for Round 3 Jal el Dib for Chloride........................... 110

Table 5-34: Field measurements (WQ_{Field}) matching with EPIK Protection Factor (WQ_{EPIK}) ranges Version 2 produced by this study for Round 3 Jal el Dib for TDS 111

Table 5-35: Field measurements (WQ_{Field}) matching with EPIK Protection Factor (WQ_{EPIK}) ranges Version 2 produced by this study for Round 7 Jal el Dib for Chloride........................... 111

Table 5-36: Field measurements (WQ_{Field}) matching with EPIK Protection Factor (WQ_{EPIK}) ranges Version 2 produced by this study for Round 7 Jal el Dib for TDS 112

Table 5-37: Field measurements (WQ_{Field}) matching with EPIK Protection Factor (WQ_{EPIK}) ranges Version 2 produced by this study for Round 1 Tripoli for Chloride 112

Table 5-38: Field measurements (WQ_{Field}) matching with EPIK Protection Factor (WQ_{EPIK}) ranges Version 2 produced by this study for Round 1 Tripoli for TDS 113

Table 5-39: Field measurements (WQ_{Field}) matching with EPIK Protection Factor (WQ_{EPIK}) ranges Version 2 produced by this study for Round 2 Tripoli for Chloride 113

Table 5-40: Field measurements (WQ_{Field}) matching with EPIK Protection Factor (WQ_{EPIK}) ranges Version 2 produced by this study for Round 2 Tripoli for TDS 114

Table 5-41: Field measurements (WQ_{Field}) matching with EPIK Protection Factor (WQ_{EPIK}) ranges Version 3 produced by this study for Round 1 Beirut for Chloride 114

Table 5-42: Field measurements (WQ_{Field}) matching with EPIK Protection Factor (WQ_{EPIK}) ranges Version 3 produced by this study for Round 1 Beirut for TDS....................................... 115

Table 5-43: Field measurements (WQ_{Field}) matching with EPIK Protection Factor (WQ_{EPIK}) ranges Version 3 produced by this study for Round 3 Jal el Dib for Chloride........................... 115

Table 5-44: Field measurements (WQ_{Field}) matching with EPIK Protection Factor (WQ_{EPIK}) ranges Version 3 produced by this study for Round 3 Jal el Dib for TDS 116

Table 5-45: Field measurements (WQ_{Field}) matching with EPIK Protection Factor (WQ_{EPIK}) ranges Version 3 produced by this study for Round 7 Jal el Dib for Chloride........................... 116

Table 5-46: Field measurements (WQ_{Field}) matching with EPIK Protection Factor (WQ_{EPIK}) ranges Version 3 produced by this study for Round 7 Jal el Dib for TDS 117

Table 5-47: Field measurements (WQ_{Field}) matching with EPIK Protection Factor (WQ_{EPIK}) ranges Version 3 produced by this study for Round 1 Tripoli for Chloride 118

Table 5-48: Field measurements (WQ_{Field}) matching with EPIK Protection Factor (WQ_{EPIK}) ranges Version 3 produced by this study for Round 1 Tripoli for TDS 118

Table 5-49: Field measurements (WQ_{Field}) matching with EPIK Protection Factor (WQ_{EPIK}) ranges Version 3 produced by this study for Round 2 Tripoli Tripoli for Chloride.................. 119

Table 5-50: Field measurements (WQ_{Field}) matching with EPIK Protection Factor (WQ_{EPIK}) ranges Version 3 produced by this study for Round 2 Tripoli for TDS 119

Table 5-51: calculations of GQI 123

Table 5-52: WHO standards 123

Table 5-53: Calculation of GQISWI... 123

Table 5-54: List of all the Interpolation scenarios conducted for this study (Total of 380) with their respective names in the agreed codes 130

Table 5-55: Coding system for the Interpolation and Vulnerability Assessment Analysis........ 134

Table 5-56 : All interpolation scenarios conducted for Jal el Dib Round 3 (January 2013) wells (Blue highlight are the ones performed the best)... 135

Table 5-57: All interpolation scenarios conducted for Jal el Dib Round 7 (September 2013) wells (Blue highlight are the ones performed the best) 136

Table 5-58: All interpolation scenarios conducted for Beirut Round 1(May June 2013) wells (Blue highlight are the ones performed the best) 138

Table 5-59: All interpolation scenarios conducted for Tripoli Round 1 (July 2007) wells (Blue highlight are the ones performed the best) 139

Table 5-60: All interpolation scenarios conducted for Tripoli Round 2 (September 2006) wells (Blue highlight are the ones performed the best) 140

TABLE OF CONTENTS

1 Introduction 3

2 Groundwater Vulnerability Assessment Applications 5

3 Material and Methods 9

3.1 Study area characteristics 9

3.2 Field sampling program 11

3.3 GVA Model Selection 11

3.4 DRASTIC 13

3.5 EPIK 15

3.6 Validation of OI groundwater vulnerability assessment models 20

3.7 Setting validation criteria (water quality standards) 21

4 Results and Discussion 23

4.1 DRASTIC 23

4.1.1 Water quality vs. PP values 24

4.2 EPIK 27

4.2.1 Water quality vs. PF values 32

4.3 EPIK v/s DRASTIC 35

5 Concluding remarks 36

1 Introduction 40

2 Material and Methods 45

2.1 Geospatial Analysis of Groundwater Quality 45

2.2 Contaminants 47

2.3 Study area characteristics 48

2.4 Field sampling program 50

3 Results and Discussion 50

3.1 Water Quality Category Matching 56

3.2 GQA V/S GVA 60

4 Concluding remarks 66

5 Annexes 78

5.1 Annex 1: Detailed explanation on the definitions of EPIK components for the three versions 78

5.2 Annex 2: DRASTIC ranges for field measured water quality parameters Matching with Metni, (2002) DRASTIC Pollution Protection (PP) ranges 81

5.3 Annex 3: Error of 3% calculated for field measured (Cl & TDS) 86

5.3.1 Jal el Dib 86

5.3.2 Beirut 89

5.3.3 Tripoli 97

5.4 Annex 4: EPIK ranges for field measured water quality parameters matching with the Protection Factor (PF) ranges of three versions of EPIK 104

5.4.1 EPIK Version 1 104

5.4.2 EPIK Version 2 109

5.4.3 EPIK Version 3 114

5.5 Annex 5: Validation of water quality assessment interpolation methods 121

5.6 Annex 6: Multi-Contaminant quality indicator 123

5.7 Annex 7: Semivariogram Models 125

5.8 Annex 8: Interpolation Methods 126

5.8.1 Inverse Distance Weight 126

5.8.2 Kriging interpolation 127

5.8.3 Co-Kriging 128

5.9 Annex 9: List of all 380 scenarios conducted and validated 130

5.10 Annex 10: Results of Leave one Out Validation 135

GENERAL BACKGROUND

The sustainability of groundwater resources along coastal areas under increasing urban development stress is a global problem (Chang, 2010; Howard, 2002). Challenges include increased water extraction due to expanding populations, changing standards of lifestyle, as well as decreased infiltration and recharge capacities caused by land use changes associated with urbanization. Potential climate change impacts present another challenge that is likely to affect components of the water cycle (increased evaporation, change in precipitation spatial and temporal pattern, hence increased run-off), which are known to hinder groundwater recharge (Elewa et al., 2013; Loáiciga et al., 2012; Ranjan et al., 2006; Vorosmarty et al., 2000; Werner et al., 2012). Developing countries are particularly more vulnerable to global climate change impacts due to the lack of adaptive and mitigation capabilities to cope with the impact of this change, as a result of weak institutional structure and lack of awareness regarding the scale of the impact (Howard, 2002).

Unrestricted urbanization has led to water shortages in many developing countries as water demand exceeds existing sources (Howard, 2002). Urban residents often attempt to alleviate the shortage by drilling more wells and over-abstracting groundwater; an action that would lead to lowering of the water table and accelerating saltwater intrusion (Fetter, 2001).

The impact of saltwater intrusion in an aquifer varies spatially, depending on several factors that can be categorized into three major types: the contaminant, the aquifer media, and the urbanization activities. In an effort to assess the spatial variability of the contaminant in the groundwater or the distribution of vulnerable zones in a study area, several approaches have been developed, namely: 1) Groundwater Vulnerability Assessment 2) Groundwater Quality Assessment; and 3) Physical-Mathematical Modeling1.

This work targets the first two approaches, groundwater vulnerability assessment (Part I) and groundwater quality assessment (Part II) under the stress of saltwater intrusion along coastal areas with karstic or semi-karstic geological setting under urban development stress.

The first part "Assessment of methodologies for groundwater vulnerability to seawater intrusion along coastal and urban areas" analyzes two major groundwater vulnerability assessment methods and validates them with field measured water quality parameters. The second part "Variation of the Spatial distribution of Groundwater Quality in Karstic aquifers under urbanization stress" discusses scenarios of interpolation methods which are used for water quality assessment in the study area to highlight the best method under the given conditions of urbanization, karstification, and climate change. It then validates the results and compares them with the in-situ groundwater vulnerability results. Accordingly, the objectives of both parts can be summarized as follows:

---

[1] Along with groundwater vulnerability assessment and groundwater quality assessment, some studies relied on mathematical-physical modeling for a dynamic representation of groundwater vulnerability and/or quality. Physical-Mathematical modeling also helps in defining groundwater flow patterns and the freshwater-saline water interface encroachment. Mathematical modeling becomes more complex in Karstic media (because of vertical and horizontal heterogeneity

- Conducting groundwater vulnerability assessment using different methods and variations of the same method for the entire country of Lebanon based on information from the literature
- Delineating high and low vulnerability zones and evaluating the difference in results across methods
- Validating the applicability of the groundwater vulnerability assessment methods in groundwater quality assessment of coastal urban areas with seawater intrusion
- Comparing the performance of several interpolation methods for several groundwater quality pollutants (single and composite) over three coastal cities to highlight the groundwater contamination with seawater
- Validating the accuracy of the interpolation by leave-one-out cross validation method
- Comparing the results of groundwater vulnerability assessment and the groundwater quality assessment on the same areas and evaluate the applicability of the methodologies for the purpose of seawater intrusion analysis.

CHAPTER I

GROUNDWATER VULNERABILITY TO SEAWATER INTRUSION ALONG COASTAL URBAN AREAS: A QUANTITATIVE COMPARATIVE ASSESSMENT OF EPIK AND DRASTIC

ABSTRACT

Groundwater vulnerability assessment models are invariably coupled with Geographic Information Systems to provide decision makers with easier visualization of complex systems. In this study, we examine the uncertainty associated with two GIS-based groundwater vulnerability models: DRASTIC and EPIK. These two model are used to assess seawater intrusion, a growing threat along coastal urban cities due to overexploitation of groundwater resources. For this purpose, a national mapping of groundwater vulnerability was first conducted and followed with a groundwater quality monitoring program along three coastal cities. EPIK and DRASTIC model results were categorized into six predefined water quality categories based on water quality standards; these categories ranged between groundwater suitable for drinking purposes to seawater. Finally, the results of the groundwater monitoring program were compared with the modeled vulnerability predictions using two indicators (Chloride and TDS). While field measurements demonstrated a high spatial vulnerability in seawater intrusion along the coastal urbanized areas, the modelling results failed to capture these dynamics. These results clearly indicate that vertical-based vulnerability models perform poorly when the anthropogenic impacts depend on lateral groundwater flow. As such, EPIK and DRASTIC have limited abilities to capture vulnerability to lateral seawater intrusion induced primarily by vertical groundwater withdrawal. If these models are to be used to assess seawater intrusion, then both models require modification so as to incorporate data on water depth and the underlying lithology.

Keywords: Groundwater Vulnerability, Seawater intrusion, DRASTIC, EPIK

1 Introduction

Groundwater vulnerability assessments are often coupled with Geographic Information Systems (GIS) based models to provide decision makers with easier visualization of complex systems. However, most vulnerability assessment models are commonly set for surface-based contamination and typically not tailored for coastal urban cities characterized with seawater intrusion. The vulnerability of groundwater to seawater intrusion is increasing exponentially under unsustainable extraction practices along coastal urban areas, where population growth resulted in increased water extraction rates that exceed natural recharge (Chang, 2010; Howard, 2002). Groundwater vulnerability is further accentuated with the decrease in infiltration and recharge capacities caused by land use changes associated with urbanization (IPCC, 2013) and expected to get exacerbated with the potential climate change impacts. The latter affects components of the water cycle (increased evaporation, change in spatial and temporal precipitation patterns, hence increased run-off), which results in hindering groundwater recharge, particularly in karstic and semi-karstic areas (Fetter, 2001; Howard, 2002; Loáiciga, et al., 2012; Ranjan, et al., 2006; Vorosmarty, et al., 2000; Werner, et al., 2012).

Aquifer vulnerability, defined as sensitivity of the studied factor to various stresses (climatic or anthropogenic), was first used by Margat (1968) to evaluate the exposure of aquifers to contaminants (Magiera, 2000; Vlaicu & Munteanu, 2008). A comprehensive vulnerability analysis factors the *sensitivity* of the study area, which is defined by the intrinsic characteristics of the system or the aquifer to various stresses, and the *exposure*, which introduces potential impacts from contamination of anthropogenic or natural sources. Adaptive systems are more resilient to exposure parameters than sensitive systems, because they can utilize their adaptive capacity to reduce vulnerability (Walthall et al., 2012; IPCC, 2007).

Groundwater vulnerability assessment (GVA) models have been developed to provide insight on groundwater conditions based on physical parameters of the medium containing the groundwater. The medium are usually static systems that vary only over geological time spans. Their inputs require the intrinsic characteristics of the groundwater bearing formations (aquifers) including geology, geomorphology, and hydrogeology (Fijani et al., 2013; Vlaicu & Munteanu, 2008) or layers that impact these formations. These include soil cover, land use, topography, and hydrology. GVA models usually utilize the Index and Overlay (IO) system to generate scores based on ranks or weights given to several parameters intrinsic to the aquifer medium. Those weights are then aggregated to produce a dimensionless value referred to as the total vulnerability of the study area (Elewa, et al., 2013; R. C. Gogu & A. Dassargues, 2000; Milnes, 2011; Shirazi et al., 2012).

Given the nature of input parameters, GVA models are usually suitable for data-scarce regions (Panagopoulos et al., 2006; Vlaicu & Munteanu, 2008). Newly developed IO vulnerability assessment models have attempted to add new external factors such as contaminant source and type or climate change and other regional impacts into their modeling framework (Ahmadian, 2013; Fijani, et al., 2013; Rangel-Medina et al., 2004; Shirazi, et al., 2012). A summary of the parameters used in selected IO groundwater vulnerability assessment methods is presented in Table 1-1. Note that the inclusion of too many input parameters does not necessarily increase the reliability of one method over the other. Method classification is highly dependent on applicability and relevance to the study area characteristics.

Table 1-1: Comparison of commonly used intrinsic vulnerability assessment methods with corresponding parameter

Included Parameter	DRASTIC[a]	SINTACS[b]	EPIK[c]	COP+K[d]	GOD[e]	IP /PI[f]	GALDIT[g]	WMCDSS[h]
Depth to water table	X	X	-	-	X	X	X	-
Precipitation/recharge rate/ water balance	X	X	X	X		X	-	X
Vadose (unsaturated) zone	X	X	X	X	X	X	-	-
Aquifer Media/ lithology/Hydrogeological characteristics	X	X	X	X	X	X	-	-
Soil	X	X	X	X	X	X	-	-
Topography	X	X	X	X	-	X	-	-
Aquifer thickness	-	X	-	-	X	-	X	-
Hydraulic conductivity	X	X	X	X	-	-	X	X
Land Use	-	X	X	X	-	X	-	-
Hydrology/steams	-	-	-	X	-	X	-	-
Distance from shoreline	-		-		-		X	-
Water quality	-		-		-		X	X

Source: [a] Aller et al., 1987; Jamrah et al., 2008; Panagopoulos, et al., 2006; Shirazi, et al., 2012; Vlaicu & Munteanu, 2008

[b] Civita & de Maio, 1997; Rangel-Medina, et al., 2004; Gogu et al., 2003; Polemio et al., 2009; Vlaicu & Munteanu, 2008

[c] Barrocu et al., 2006; Doerfliger, 1996; Doerfliger et al., 1999; Doerfliger & Zwahlen, 1998; Radu Constantin Gogu & Alain Dassargues, 2000; Pera & Valcarce, 2009; Polemio et al., 2009 Rangel-Medina, et al., 2004SAEFL, 1998; Vlaicu & Munteanu, 2008

[d] Marín et al., 2010; Polemio et al., 2009; Rangel-Medina, et al., 2004; Vlaicu & Munteanu, 2008

[e] Gogu, et al., 2003; Polemio et al., 2009; Rangel-Medina, et al., 2004; Vlaicu & Munteanu, 2008

[f] Goldscheider, 2005; Polemio et al., 2009; Rangel-Medina, et al., 2004; Vlaicu & Munteanu, 2008

[g] Chachadi & Lobo-Ferreira, 2005; Chachadi & Lobo-Ferreira, 2001

[h] Elewa, et al., 2013

For this study, two commonly used groundwater vulnerability assessment models (DRASTIC and EPIK) were used to assess groundwater vulnerability to seawater intrusion in urban and coastal regions characterized with karstic aquifers. For this purpose groundwater vulnerability maps were generated using basic physical inputs, and validated by data from field sampling campaigns. Model results were then compared and used to assess the advantages and drawbacks of each model in the context of an urban environment under seawater intrusion stress.

2 Groundwater Vulnerability Assessment Applications

GVA methods have become user-friendly with the increased use of Geographic Information System (GIS). This has made them attractive tools for use by decision and policy makers.

Accordingly, decision makers are able to use the generated results to aid their decision making process. While such tools have often resulted in improved decision making, they have also produced similar amount of non-validated or unreliable data based on their failure to recognize the complexity of the system, its adaptive capability, or the model of exposure (Focazio et al., 2002). These models utilize generalized assumptions and parameters and may not be representative of the peculiarities or actual conditions of some study areas (Doerfliger, et al., 1999; Doerfliger & Zwahlen, 1998; R. C. Gogu & A. Dassargues, 2000).

Common groundwater vulnerability assessment models/methods (R. C. Gogu & A. Dassargues, 2000; Gogu, et al., 2003; Goldscheider, 2005; Marín, et al., 2010; Polemio, et al., 2009; Vlaicu & Munteanu, 2008) vary in their ability to account for vertical and non-vertical contamination (Chachadi & Lobo-Ferreira, 2001; Elewa, et al., 2013; Rangel-Medina, et al., 2004; Selmi, 2013). In some cases, models designed specifically for surface contamination were used for non-vertical contamination with (Chachadi & Lobo-Ferreira, 2005; Chachadi & Lobo-Ferreira, 2001; Elewa, et al., 2013; Selmi, 2013) or without modifications (Jamrah, et al., 2008). A summary of common intrinsic GVA methods applied in various study areas is shown in Table 2-1.

Table 2-1: Summary of intrinsic Vulnerability Assessment Methods applied in various study areas
For analysed water quality parameters refer to Table 1-1 in Chapter 2)
(N/A: not applicable and (-) means not found, WL: water Level, LS: Limestone)

Reference	Modify (Y/N)	Validation (Y/N)	Method	# sample points	Area	Notes
Barrocu et al., 2006	N	N	EPIK[a]	N/A	110 km^2	North-central Sardinia
Chachadi et al., 2002	N	N	GALDIT[b]	56 wells	-	Goa: application for Local sea level rise
Doerfliger et al., 1999	N	N	EPIK	N/A	110 km^2	Application Saint-Imier test site (Swiss Jura)
Elewa, et al., 2013	N (New method)	Y	WMCDSS	46 wells	7593 km^2	WMCDD: weighted multi-criteria decision support system Northeastern part of Nile Delta
Fijani et al., 2013	Y	Y	DRASTIC[c]	131 wells	~1000 km^2	Validation using SCMAI (supervised committee machine with artificial intelligence) which was calibrated with NO_3-N concentration data Maragheh–Bonab plain aquifer, Iran
Radu Constantin Gogu & Alain Dassargues, 2000	N	Y	EPIK	N/A	2.5 km^2	Sensitivity analysis to evaluate the influence if each parameter to the overall result The Beauraing Southern Belgium
Gogu, et al., 2003	N (comparison)	N	EPIK, DRASTIC, The German method, GOD, ISIS	N/A	65 km^2	Neblon river basin (Begium)
Goldscheider, 2005	N (comparison)	N	PI, EPIK, The German method	N/A	36 km^2	Engen Test site Swabian Alb, Germany
Jamrah, et al., 2008	N	Y	DRASTIC	>50 wells	-	For water level 50wells Water quality measurements from 111 water samples Coastal Region Oman
Kallioras et al., 2011	N	Y	DRASTIC	6 wells (geophysical analysis) 25 wells (WL & quality)	-	DRASTIC was checked with main water quality parameters (without interpolating) Rhodope Greece
	N	Y	GALDIT		-	GALDIT was checked with main water quality parameters (without interpolating) Rhodope Greece
Lobo-Ferreira et al., 2005	N	N	GALDIT	9 wells	10 km^2	Based on scenarios for GW level above the sea level Monte Gordo
Marín, et al., 2010	N (comparison)	N	COP, PaPRIKA	N/A	350km^2 (110 km^2 of LS outcrop)	Lez Karst System (Montpellier, South France).

Reference	Modify (Y/N)	Validation (Y/N)	Method	# sample points	Area	Notes
M. Metni et al., 2004	N	N	DRASTIC	N/A	10,452km^2	Modified the classes for each parameter to fit to the Lebanese context Lebanon
Najib et al., 2012	N	N	GALDIT	N/A	-	Aquifer of Chaouia Coast (Morocco)
Panagopoulos, et al., 2006	Y	Y	DRASTIC	GW 145 sampling points Soil 46 sites	285 km^2	Using geostatistical analysis weights and ranks were modified and some parameters were removed and/or added Trifilia province, Greece,
Pera & Valcarce, 2009	N	N	EPIK	N/A	-	La Habana city area, Cuba
Polemio, et al., 2009	N (comparison)	N	GOD, DRASTIC, SINTACS, EPIK, PI & COP	N/A	78.2 km^2	Karst feature = maximum vulnerability Apulian test site
Selmi, 2013	N	Y	GALDIT	N/A	365 km^2	Gaza Strip
Shirazi, et al., 2012	Y	Y	DRASTIC	N/A	N/A	Conceptually rescaling of rating ranges DRASTIC was evaluated using nitrates using Susceptibility Index (SI) method
Vlaicu & Munteanu, 2008	N (comparison)	N	Application by PI method and selected parameters (P, K, C, O factors)	N/A	-	5 groups of vulnerability assessment in Karst Aquifers (Hydrogeological complex method, Analogical, parametric, Mathematic, Statiscal) Compared methods: DRASTIC, DWSAP, SINTACS, SI, GOD, EPIK, REKS, GSI, GLA, AF, ΔhT, VULK, FAVA, CALVUL O: overlaying layers C: concentration of flow K: Karst Network development P: precipitation regime EPIK: in northern unit of Banat Mountains, Romania PI in Bihor Mountains, Romania

a SAEFL, 1998 *AND* Doerfliger & Zwahlen, 1998 set the methodology

b Chachadi & Lobo-Ferreira, 2001 *AND* Chachadi & Lobo-Ferreira, 2005 set the methodology

c Aller et al., 1987 Set the methodology

3 Material and Methods

3.1 Study area characteristics

The modeling domain covers the entire country of Lebanon; yet field monitoring was restricted to the Lebanese coastal plain that stretches along the eastern Mediterranean. The monitored area stretched between Beirut and Tripoli and is known to have a semi-karstic aquifer (Figure 3-1). The area is characterized by a semi-arid climate with mild wet winters and moderately hot dry summers. With a predominantly residential and commercial land use, the area has high population density and high density of drilled wells.

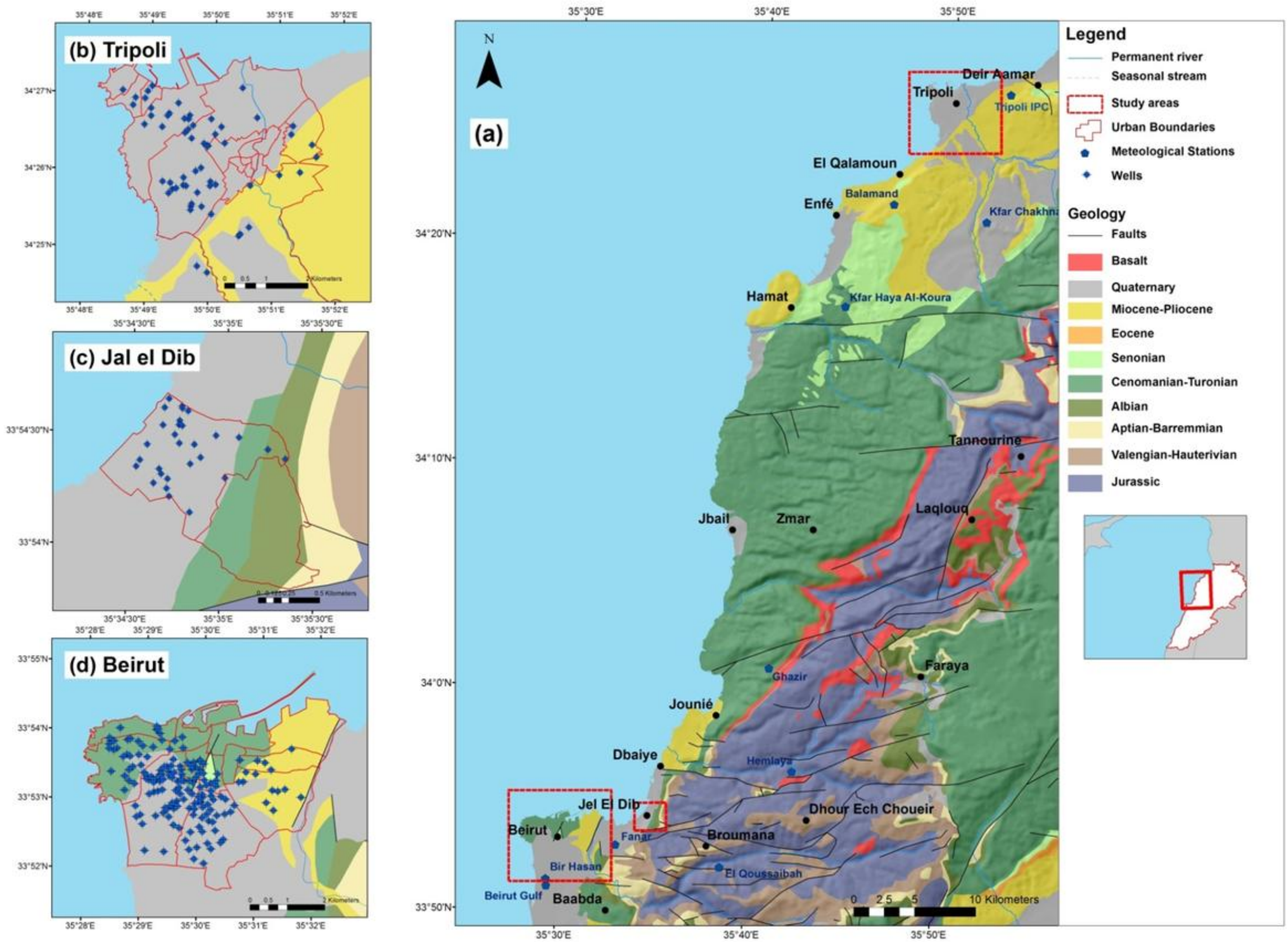

Figure 3-1: (a) Geological formations of the Northern Coast of Lebanon with the focus study areas and the wells' locations for the three areas of study (b) Tripoli (c) Jal el Dib (d) Beirut

3.2 Field sampling program

Groundwater sampling in the study area was conducted in three coastal cities (Figure 3-1). The first zone, Jal el Dib, was monitored through 6 groundwater sampling campaigns that were conducted every two months starting in October 2012 and ending in October 2013. Samples were collected from 29 privately owned wells. The second zone, Beirut, was assessed through a single sampling campaign that was conducted between May and June 2013. Samples from 165 privately owned wells were collected (Mutasem El-Fadel et al., 2014). The last zone was Tripoli, which was surveyed through two sampling campaigns one in June 2007 and another in September 2006. In Tripoli, 60 privately owned wells were monitored (M. El-Fadel et al., 2014; Tomaszkiewicz et al., 2014). The locations of the sampled wells are shown in Figure 3-1 b, c and d, Tripoli, Jal el dib, and Beirut, respectively. At each sampling point, the water system was checked to ensure that the water sample can be obtained directly from the well to limit potential cross-contamination from the existing public water supply system. The collected samples were transported on ice to the Environmental Engineering Research Center at the American University of Beirut and analyzed for various physical and biochemical indicators in accordance with *Standard Methods for the Examination of Water and Wastewater* (APHA, 1998).

3.3 GVA Model Selection

The DRASTIC and EPIK model were adopted as the GVA models. DRASTIC was designed for large areas and to work over any aquifer type (porous/karstic/mixed). It was applied in Lebanon (Figure 4-1) in a similar fashion to its uses in many other large-scale study areas (Fijani, et al., 2013; Kallioras, et al., 2011; Khan et al., 2010; Panagopoulos, et al., 2006; Salemi et al., 2011;

Shirazi, et al., 2012; Werner, et al., 2012). Given the karstic environment and scarcity of data along the Lebanese coastal zone, EPIK and COP+K were also considered (Jiménez-Madrid et al., 2010). Even though COP+K is easy to apply and accounts for climatic variables, it has been reported that it usually under-estimates the vulnerability of karstic areas (Civita & de Maio, 1997; R. C. Gogu & A. Dassargues, 2000; Polemio, et al., 2009). EPIK on the other hand has been applied on several test sites and has been more rigorously cross-validation with actual field measured parameters when compared with COP+K; therefore EPIK was chosen as the second intrinsic vulnerability assessment method.

With respect to the other potential methods (Table 1-1), the GOD method is not very sensitive to minor changes, thus it is used where the vulnerability variations are large within a small area (Polemio, et al., 2009). PI method was designed for Karstic environment, and maps groundwater vulnerability in a GIS-environment based on the "origin-pathway-target" model[2] (Goldscheider, 2005; Goldscheider et al. 2000 cited in Voigt et al., 2004; Vlaicu & Munteanu, 2008). However, this method was compared with EPIK and the result were found to be very similar (Polemio, et al., 2009). SINTACS and IP/PI are the most comprehensive with respect to the number of parameters that are included; however over parameterization limits their use in data scarce regions. The WMDCSS model is highly regionalized to the original study area and this difficult

[2] Origin-pathway-target model takes into consideration the location where the contaminant is introduced, the phreatic zone until it reaches the aquifer, and the aquifer which is the target

to implement (Elewa, et al., 2013). Some of the more recent vulnerability assessment methods designed for lateral contamination (seawater intrusion), such as the GALDIT, would have also been ideal, however they have not been adequately tested, with no application in any Mediterranean city (Chachadi & Lobo-Ferreira, 2005; Chachadi & Lobo-Ferreira, 2001; Chachadi, et al., 2002; Lobo-Ferreira, et al., 2005; Kallioras, et al., 2011; Najib, et al., 2012; Selmi, 2013).

3.4 DRASTIC

DRASTIC is an intrinsic vulnerability assessment method which uses OI of its 7 different aquifer related parameters, to assess the vulnerability of the aquifer to groundwater contamination. The method has been established and implemented by Aller et al. (1987) and published by the U.S. Environmental Protection Agency (EPA). This method is suitable for porous/granular aquifers at a large scale.

The seven parameters that make up the acronym of DRASTIC are **D**epth to water level, **R**echarge, **A**quifer Media, **S**oil Media, **T**opography, **I**mpact of the Vadose Zone, Hydraulic **C**onductivity. Each of the 7 parameters are separately given a weight (W=1 to 5), relative to its impact on the aquifer vulnerability and each sub-category within one parameter, is given a rating (R=1 to 10) based on its influence on that parameter (Figure 3-2). The rankings and the weights can differ from one study area to another (Aller, et al., 1987; Fijani, et al., 2013; M. Metni, et al., 2004).

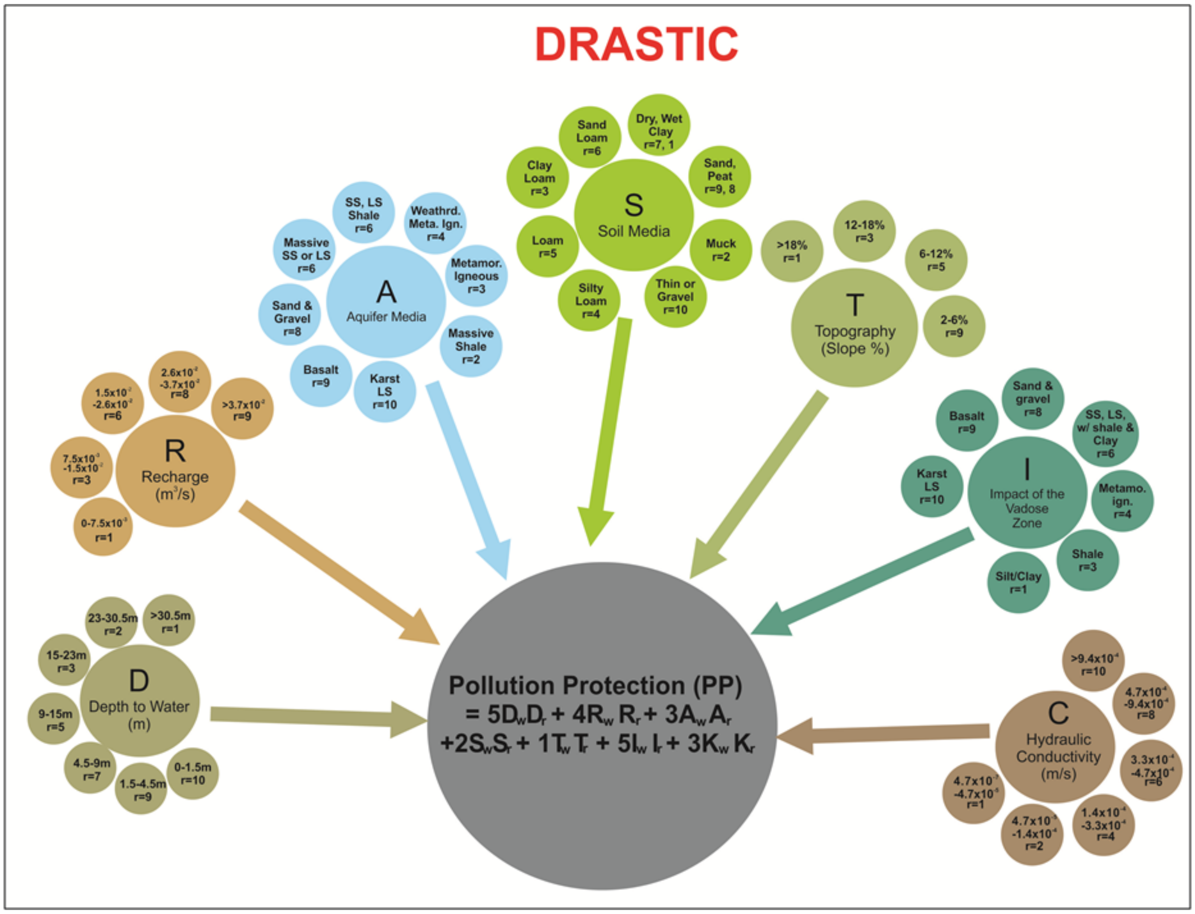

Figure 3-2: Diagram showing the parameters of the analysis of DRASTIC and the weights and ranks for each parameter NOTE: SS is Sandstone, LS is Limestone, weathrd is weathered, Meta. & metamor. is metamorphic, ign. is igneous

The **Pollution Protection** (PP) index is then calculated from multiplying the weight (W) and the rating (R) of each of the 7 parameters. The higher the Pollution Protection value, the higher the vulnerability of that area, as shown in the formula below:

Pollution Protection (PP) $= D_R D_W + R_R R_W + A_R A_W + S_R S_W + T_R T_W + I_R I_W + C_R C_W$

Where: D: Depth to Water; R: Recharge; A: Aquifer Media, S: soil media; T: Transmissivity; I: Impact of the Vadose zone; C: Hydrauilic Conductivity; R: Rating and W: Weight

In terms of limitations, DRASTIC (Fijani, et al., 2013; Panagopoulos, et al., 2006; Sener & Davraz, 2012) does not differentiate between porous media and fractured media; and does not account for structural geology (faults, folds). It only assesses the shallowest aquifer, discarding the aquifers underneath and assumes contamination is introduced evenly all over the study area. Moreover, DRASTIC parameters are chosen based on qualitative judgment not quantitative, and its results are not calibrated by the concentration of the contaminants nor are they validated.

On the other hand, DRASTIC's main advantage is its flexibility to adjust the ratings and the weights to better fit the specifications of the study area (Fijani, et al., 2013; Aller et al. 1987; Panagopoulos, et al., 2006). In this study DRASTIC model results are used from an existing national comprehensive study (Marc Metni, 2002).

3.5 EPIK

EPIK is an intrinsic vulnerability assessment method, which is used for spring catchment areas and well radius of influence. It was produced by the Swiss Agency for the Environment, Forests and Landscape to deal specifically with Karstic environments. It has four parameters (Figure 3-3) as indicated in the acronym (**E**pikarst, **P**rotective cover, **I**nfiltration condition, **K**arst network) (Barrocu, et al., 2006; SAEFL, 1998). Every parameter is given a weight depending on its impact; these parameters are divided into sub-categories, each with a specific rating.

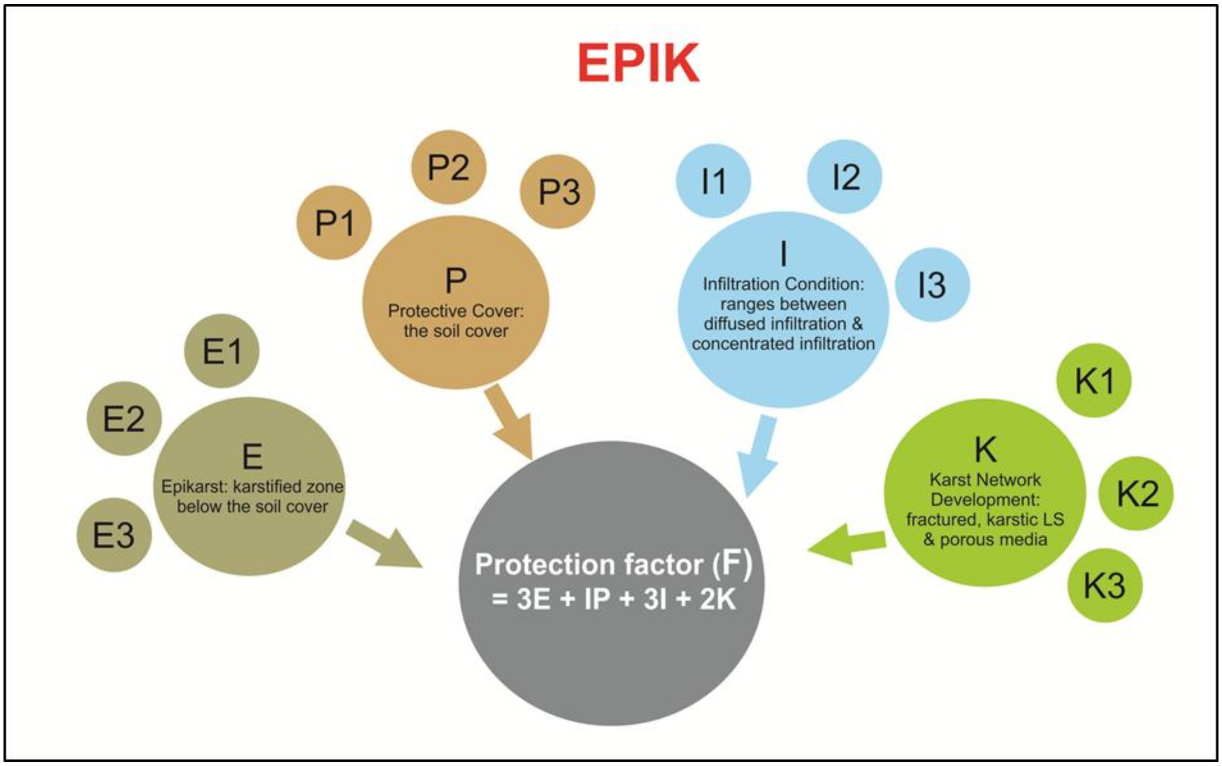

Figure 3-3: Diagram showing the parameters of the analysis of EPIK and the vulnerability zones based on the Protection Factor (F) calculation

The **Protection Factor** (PF) is calculated by multiplying the ratings with the weight as shown in the formula below (Figure 3-3)

Protection factor (F) = 3E + 1P + 3I + 2K

Where E: Epikarst; P: Protective Cover; I: Infiltration Condition; K: Karst Network, and the values are weight suggested by the reference

Since EPIK was not tailored to be used in urbanized areas, it is essential to analyze its applicability in an urban context, given accelerating coastal urban expansion. In fact, EPIK (in its original form) considers urban areas as relatively low vulnerability, since asphalted areas or concrete structures are considered to be impermeable surfaces for the downward percolation of contaminants'.

For this study, EPIK was used on a country scale; moreover EPIK's flexibility was utilized to vary the input parameters so as to include the urbanization factor into the analysis (Table 3-1). This was achieved by generating three different parameterizations of EPIK. These modification were introduced by changing the properties of the outcropping geological properties, thus adding dynamic features to the methodology since urbanization changes occur at a shorter time span than geological changes. In summary, V2 is the EPIK as it is suggested in the reference, and urbanization factor is the varying factor in V1 and V3

Table 3-1: Different versions of EPIK methodology with corresponding definition (the main variation is the variation of the urban areas factor)
NOTE: The buffer around the coast is not dynamic, it uses a fixed value without taking topography into consideration (For more details per version see section 5.1 – Annex 1)

Parameter	Versions			Weight/ Rank
Epikarst	V1	V2	V3	3
E1	Fractures, developed faults, current/paleo channels/Rivers, flood plains + Buffer (500m) around faults + Buffer 500m around Rivers	Same as V1	Same as V1	2
E2	Karst outcropping formations	Same as V1	Same as V1	3
E3	The rest of the area, where karstic morphology absent	Same as V1	Same as V1	4
Protective Cover	V1	V2	V3	1
P1	No protective cover (rest of the area)	Same as V1	No protective cover (rest of the area)*+urban areas*	1
P2	Quaternary cover + dynamic buffer to an elevation of 100m asl on the coastline[3]	Same as V1	Same as V1	2
P3	500m buffer around rivers channels	Same as V1	Same as V1	3
P4	Aquicludes + urban areas	Aquicludes without urbanization	Aquicludes	4
Infiltration	V1	V2	V3	3
I1	Slopes greater than 10% in Karstic area	Same as V1	Slopes greater than 10% in Karstic area + *coastal urban areas*	2

[3] The well of the highest elevation in the surveyed wells is at an elevation of 99 m asl, and accordingly 100m asl was chosen as the maximum distance from the coast to build the buffer

Parameter	Versions			Weight/ Rank
I2	Slopes less than 25% around the coast	Same as V1	Same as V1	3
I3	Rest of the area	Same as V1	Same as V1	4
Karst network development	V1	V2	V3	2
K1	Well-developed karst formation (including the C4, C5, e, J, m2 formations + Fault buffers)	Same as V1	Well-developed karst formation (including the C4, C5, e, J, m2 formations + Fault buffers) *including coastal urbanization*	1
K2	Poorly developed karst or aquifers (C1, C2, Q, ncg, ml, p)	Same as V1	Same as V1	2
K3	Rest of the area (bc, bj, bm, bp, C3) + *urban areas*	Rest of the area (bc, bj, bm, bp, C3)	Rest of the area (bc, bj, bm, bp, C3)	3

3.6 Validation of OI groundwater vulnerability assessment models

The OI groundwater vulnerability assessment models typically do not include a validation step, whereby results are compared with field measured water quality values. Validation could be implemented by developing a categorization that links the resulting Protection Factor (PF) in EPIK or the Pollution Protection (PP) in DRASTIC values with standardized water quality categories of different pollutants obtained from water quality measurements. In this paper, five different water quality categories based on Chloride and TDS were used to assess the performance of DRASTIC and EPIK. Those water quality categories, ranging from freshwater to seawater, were assigned corresponding ranges of PF and PP scores based on their qualitative description. This proposed evaluation methodology (Figure 3-4) bridges the missing gap between vulnerability assessment based on intrinsic properties of the aquifer and the current status of the groundwater quality (Fijani, et al., 2013; Panagopoulos, et al., 2006; Sener & Davraz, 2012).

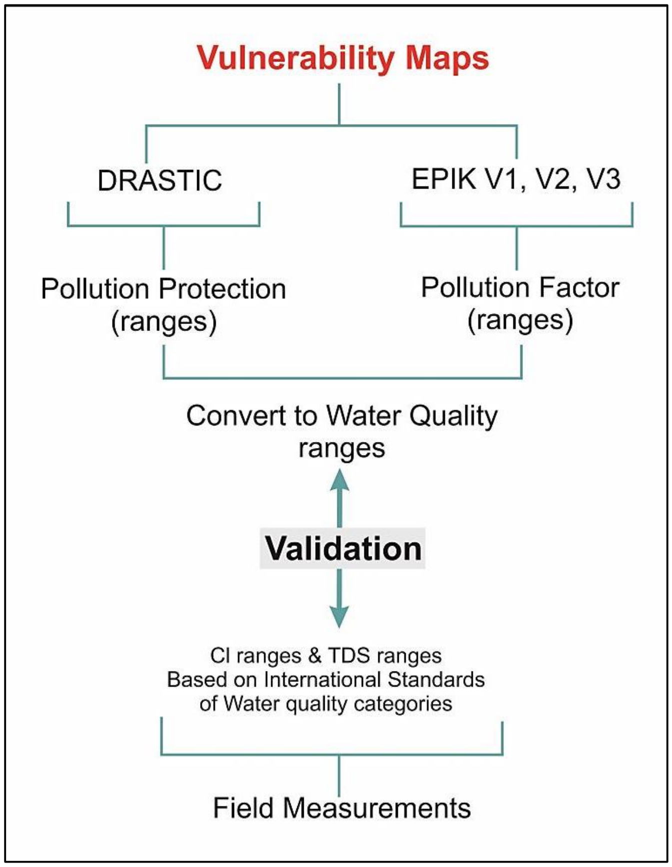

Figure 3-4: Diagram showing the work flow for this study

3.7 Setting validation criteria (water quality standards)

Validating with field water quality measurements has been commonly done in the literature (Table 2-1), although GVA models are static whereas field measured water quality are dynamic and can highly be affected by anthropogenic activities like over-pumping, which can promote seawater intrusion.

With both methods, it was assumed that lower vulnerability zones are more likely to have steady water quality levels with little to no changes (deterioration). Hence, it is hypothesized that urbanized coastlines areas that have been categorized as high-vulnerability zones are more likely to have deteriorated groundwater quality as a result of saltwater intrusion. Thus, the "Drinking

Water" category was expected to be more commonly found in areas that were within low vulnerability zones and the "Sea Water" category more probable in areas falling within high vulnerability zones. Table 3-2 presents the standard water quality categorization and the proposed matching with the DRASTIC and EPIK vulnerability ranges. Note that in cases of lateral flow (seawater intrusion) or when the recommended protection measures are not enforced, the water quality would not match with the vulnerability criteria. The proposed categories of PP and PF were divided equally to range between the low and high vulnerability thresholds as per the vulnerability level (low to high); unlike the TDS and Cl^- ranges of water quality class which follow non-linear trend.

Table 3-2: Water Quality categories and their equalivalent PP and PF ranges

Water Types	**TDS range (ppm)**	**Cl^- range (mg/L)**	**DRASTIC PP ranges (Aller, et al., 1987; Marc Metni, 2002)**	**EPIK PF ranges (SAEFL, 1998)**	**EPIK PF ranges (modified)**	**Vulnerability**
Drinking water	0-500	1-200	27-85	34 AND 34+P=4 I=3 or 4[1]	32-34	Low
Fresh Water	500-1,000	200-300	86-106	29-33	28-31	
Brackish	1,000-5,000	300-500	107-127	24-28	24-27	Moderate
Highly Brackish	5,000-15,000	500-5,000	128-148	19-23	21-23	
Saline Water	15,000-30,000	5,000-15,000	149-169	14-18	18-20	High
Sea Water	30,000-40,000	15,000-20,000	170-236	9-13	15-17	

Source: Aller, et al., 1987; Oram et al., 2010; SAEFL, 1998; USGS, 2000; Water Quality Assosciation, 2013; WHO, 2003

[1] ONLY the locations where PF=34 AND P=4 and I=3 or 4; All these conditions should be found together for this category

After applying DRASTIC and EPIK methods on the study area, the PP and the PF values of each zone were validated with their corresponding TDS or Chloride categories obtained from the field water quality campaign, as shown in Table 3-2. A cross validation table was then constructed to evaluate the extent of match between the results of the intrinsic vulnerability assessment methods and the actual measured water quality data in terms of chloride and TDS levels. Results and Discussion

4 Results and Discussion

4.1 DRASTIC

Figure 4-1 shows the DRASTIC vulnerability map for Lebanon (Marc Metni, 2002). The karstification regions in the high elevation of Mount Lebanon are marked with red color indicating high vulnerability, and the Bekaa plain with soil cover and recent less-permeable outcrops show lower vulnerability, depicted in blue to green colors. The coast varies from low vulnerability in the south, moderate vulnerability in the north, and high vulnerability in Jounieh-Jbeil area (area between Beirut and Tripoli). The vulnerability map is highly conformable with the 1:200,000 scale geologic map of Lebanon, which highlights the focus of this methodology on the outcropping lithology and not the underlying aquifers, even if they are the tapped/used aquifers. The overall map also shows that this method excludes the anthropogenic factor when analyzing the vulnerability of a system.

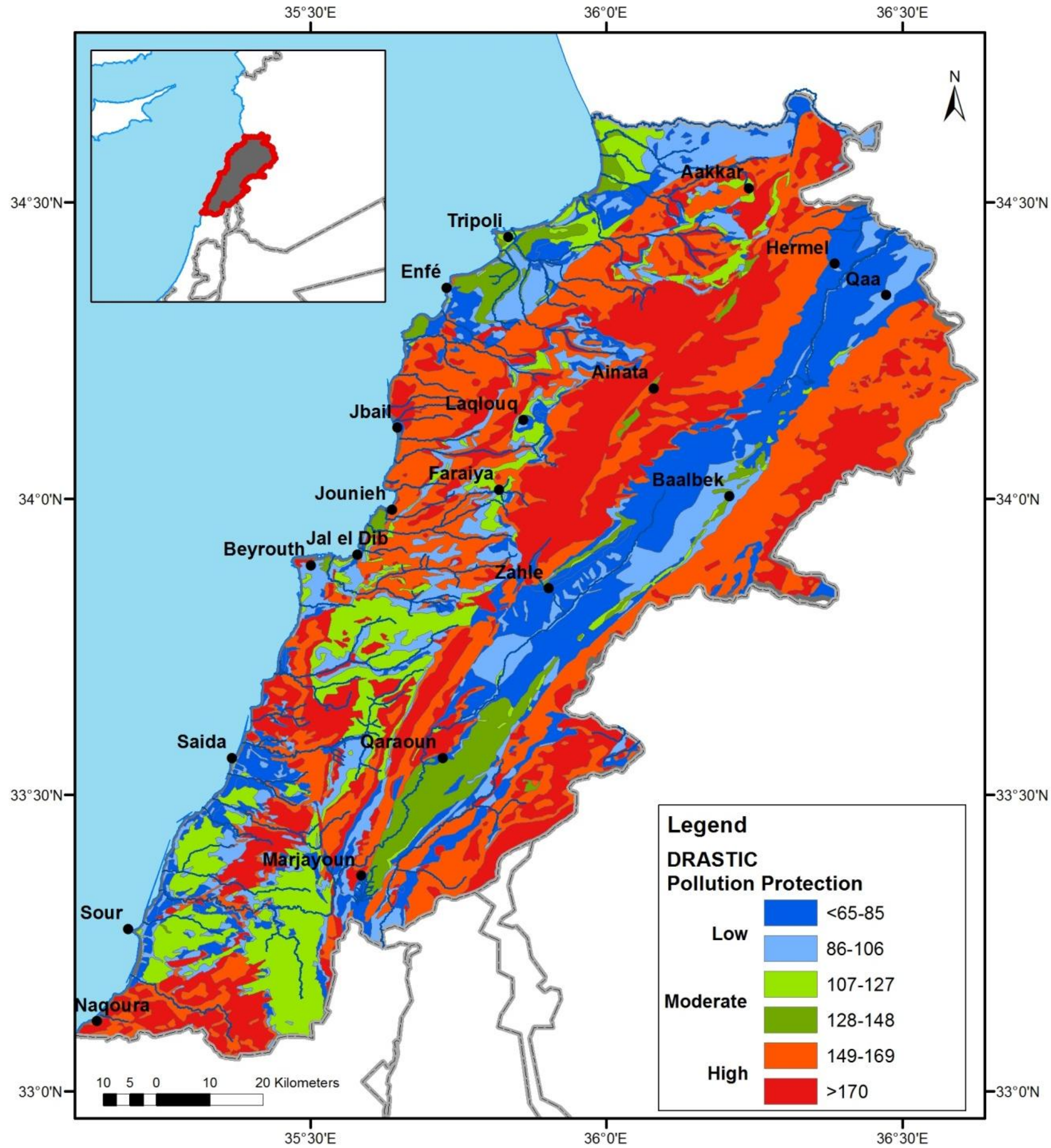

Figure 4-1: Map of showing the Groundwater Vulnerbaility of Lebanon based on DRASTIC Pollution Protection values (redrawn after M. Metni, et al., 2004)

4.1.1 Water quality vs. PP values

After conducting a visual check of the vulnerability display of Lebanon, the focus shifted to the three coastal areas in our study area where seawater intrusion already occurs, and groundwater samples have already been collected and analyzed. According to the water quality categories defined earlier (Section 3.7), analysis for the percentage of match between water quality categories predicted by DRASTIC and obtained from groundwater quality analysis was conducted to verify the extent of match between the ranges based on field measured water quality values and the water quality ranges generated by DRASTIC (Table 3-2).

Results for the three cities at different sampling periods were reported in tables similar to Table 4-1 showing the assessment for the city of Beirut, while using Chloride levels as an indicator. In the table, columns represent the water quality categories based on water quality analysis, while rows represent the different water quality categories predicted by the PP values of DRASTIC. The ideal case occurs when the table only has diagonal entries and zeros everywhere else. The cross validation table also gives an idea on the tendency of DRASTIC to over-estimate or under-estimate. Values to the upper triangle indicate that the DRASTIC is over-estimating; while having more points in the lower triangle indicates that the VA methodology is under-estimating (the results of cross-checking with all the cities and parameters are shown in section 5.2 – Annex 2).

Results showed that DRASTIC matched only 12.1 percent of the field Chloride results in Beirut. DRASTIC matched a cumulative of 40.6 and 86.1 percent of the wells' water quality with ±1 and ±2 water quality category, respectively. The results also show that the methodology tended to over-estimation 33 percent of the times and under-estimated the water quality values 54 percent. It should be noted that the performance of DRASTIC was found to vary over cities, seasons, and measured parameter.[4]

Table 4-1: Field measured Chloride levels (WQ_{Field})and Metni, 2002 DRASTIC ranges for Round 1 Beirut matching with DRASTIC Pollution Protection (PP) ranges($WQ_{DRASTIC}$)

WQ_{Field} / $WQ_{DRASTIC}$	Drinking water 1-200	Fresh Water 200-300	Brackish 300-500	Highly Brackish 500-5,000	Saline Water 5,000-15,000	Sea Water 15,000-20,000
Drinking water 27-85						
Fresh Water 86-106	29	20	8	35	10	
Brackish 107-127		1		2		
Highly Brackish 128-148	6		1			
Saline Water 149-169						
Sea Water 170-236		4	3	40	6	
e.g. BEY_R1_DR_Cl	Match	±1	±2	±3	±4/5	Total
Number of wells	20	47	75	19	4	165
Percent per category	12.1	28.5	45.5	11.5	2.4	100.0
Cumulative Percent	12.1	40.6	86.1	97.6	100.0	100.0

[4] In order to make sure that the under or over estimations within categories are not based on errors in the appliances that measured the water quality, an estimation of error ±3% was added on the measurements of the Chloride and the TDS, and the number of points which crossed categories due to this error were counted, see section 3.6 (Water Quality Standards) and section 5.3 – Annex 3.

This analysis was repeated for the three cities using Chloride and TDS parameters at every measurements round. Table 4-2 presents a compilation of the cross-check results for DRASTIC. The results show that the city that performed the worst in matching with the DRASTIC measurements was Beirut, whereas results of Jal el Dib seem to exhibit the best match. This is an interesting observation since the level of urbanization is relatively higher in Beirut as compared to Jal el Dib

Table 4-2: Percent of match for the DRASTIC methodology Validation (the highlighted blue are when the 50 percentile is crossed)

NAME	Match (%)	±1 (%)	±2 (%)	±3 (%)	±4/5 (%)	Total (%)
BEY_R1_DR_Cl	12.1	40.6	86.1	97.6	100	100.0
BEY_R1_DR_TDS	27.3	49.1	71.5	98.2	100	100.0
JD_R3_DR_Cl	45.5	68.2	100	100	100	100.0
JD_R3_DR_TDS	22.7	90.9	100	100	100	100.0
JD_R7_DR_Cl	14.8	77.8	88.9	100	100	100.0
JD_R7_DR_TDS	55.6	77.8	96.3	100	100	100.0
TRP_R1_DR_Cl	26.2	43.1	89.3	100	100	100.0
TRP_R1_DR_TDS	8.3	55	91.7	100	100	100.0
TRP_R2_DR_Cl	18.3	35	85	100	100	100.0
TRP_R2_DR_TDS	8.3	38.3	86.6	100	100	100.0

CITY		**VULNERABILITY ASSESSMENT (VA) METHOD**	
BEY	Beirut	DR	DRASTIC
JD	Jal el Dib	EP1	EPIK-Version 1 (urbanization low impact)
TRP	Tripoli	EP2	EPIK-Version 2 (no urbanization)
SAMPLING ROUND		EP3	EPIK-Version 3 (urban areas high vulnerability)
R1	Round 1- Early Summer - May/June	**PARAMETERS**	
R2	Round 2 - Late Summer – Sept./Oct.	Cl^-	Chloride Level (mg/L)
Rx	Other Rounds	TDS	Total Dissolved Solids (ppm)

4.2 EPIK

As was mentioned in section 0, there are three variations of EPIK that were implemented at the country scale; the variations were focused on the approach used to integrate the urbanization impact factor. The first version (EPIK_V1) included urbanization as a surface of protection, which may be true in surface-introduced-contaminants, but not necessarily true for most coastal cities in developing countries, where urbanization is adding on the vulnerability (increased abstraction, seawater intrusion) (Figure 4-2).

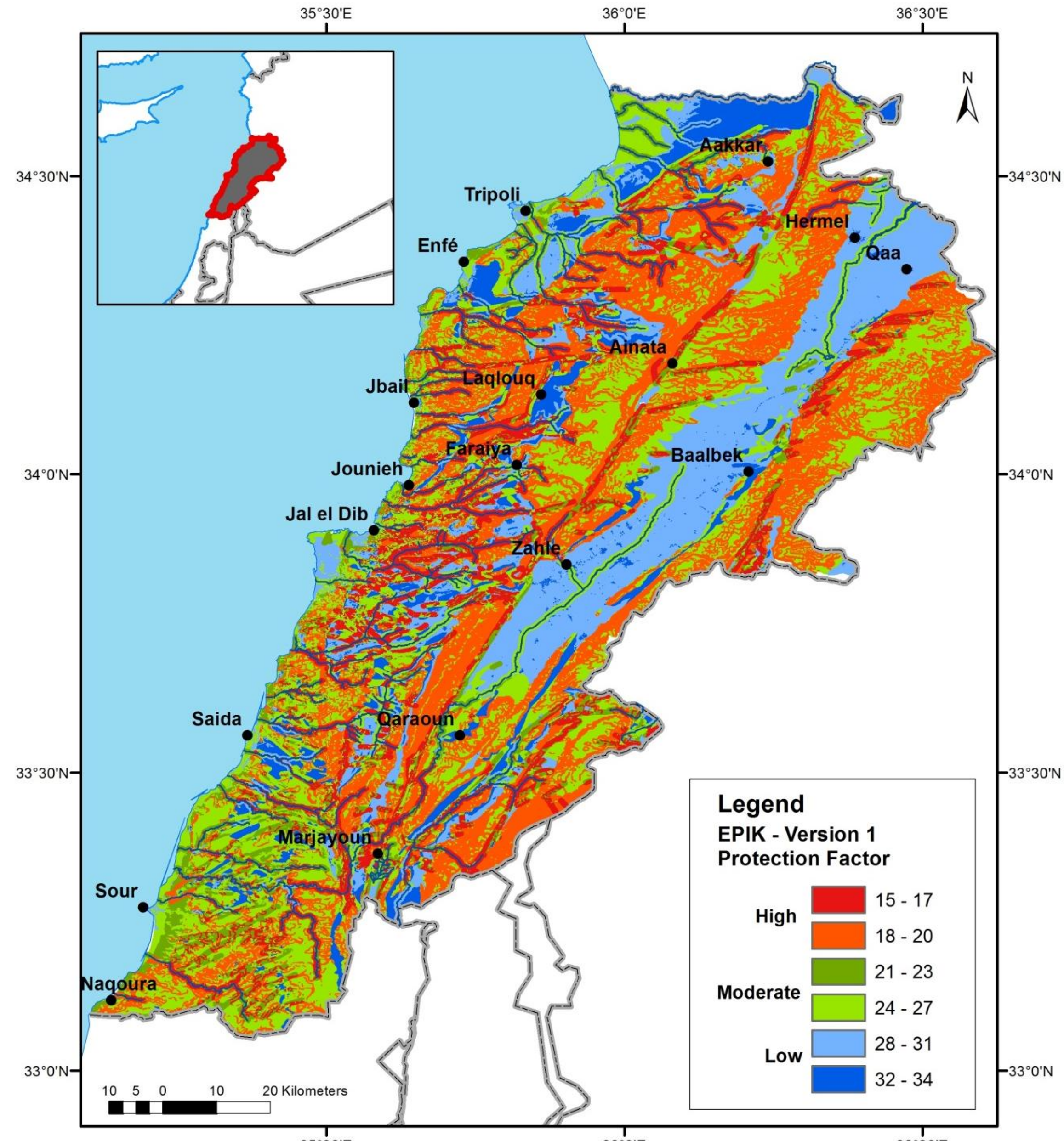

Figure 4-2: Map of showing the Groundwater Vulnerability of Lebanon based on EPIK Protection Factor as defined in Version 1

After conducting a visual analysis for this map, low vulnerability can be noted in the Bekaa valley similar to the DRASTIC results, the coastline is mainly moderate vulnerability, and the Mount Lebanon is not entirely highly vulnerable, in contrast to what the lithological characteristic would suggest (highly karstic). This method depicts the impact of faults and river channels at a finer resolution.

The second version (EPIK_V2) is where urbanization is not accounted for at all, and the vulnerability is taken according to the geological outcrops only (Figure 4-3). When validating the map visually, the variation between the first version and the second is shown in the Lebanese Western Mountain Chain and the Biqaa Valley and the difference varies between the two ranges of moderate and the two ranges of low vulnerability, with an overall increased vulnerability as compared to the first version (urbanization).

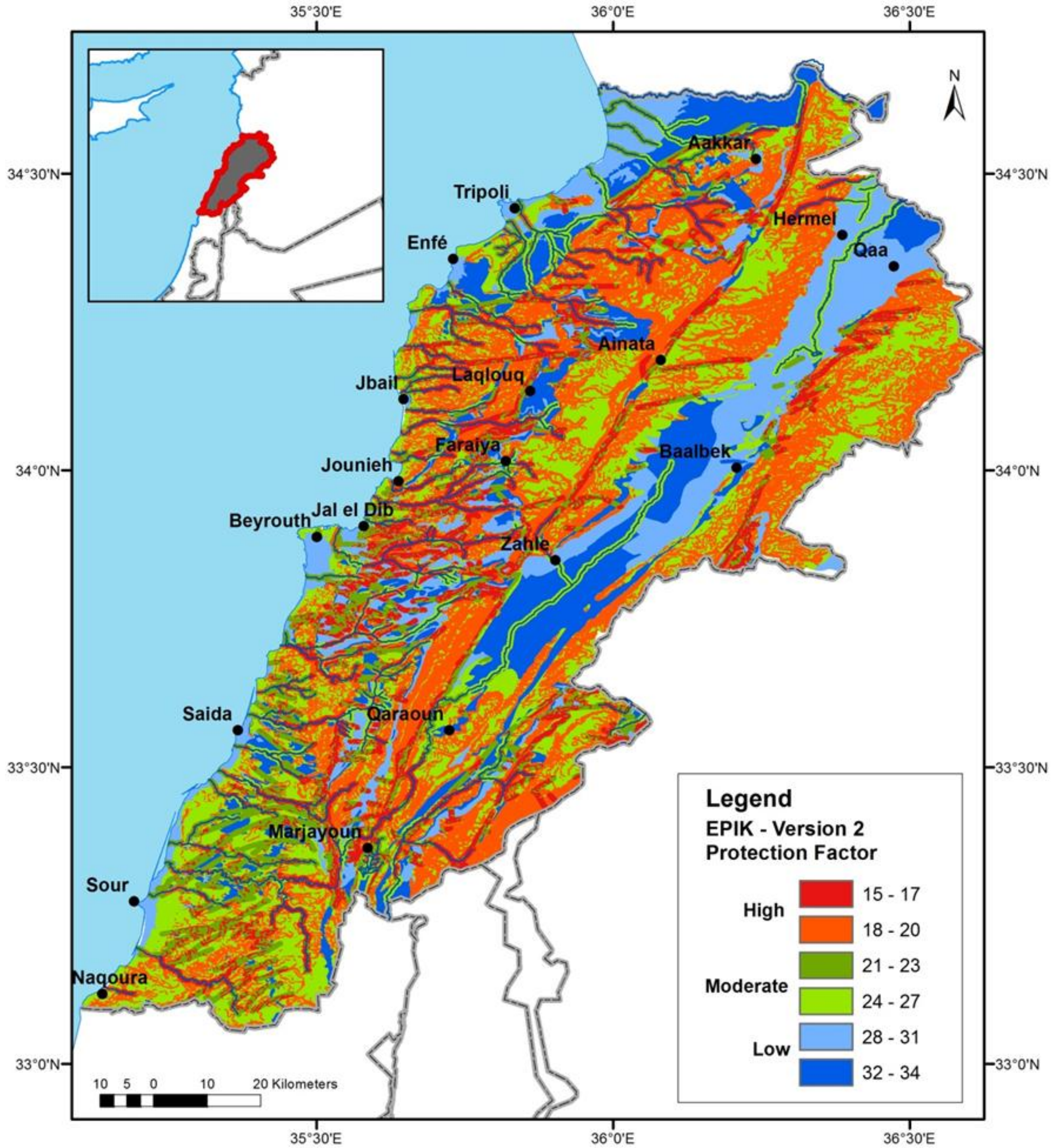

Figure 4-3: Map of showing the Groundwater Vulnerability of Lebanon based on EPIK Protection Factor as defined in Version 2

The third version of EPIK assigns higher vulnerability values to the coastal urban areas (EPIK_V3), to emphasize the anthropogenic impact of heavy extraction (Figure 4-4). Visual analysis of the map shows a noticeable increase along the coastal areas. This version is the most suitable for coastal Lebanon.

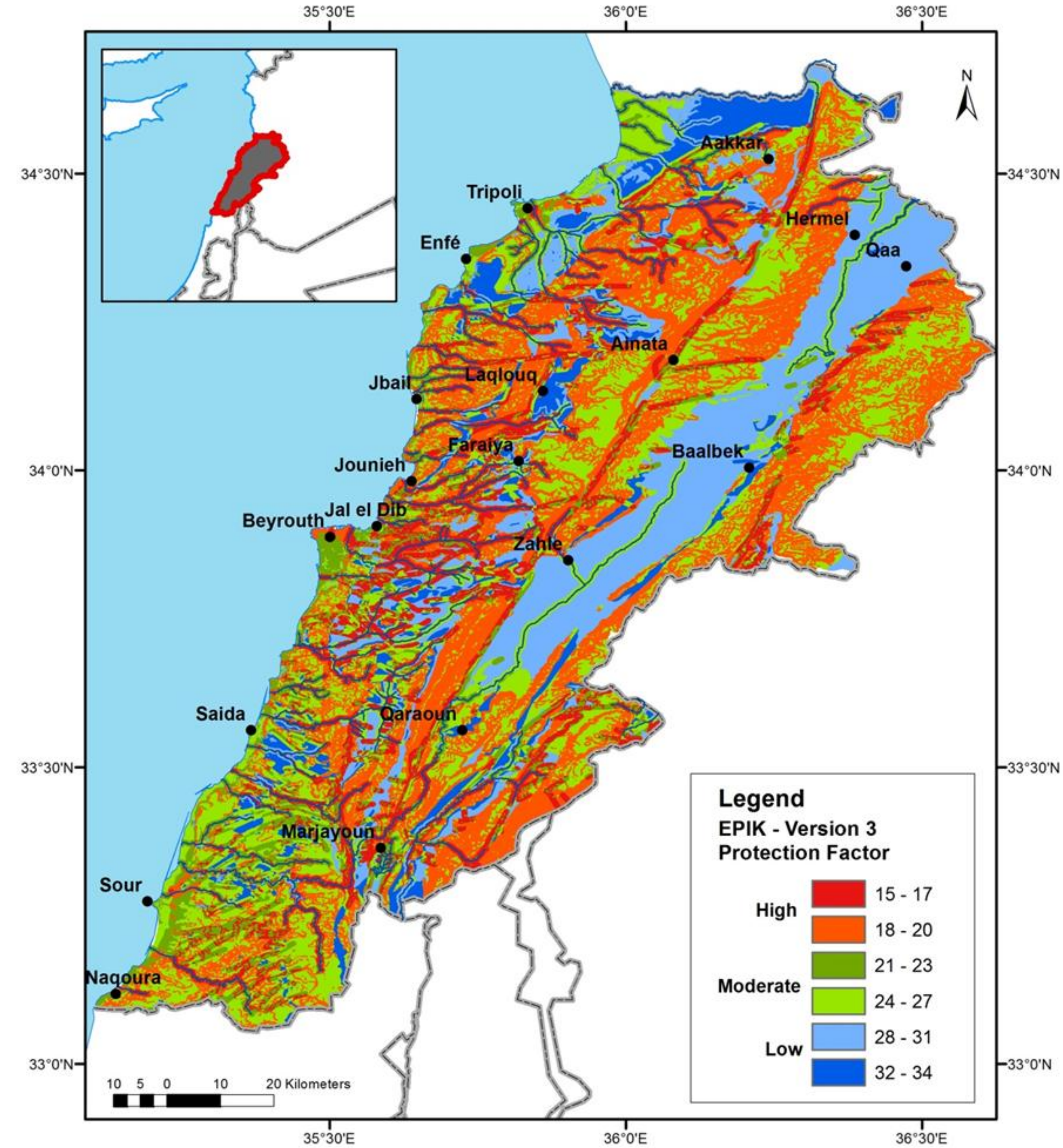

Figure 4-4: Map of showing the Groundwater Vulnerability of Lebanon based on EPIK Protection Factor as defined in Version 3

A comparison between the three versions of EPIK is shown in Figure 4-5.

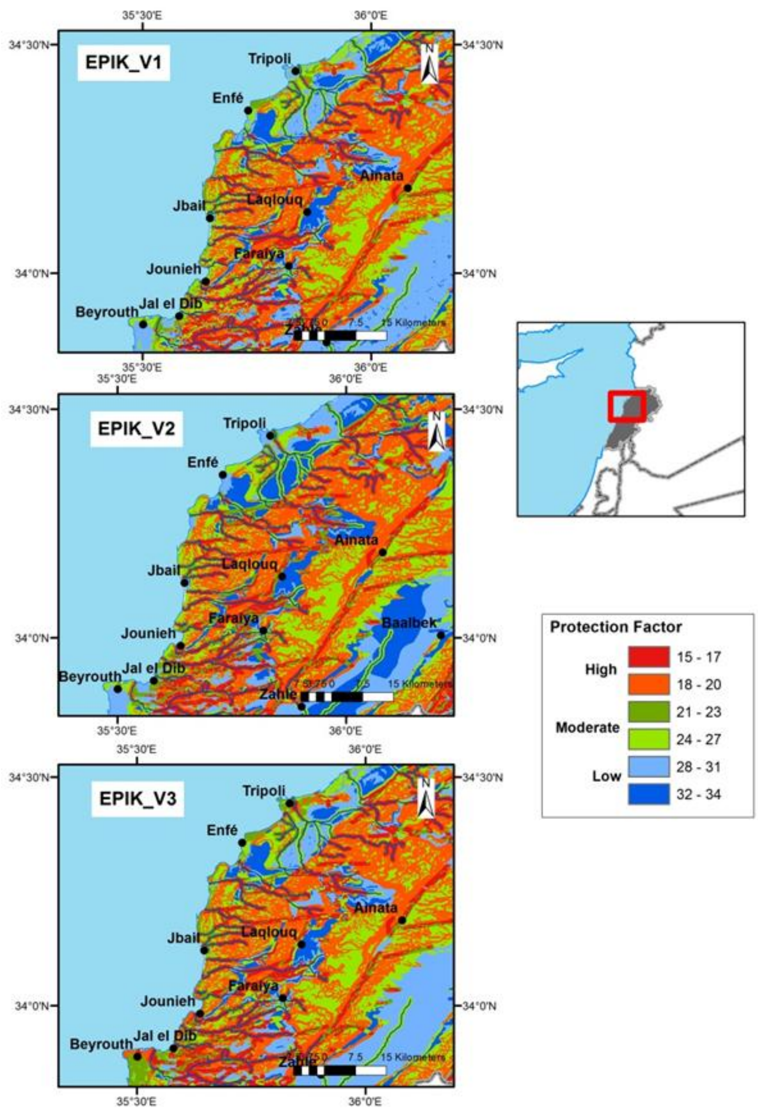

Figure 4-5: Comparing the three versions of EPIK

4.2.1 Water quality vs. PF values

Validation process similar to the one used in DRASTIC was used for the three versions of EPIK. Results for the city of Tripoli while using TDS vales collected in Round 2 are shown in Table 4-3). Similar tables across the three different model versions, cities, seasons, and water quality parameters are shown in section 5.3 – Annex 4.

Table 4-3: Field measured TDS (WQ_{Field}) and EPIK version 3 ranges for Round 2 Tripoli matching with EPIK Protection Factor (PF) ranges (WQ_{EPIK})

WQ_{Field} / WQ_{EPIK}	Drinking water 0-500	Fresh Water 500-1,000	Brackish 1,000-5,000	Highly Brackish 5,000-15,000	Saline Water 15,000-30,000	Sea Water 30,000-40,000
Drinking water 32-34						
Fresh Water 28-31	1					
Brackish 24-27	8	4				
Highly Brackish 21-23	25	10	7			
Saline Water 18-20	2					
Sea Water 15-17		1				
e.g. TRP_R2_EP3_TDS	Match	±1	±2	±3	±4/5	Total
Number of wells	0	12	18	25	5	60
Percent per category	0.0	20.0	30.0	41.7	8.3	100.0
Cumulative Percent	0	20	50	91.7	100	100.0

With EPIK version 1, it can be noted that the model performed well for Beirut and Jal el Dib but poorly for Tripoli (Table 4-4).

Table 4-4: Percent of match for the EPIK Version 1 methodology Validation (the highlighted blue are when the 50 percentile is crossed)

NAME	Match (%)	±1 (%)	±2 (%)	±3 (%)	±4/5 (%)	Total (%)
BEY_R1_EP1_Cl	20	66.1	82.5	92.7	100	100.0
BEY_R1_EP1_TDS	23.6	64.8	84.2	98.8	100	100.0
JD_R3_EP1_Cl	22.7	72.7	77.2	100	100	100.0
JD_R3_EP1_TDS	27.3	90.9	100	100	100	100.0
JD_R7_EP1_Cl	22.2	100	100	100	100	100.0
JD_R7_EP1_TDS	77.8	100	100	100	100	100.0
TRP_R1_EP1_Cl	16.7	30	91.7	100	100	100.0
TRP_R1_EP1_TDS	11.7	50	90	100	100	100.0
TRP_R2_EP1_Cl	8.3	25	90	100	100	100.0
TRP_R2_EP1_TDS	11.7	36.7	90	100	100	100.0

CITY		**VULNERABILITY ASSESSMENT (VA) METHOD**	
BEY	Beirut	DR	DRASTIC
JD	Jal el Dib	EP1	EPIK-Version 1 (urbanization low impact)
TRP	Tripoli	EP2	EPIK-Version 2 (no urbanization)

SAMPLING ROUND		EP3	EPIK-Version 3 (urban areas high vulnerability)
R1	Round 1- Early Summer - May/June	PARAMETERS	
R2	Round 2 - Late Summer – Sept./Oct.	Cl^-	Chloride Level (mg/L)
Rx	Other Rounds	TDS	Total Dissolved Solids (ppm)

When analyzing the extent of match for the second version of EPIK (no anthropogenic impact), it can be noticeable that the difference between the two version was minimal. This indicates that the geological outcrops on the coast are not highly vulnerable (Table 4-5).

Table 4-5: Percent of match for the EPIK Version 2 methodology Validation (the highlighted blue are when the 50 percentile is crossed)

NAME	Match (%)	±1 (%)	±2 (%)	±3 (%)	±4/5 (%)	Total (%)
BEY_EP2_Cl	22.4	66.6	83	93.9	100	100.0
BEY_EP2_TDS	24.2	67.2	86	98.7	100	100.0
JD_R3_EP2_Cl	22.7	72.7	77.2	100	100	100.0
JD_R3_EP2_TDS	27.3	90.9	100	100	100	100.0
JD_R7_EP2_Cl	22.2	100	100	100	100	100.0
JD_R7_EP2_TDS	77.8	100	100	100	100	100.0
TRP_R1_EP2_Cl	16.7	30	93.3	100	100	100.0
TRP_R1_EP2_TDS	11.7	50	91.7	100	100	100.0
TRP_R2_EP2_Cl	8.3	25	91.7	100	100	100.0
TRP_R2_EP2_TDS	11.7	36.7	91.7	100	100	100.0

The third version of EPIK, where urbanization causes larger impact and produces high vulnerability, had overall a poor fit as shown in Table 4-6. It was observed that when there is little or no anthropogenic activities, the studied setting is closer to its natural condition, which is what EPIK (or other vulnerability assessment methods) reflect best. Accordingly, whenever there is higher urbanization impact, and higher seawater intrusion, and thus higher diversion from the natural condition, there is poorer fit between the GVA models and water quality values.

Table 4-6: Percent of match for the EPIK Version 3 methodology Validation (the highlighted blue are when the 50 percentile is crossed)

NAME	Match (%)	±1 (%)	±2 (%)	±3 (%)	±4/5 (%)	Total (%)
BEY_R1_EP3_Cl	21.2	48.5	66.7	80.6	100	100.0
BEY_R1_EP3_TDS	10.9	37	67.3	82.5	100.1	100.0

JD_R3_EP3_Cl	18.2	72.7	77.2	100	100	100.0
JD_R3_EP3_TDS	4.5	27.2	90.8	100	100	100.0
JD_R7_EP3_Cl	40.7	81.4	100	100	100	100.0
JD_R7_EP3_TDS	11.1	77.8	100	100	100	100.0
TRP_R1_EP3_Cl	10	25	40	93.3	100	100.0
TRP_R1_EP3_TDS	0	26.7	55	91.7	100	100.0
TRP_R2_EP3_Cl	13.3	21.6	41.6	93.3	100	100.0
TRP_R2_EP3_TDS	0	20	50	91.7	100	100.0

4.3 EPIK v/s DRASTIC

A comparison between the second version of EPIK (geological outcrops) and the DRASTIC model results indicate that the main differences are in the ability of EPIK to account for local details such as fault lines, river channels, and high slope topographies (Figure 4-6).

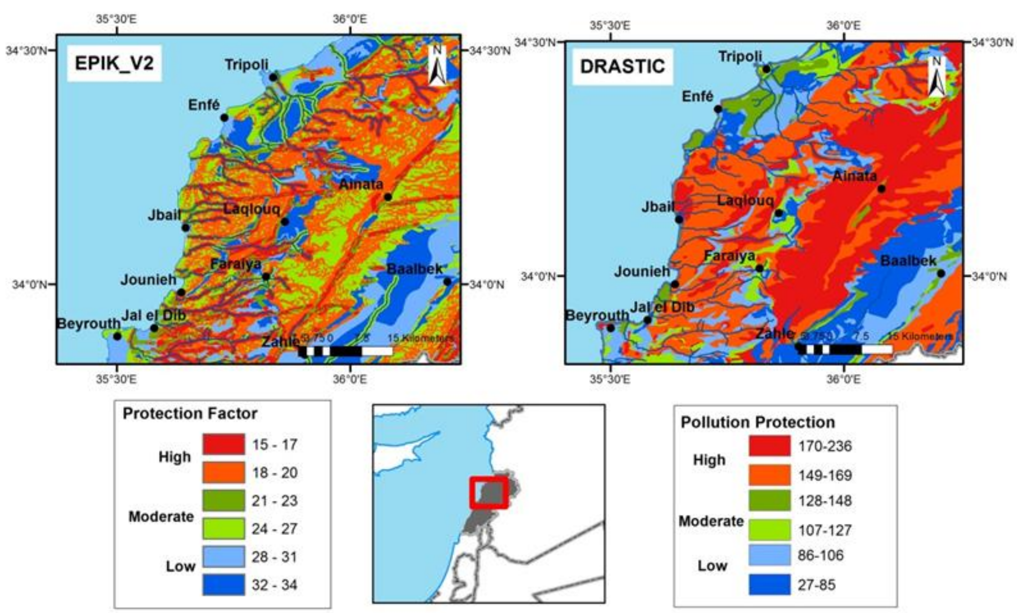

Figure 4-6: Comparison between EPIK and DRASTIC

Regarding the water quality classes and cross-validation, in general EPIK_V3 performed the worse, and the other two versions of EPIK (EPIK_V1 and EPIK_V2) performed relatively better than DRASTIC (Table 4-2, Table 4-4, Table 4-5, Table 4-6). Nevertheless, both of these methodologies use physical characteristics and focus on vertically introduced contaminants, whereas the high salinity in the water samples analyzed are indicative of horizontally introduced contaminants, which is the seawater in this case.

5 Concluding remarks

This study evaluated the vulnerability of groundwater resource in a karstic environment under both geological parameters and local anthropogenic impact. The commonly used vulnerability assessment models DRASTIC and EPIK, were run independently on the specific characteristics of the introduced contamination and the anthropogenic impact. These models were selected based on a comprehensive literature analysis and comparison of existing vulnerability assessment methodologies taking into consideration the karstification. These methods were compared at the national level and then cross-validated with measurements collected from three different coastal cities.

The results of the comparison demonstrated first the coarse resolution of the two models. Secondly, the models exhibited poor correlation in quality standards (between GVA values and the water quality standards) when anthropogenic factors dominated an area, highlighting their weakness especially in the context of seawater intrusion which is greatly induced by anthropogenic activities.

Future work should be oriented on improving the resolution of the chosen models. Other models such as COP+K can provide a different aspect on the vulnerability status of the groundwater. Moreover, for improved results continuous groundwater level monitoring is needed (Murgulet & Tick, 2007). Accurate knowledge of tapped aquifer and other subsurface lithological information is also essential.

With these vulnerability maps, highly vulnerable areas are delineated, thus setting management or legal guideline to control further exploitation.

CHAPTER II

WATER QUALITY IN KARSTIC AQUIFERS UNDER URBANIZATION STRESS: A METHODOLOGICAL ASSESSMENT

ABSTRACT

Decision makers are increasingly relying on maps that ate generated from limited monitoring locations through the use of geospatial models. These tools are often applied without proper knowledge of the underlying assumptions. This study examines the accuracy of commonly used interpolation schemes using field measurements collected during groundwater sampling campaigns in three coastal cities along the eastern Mediterranean. Different interpolation methods and semi-variogram models were compared using multiple water quality criteria. The performance and accuracy of interpolation methods was scrutinized by conducting a leave-one-out analysis. The results showed that Kriging and Co-Kriging produced relatively good model fits. Inverse Distance Weighting (IDW) results were in general poor, except when the comparison was based on a six water quality categories classification. Nevertheless, all GIS-based interpolation methods exhibited better performance as compared to the output of the groundwater vulnerability assessment models DRASTIC and EPIK.

Keywords: Interpolation, Kriging, Co-Kriging, IDW, Semivariogram models, Water Quality

1 Introduction

The overexploitation of groundwater resources in urban coastal areas has grown into a global problem manifested in the acceleration of saltwater intrusion inland (Fetter, 2001). The issue is expected to get accentuated with population growth, increased water demand, and the projected climate change impacts (Chang, 2010; Elewa, et al., 2013; Howard, 2002; Loáiciga, et al., 2012; Ranjan, et al., 2006; Vorosmarty, et al., 2000; Werner, et al., 2012). Seawater intrusion is particularly more accentuated in developing countries where mitigation strategies, regulatory enforcement and institutional capacities are generally weak. The extent and impact of saltwater intrusion varies spatially depending on several factors that can be categorized into three major types: the contaminants, the aquifer media, and the urbanization (anthropogenic) activities.

With the increase in the use of Geographic Information System (GIS), interpolated and user-friendly maps are generated from point data to help decision makers take informed decisions (Focazio, et al., 2002). In general, groundwater quality assessment methods rely on statistical models to interpolate the specific characteristics of groundwater (or the contaminant in groundwater) at monitored points. The assumptions that accompany these approaches depend on the interpolation method, which typically assumes homogeneity and isotropy. Examples for case studies in the literature with the mostly used interpolation methods and semivariogram models are shown in Table 1-1. Yet, many of these statistical analysis tools are used without proper knowledge of the underlying model assumptions thus producing large amounts of non-validated or unreliable data (Focazio, et al., 2002). Conducting groundwater quality assessment using spatial interpolation typically requires four steps summarized in Figure 1-1 (Arslan, 2012; Cooper & Istok, 1988; Sajil Kumar et al., 2011).

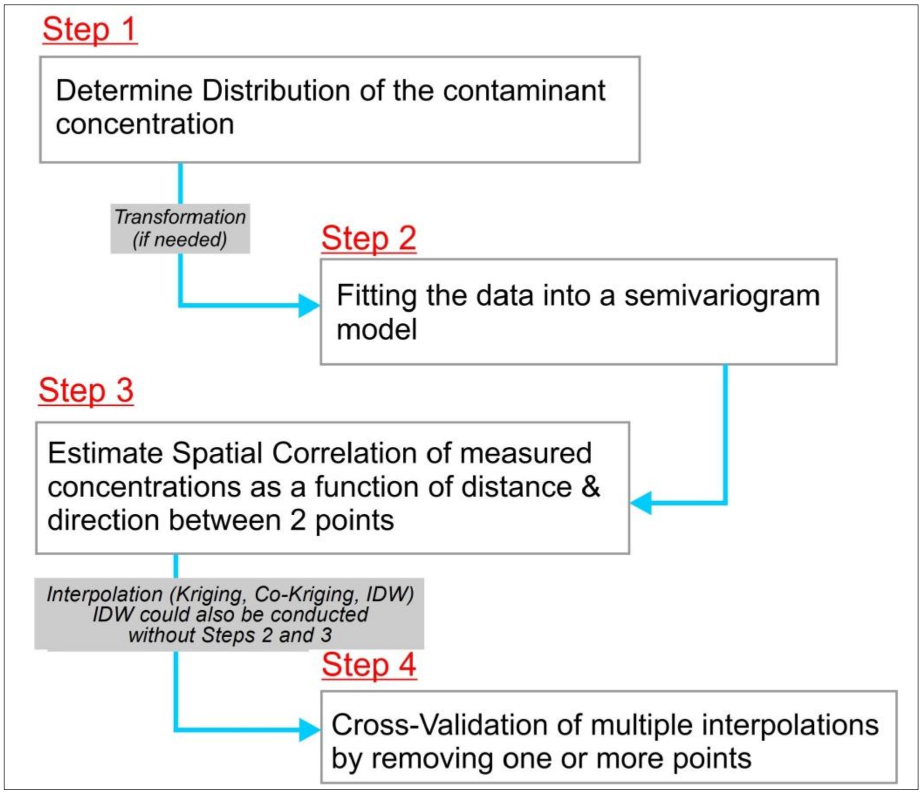

Figure 1-1: Steps to follow when conducting a spatial groundwater quality assessment

Earlier forms of interpolation software required high-level programming skills for the 3 first steps of spatial analysis, and if cross validation was needed (Step 4), often a separate software was required (Cooper & Istok, 1988). However, with the development of GIS software, spatial analysis became user-friendly.

Conducting a saltwater intrusion groundwater quality interpolation assumes the following: (Moujabber et al., 2006; Ozler, 2003; Panteleit et al., 2010; Pulido-Leboeuf et al., 2003; Sheikhy Narany et al., 2014; Vengosh & Rosenthal, 1994):

- Data is stationary and normally distributed[5]
- Water-rock interaction is neglected
- Dissolution of salt pockets is not important
- Discarding other natural salinity sources leading to saline groundwater not from the sea (common in arid and semi-arid regions)
- Discarding chemical reactions such as dolomitization and salinization (cation exchange)

This study examines the accuracy of commonly used interpolation schemes by cross-validation with field measurements collected at three coastal cities along the eastern Mediterranean, in Lebanon. Groundwater quality assessment results using interpolation methods are then compared with groundwater vulnerability assessment results from DRASTIC and EPIK models, highlighting differences and similarities between the two approaches.

[5] Although the Geostatistics Tool do not require to have the input data normally distributed, the results will not be optimal (ESRI, 2008).

Table 1-1: Some of the references reviewed in this study that used interpolation models in various study areas (N/A: not applicatble and (-) means not found), WL: water Level)

Reference	Modify (Y/N)	Validation (Y/N)	Interpolation-model	WQ parameters	# sample points	Area	Notes
Ahmadian, 2013	N	Y	OK[a], SK[b], UK[c], DK[d], co-K[e]	TDS, EC, NO_3^-, Na^+	70-90wells	4410 km^2	Tehran-Karaj Plain
Arslan, 2012	N	Y	OK, IK[f]- EX[g], SP[h], Rational	EC	97 wells	10350 ha 103.5km^2	Semivariogram models varied by year OK: analysis og spatial variability of GW salinity IK: analysis of GW salinity with respect to pollution thresholdss Bafra Plain in Samsun province, Turkey
Bajjali, 2005	N	N	GPI[i]; IDW[j]; TSA[k]; K[l]	TDS	2429 wells	189.49km^2; 16.80km^2; 45.86km^2	3 different basins/watersheds (Ma'awil, Samail, Sahanawat) in Oman
Cooper & Istok, 1988	N	N	TFORTRAN subroutine VARIO	N/A	N/A	N/A	Geostatistical program coded by the authors to compute the semivariogram. Point kriging: SS2DGRID in STATPAC The cross-validation:by the SS2DXVAL program in STATPAC[m]
Delbari et al., 2013	N	Y	K-SP, G[n]	EC, TDS, Na^+, SAR[o]	172 well	122608 km^2	Using GS+ to analyse the most suitable semivariogram EC, TDS, Na+ - SP & SAR - G To produce zonations of potable water standards Fars province
Elewa, et al., 2013	N	Y	K (Spatial analyst tool)	TDS, SAR, Cl/HCO_3, K^+, water types	46 wells	7593 km^2	The model is validated with GW quality data and Piper trilinear diagram Northeastern part of Nile Delta
Kura et al., 2014	N	Y	IDW	HNO_3^-, pH, DO[p], EC, WL, Temperature, Cl^-, HCO_3^-, SO_4^{2-}, Ca^{2+}, Mg^{2+}, Na^+, K^+	11 wells 22 samples	2 km^2	Geochemical and geostatistical analysis to verify geophysical (resistivity) profiles. Kapas Island
Murgulet & Tick, 2007	N	Y	K	EC, Cl^-, TDS	200 wells (400 samples)	4130 km^2	Validation of geostatistical method using *Surfer* Baldwin County in Alabama
Nas & Berktay, 2010	N	Y	OK (12 semivariogram models[q])	pH, EC, Cl^-, SO_4^{2-}, NO_3^-, hardness	177 wells	38,183 km^2	pH: normal distribution EC, Cl, SO_4, Hardness, NO_3: log transformation Konya province in Turkey
Saadeh, 2008	N	N	OK	pH, EC, TDS, Na^+, Ca^{2+}, NO_3^-, PO_4^{3-}, SO_4^{2-}, Br^-, Mg^{2+}, Alkalinity, Hardness, F^-	70	130 km^2	Coast of Greater Beirut Area
Sajil Kumar, et al., 2011	N	Y	K-SP	Ca^{2+}, TDS, hardness EC,	62 well	-	K-SP: Ca, TDS, hardness EC

Reference	Modify (Y/N)	Validation (Y/N)	Interpolation-model	WQ parameters	# sample points	Area	Notes
			K-EX-Log[r]	Mg^{2+}, K^{+}			K-EX-Log: Mg, K Palar River basin in Tamil Nadu state
Sajil Kumar et al., 2013	N	N	K-SP	EC, pH, Cl-, HCO_3^-, Ca^{2+}, Mg^{2+}, Na^{+}, K^{+}, SO_4^{2+}, hardness, SAR, Na %	25 wells	-	Used as a complimentary method for WQI method South Chennai, India
Selmi, 2013	N	Y	OK	WL, NO_3^-, Cl-	95 wells	365 km^2	Checked using ESDA[s] first than used ordinary kriging Gaza Strip
Sheikhy Narany, et al., 2014	N	N	OK-EX	Ratios; PCA[t]; DA[u]; CA[v]	153 wells 306 samples	1822 km^2	Multivariate statistical analyses were applied Amol-Babol Plain, Iran
Voudouris et al., 2004	N	Y	OK-SP Alluvial OK-EX: Karst	TDS, R[w], I[x]	61 samples: Alluvial aquifer 12 samples: Karst	Alluvial 25 km^2 LS:-	Using Surfer The Glafkos plain alluvial aquifer is located in the Southwestern part of Greece LS aquifer in the northern central part of Crete Island
Mutua & Kuria, 2012	N	N	IDW, GPI, K, Co-K	Rainfall	25 rainfall stations	3500 km^2	Comparison of different interpolation methods In K-G, and SP Models resulted with the same RMSE, so K-G was chosen Co-K (with DEM) resulted with the lowest RMSE values Nyando River Basin, Kenya

a Ordinary Kriging interpolation method
b Simple Kriging interpolation method
c Universal Kriging interpolation method
d Disjunctive Kriging interpolation method
e Co-Kriging interpolation method
f Indicator Kriging Interpolation method
g Exponential semivariogram model
h Spherical semivariogram model
i Global Polynomial interpolation method
j Inverse Distance weight interpolation method
k Trend Surface analysis interpolation method
l Kriging
m STATPAC: a statistical analysis computer
n Gaussian semivariogram model
o Sodium Adsorption Ratio
p Dissolved Oxygen
q Circular, Spherical, Tetraspherical, Pentaspherical, Exponential, Gaussian, Rational Quadratic, Hole effect, K-Bessel, J-Bessel, Stable
r Logarithmic transformation of the data
s Exploratory Spatial Data Analysis
t Pearson Correlation Analysis
u Discriminant Analysis
v Cluster Analysis
w Revelle index
x Ionic strength

2 Material and Methods

2.1 Geospatial Analysis of Groundwater Quality

In this study, the ArcGIS Geostatistical tool was used to conduct the water quality assessment steps (Figure 1-1). Every dataset was first checked for its distribution type and whether it needed any transformation. Then Inverse Distance Weight (IDW), Kriging, and Co-Kriging interpolation schemes were adopted. For the Kriging and Co-Kriging, the Spherical, Exponential, and Gaussian models were tested as they are the most commonly used (Arslan, 2012; Delbari, et al., 2013; Nas & Berktay, 2010; Sajil Kumar, et al., 2013; Sajil Kumar, et al., 2011; Sheikhy Narany, et al., 2014; Smith, 2014; Voudouris, et al., 2004). Moreover, Co-Kriging involved trying to use correlations between the water quality data and the distance from shoreline, hydraulic conductivity of the tapped aquifer, and the well depth to improve fit. The summary of the work flow for this study is shown in Figure 2-1.

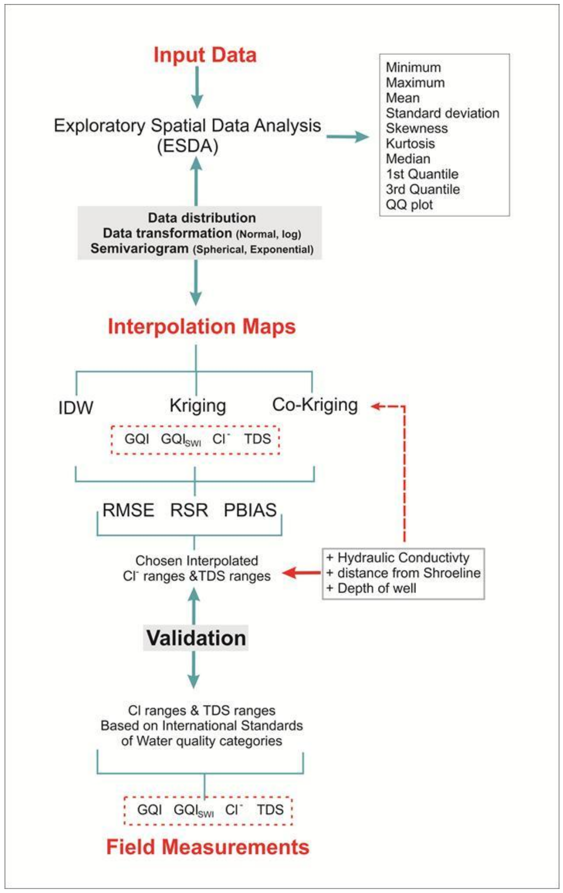

Figure 2-1: Diagram showing the work flow for this study

According to the reviewed literature, it is stated that the error difference between using different semivariogram models (with one interpolation method), and using two different interpolations methods (with one semivariogram model) using cross-validation methods. Results showed that the error difference between two different semivariogram models is less than the error difference between two interpolation methods (Ahmadian, 2013; Arslan, 2012; Delbari, et al., 2013; Smith, 2014).

In effort to compare results between models, model results were cross-validated by the "Leave-one-out" technique which produces several statistical indicators; such as Root mean square error (RMSE); Ratio of standard deviation and RMSE (RSR), and percent bias (PBIAS) among others (for more details about these techniques refer to section 5.55.5 – Annex 5).

1. RSR is the ratio of RMSE to the observations standard deviation. The lower the value, the more accurate the prediction (interpolation);
2. Coefficient of variation (CV) is the Root Mean Square value divided by the average of the measured data. The lower the value the better the performance of the model or the interpolation;
3. PBIAS is the percent BIAS and has an optimal value of 0. Positive values indicate the model's tendency to underestimate, and negative values indicate that the model has a tendency to overestimate;
4. RMS-Standardized (RMS-S) is the Root Mean square standardized by (divided by) the standard Error. The root mean square standardized error should be close to 1 if the prediction standard errors are valid. A value greater than 1 indicates underestimation of the variability in predictions whereas a value less than 1 indicates overestimation of variability in predictions.

2.2 Contaminants

Groundwater quality assessment was conducted by interpolation with a single-contaminant indicators representative of seawater intrusion, namely chlorides (Cl^-) and total dissolved solids (TDS) (Selmi, 2013; Abdul Basit S., 1971; Elewa, et al., 2013; Khayat, 2001; Moujabber, et al., 2006; Voudouris, et al., 2004) and with multi-contaminant indicators, namely the Groundwater Quality Index (GQI) developed by Babiker et al. (2006) and the GQI_{SWI}, developed by

Tomaszkiewicz et al. (2013). Previous work showed that interpolation of multiple-contaminant indicators produces less error than single-contaminant (Babiker, et al., 2006; Tomaszkiewicz, et al., 2014). Details about the two chosen multi-contaminant methods, GQI and GQI_{SWI}, are presented in section 5.6 – Annex 6[6].

2.3 Study area characteristics

This study was implemented in Lebanon at three pilot study areas along the eastern Mediterranean coast between Beirut and Tripoli overlying a semi-karstic aquifer (Figure 2-2). The area is characterized by a semi-arid climate with mild wet winters and moderately hot dry summers. With a predominantly residential and commercial land use, the area has a high population density and high density of drilled wells.

[6] Also for more explanation on Semivariogram Models and Interpolation Methods refer to sections 5.7 – Annex 7 and section 5.8 – Annex 8

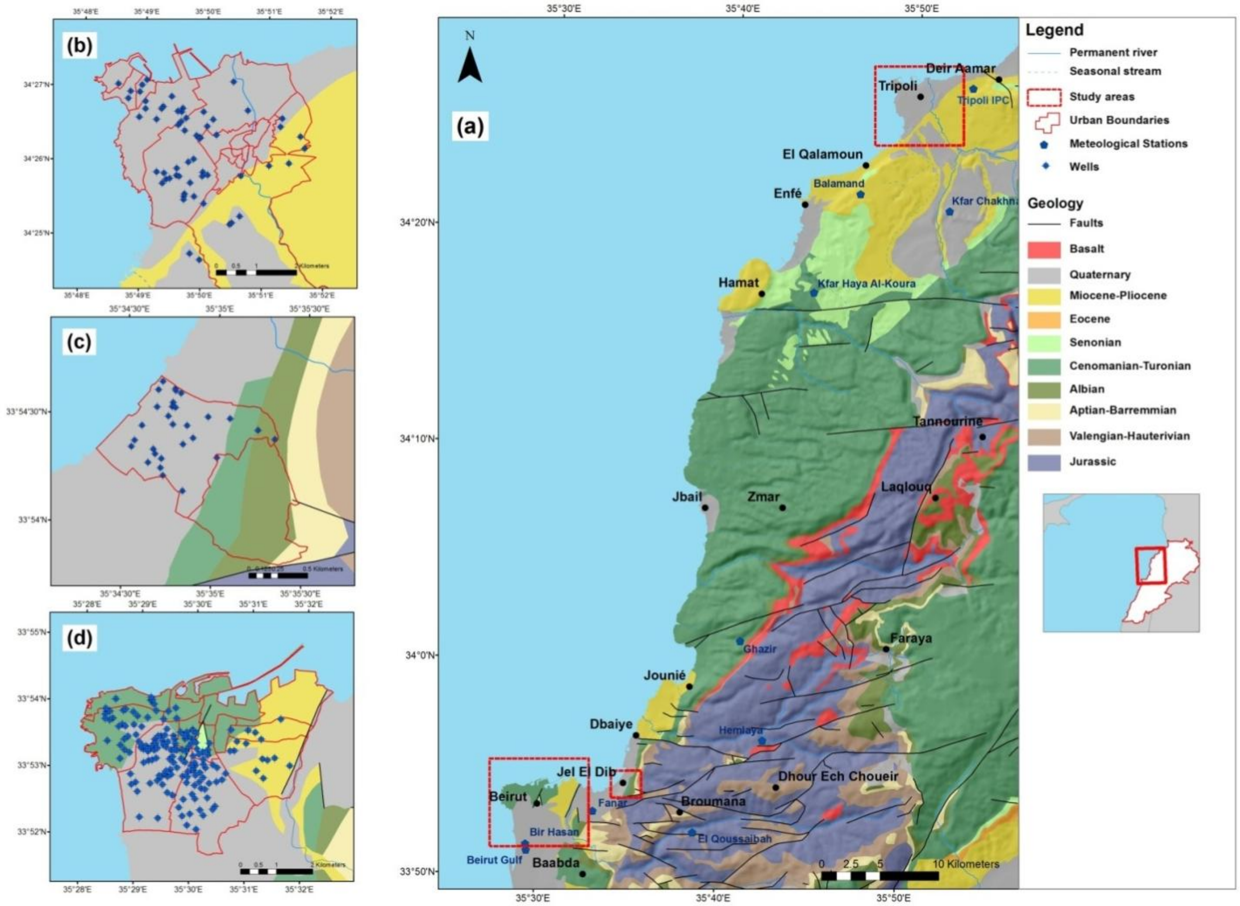

Figure 2-2: (a) Geological formations of the Northern Coast of Lebanon with the focus study areas and the wells' locations for the three areas of study (b) Tripoli (c) Jal el Dib (d) Beirut

2.4 Field sampling program

Groundwater sampling campaigns were conducted in these three cities (Figure 2-2) as part of a larger Seawater intrusion project over the Mediterranean coast. The first zone is Jal el Dib, where 6 groundwater sampling campaigns were conducted every two months starting October 2012 until October 2013 from 28 ±1 privately owned wells. The second zone is Beirut, where one sampling campaign was conducted in May/June 2013 from around 165 privately owned wells (Mutasem El-Fadel, et al., 2014). The third zone is Tripoli, where the two sampling campaigns were conducted in June 2007 and in September 2006 from 60 privately owned wells (M. El-Fadel, et al., 2014). The locations of the sampled wells are shown in Figure 2-2 b, c and d, for Tripoli, Jal el dib, and Beirut respectively. At each sampling point, the water system was checked to ensure that the water sample can be obtained directly from the well to limit potential cross-contamination from the existing public water supply system. The collected samples were transported on ice to the Environmental Engineering Research Center at the American University of Beirut and analyzed for various physical and biochemical indicators in accordance with *Standard Methods for the Examination of Water and Wastewater* (APHA, 1998).

3 Results and Discussion

The leave-one-out cross validation method was implemented to assess the adequacy of the interpolation techniques in the three cities across the four water quality metrics (for all the scenarios that were used for this study refer to section 5.9 – Annex 9). The four statistical indicators (RSR, RMS-S, PBIAS, CV) in addition to the average and the standard deviation estimates were calculated and used to compare between the different spatial interpolation methods (for all the results that were calculated for the analyzed scenarios refer to section 5.10 – Annex 10).

Tripoli

In Tripoli, Co-Kriging - of Chloride and TDS with distance of well from shoreline and transmissivity of the tapped aquifer - performed poorer than IDW across the four statistical indicators (Table 3-1, Table 3-2, Table 5-59). Yet, both methods were inferior to the results generated by the kriging model. The kriging results did not show any noticible difference between the spherical and exponential semivariogram models, nor with the different water quality parameters (Cl^- and TDS). Error maps showed no significant spatial information (Figure 3-1).

Table 3-1: The 8 chosen scenarios for City of Tripoli Round 1
(Blue highlighted cells are the statistical indicators that indicate most accurate interpolation)
(The red box is the chosen interpolation to show the error map)

Code	Statistical Indicators					
	Avg.	σ	RSR	CV	PBIAS	RMS-S
TRP_R1_Kr_E_L_Cl	216.6	249.8	0.88	1.02	-434.64	1.03
TRP_R1_Kr_E_L_TDS	639.2	528.94	0.70	0.58	-86.27	1.03
TRP_R1_IDW_Cl	216.6	249.8	0.88	1.02	-494.18	-
TRP_R1_IDW_TDS	639.2	528.94	0.76	0.63	-353.54	-
TRP_R1_CK_S_LNN_Cl_K	216.6	249.8	0.80	0.92	-605.56	3.42
TRP_R1_CK_S_LLN_Cl_K	216.6	249.8	0.80	0.92	-605.56	3.42
TRP_R1_CK_E_LNN_Cl_K	216.6	249.8	0.80	0.92	931.92	2.77
TRP_R1_CK_E_LLN_Cl_K	216.6	249.8	0.80	0.92	-589.80	2.76

CITY		PARAMETERS	
BEY	Beirut	Cl	Chloride Level (mg/L)
JD	Jal el Dib	TDS	Total Dissolved Solids (ppm)
TRP	Tripoli	GQI	Groundwater Quality Assessment
SAMPLING ROUND		GQI_{SWI}	Groundwater Quality Assessment for Seawater intrusion
R1	Round 1- Early Summer - May/June	K	Hydraulic Conductivity

R2	Round 2 - Late Summer – Sept./Oct.	TRANFORMATION	
Rx	Other Rounds	N	Normal
INTERPOLATION		L	Log
Kr	Kriging	SEMI VARIOGRAM MODEL	
IDW	Inverse Distance Weight	S	Spherical
CK	Co-Kriging	E	Exponential

Table 3-2: The 8 chosen scenarios for City of Tripoli Round 2
(Blue highlighted cells are the statistical indicators that indicate most accurate interpolation)
(The red box is the chosen interpolation to show the error map)

Code	Statistical Indicators					
	Avg.	σ	RSR	CV	PBIAS	RMS-S
TRP_R2_Kr_E_L_Cl	224.6	357.8	0.93	1.48	-348.22	1.51
TRP_R2_Kr_E_L_TDS	639.2	528.9	0.90	0.80	-177.99	1.26
TRP_R2_IDW_TDS	639.2	528.9	0.97	0.86	-440.05	-
TRP_R2_IDW_Cl	224.6	357.8	1.00	1.59	-571.71	-
TRP_R2_CK_S_LNN_Cl_K	224.6	357.8	0.95	1.51	-1,512.12	7.75
TRP_R2_CK_S_LLN_Cl_K	224.6	357.8	0.95	1.51	-1,512.12	7.75
TRP_R2_CK_E_LNN_Cl_K	224.6	357.8	0.95	1.51	-1,491.03	7.75
TRP_R2_CK_E_LLN_Cl_K	224.6	357.8	0.93	1.48	-1,491.03	6.00

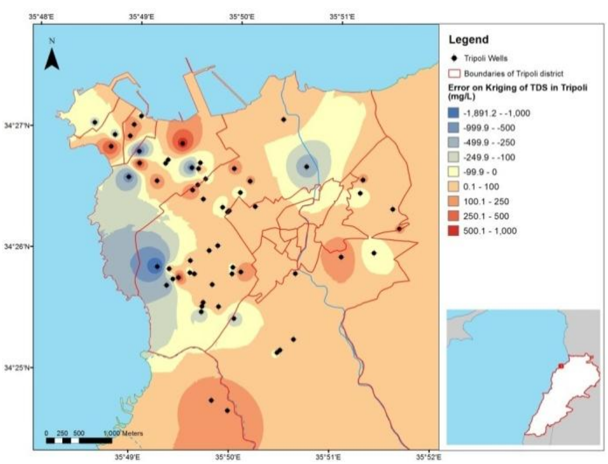

Error map in Tripoli round 1 sampling, for Kriging with Exponential semivariogram, Log transformed with TDS

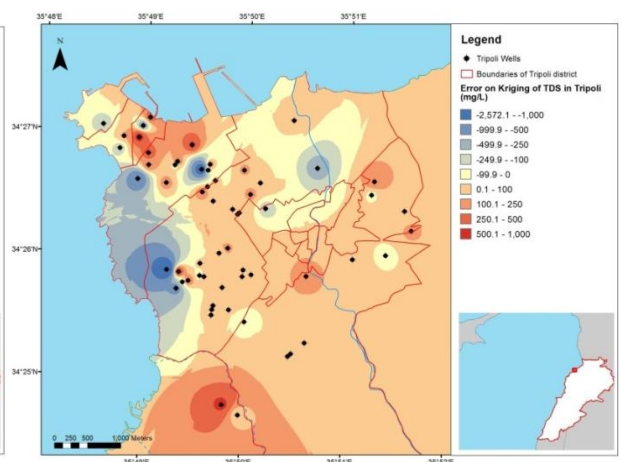

Error map in Tripoli round 2 sampling, for Kriging with Exponential semivariogram, Log transformed with TDS

Figure 3-1: Examples of error maps of Tripoli

Beirut

Based on RSR readings, Table 3-3 presents the results of the best 8 scenarios for the city of Beirut (May-June 2013). Surprisingly, IDW showed better fits compared to both kriging and co-kriging. This finding is atypical in the literature (Mutua & Kuria, 2012; Ziary & Safari, 2007). Furthermore, the spherical semivariogram models performed better than the exponential models for both kriging and co-kriging methods (Table 3-3, Table 5-58). As for the error distribution, no clear spatial trends were observed as shown in the error distribution map for Chlorides generated for IDW (Figure 3-2).

Table 3-3: The 8 chosen scenarios for City of Beirut Round 1
(the highlighted blue cells are the statistical indicators that indicate most accurate interpolation)
(The red box is the chosen interpolation to show the error map)

Code	Statistical Indicators					
	Avg.	σ	RSR	CV	PBIAS	RMS-S
BEY_R1_Kr_S_L_Cl	1,898.2	2,828.3	0.94	1.39	-256.87	1.88
BEY_R1_Kr_S_L_TDS	4,061.9	5,102.7	0.89	1.11	75.45	1.69
BEY_R1_IDW_Cl	1,898.2	2,828.3	0.98	1.46	48.84	-
BEY_R1_IDW_TDS	4,061.9	5,102.7	0.94	1.18	-97.76	-
BEY_R1_CK_S_LLL_Cl	1,898.2	2,828.3	0.95	1.41	-161.47	2.04
BEY_R1_CK_E_LLL_Cl	1,898.2	2,828.3	0.92	1.38	-34.24	1.93
BEY_R1_CK_S_LLL_Cl_K	1,898.2	2,828.3	0.93	1.39	685.17	1.55
BEY_R1_CK_E_LLL_Cl_K	1,898.2	2,828.3	0.96	1.43	-234.93	2.16
BEY_R1_CK_S_LLL_Cl_EPIK	1,898.2	2,828.3	0.91	1.36	1,004.99	1.4

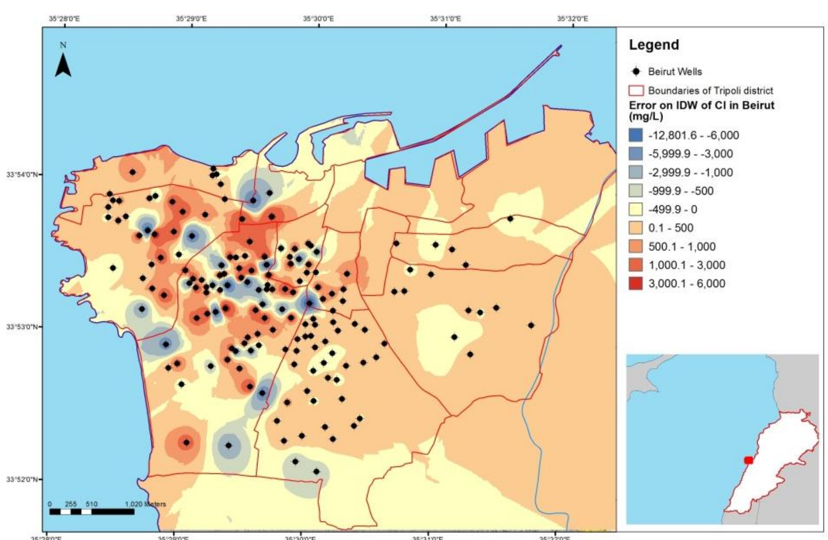

Figure 3-2: Example of Error map in Beirut round 1 sampling, for IDW with Cl^-

Jal el Dib

For Jal el Dib, the round of January and October (2013) were chosen for testing the interpolation scenarios. Most of the best performing scenarios based on the RSR values were generated by Co-Kriging the Chloride or GQI_{SWI} values as primary parameter and distance from shoreline, Hydraulic conductivity, or depth to well as secondary indicators. This favorable performance of Co-Kriging (in comparison to IDW and kriging) is in agreement with work from the literature (Ahmadian 2013; Arslan 2012; Mutua & Kuria, 2012; Ziary & Safari, 2007). In the January round, GQI performed better than other parameters (Cl^-, TDS, GQI_{SWI}) when using Kriging. In Co-Kriging, GQI_{SWI} improved the PBIAS and the CV results in both rounds, but not the RSR and the RMS-S values. When conducting error distribution maps for Jal el Dib with two examples (highlighted in red in the tables above), no significant spatial distribution for the error could be noticed (Figure 3-3).

Table 3-4: The 14 chosen scenarios for Jal el Dib Round 3
(Blue highlighted cells are the statistical indicators that indicate most accurate interpolation)
(The red box is the chosen interpolation to show the error map)

Code	Statistical Indicators					
	Avg.	σ	RSR	CV	PBIAS	RMS-S
JD_R3_Kr_E_N_Cl	388.8	182.7	1.01	0.47	69.41	1.00
JD_R3_Kr_E_L_TDS	1,090.0	825.5	0.88	0.66	-58.04	1.51
JD_R3_Kr_E_N_GQI	83.1	3.2	0.94	0.04	-2.70	1.00
JD_R3_Kr_S_N_GQISWI	58.2	10.7	0.89	0.18	-29.93	1.01
JD_R3_IDW_Cl	388.8	182.7	1.23	0.57	80.53	-
JD_R3_IDW_TDS	1,090.0	825.5	0.94	0.71	147.93	-
JD_R3_CK_S_NNN_Cl	388.8	182.7	0.99	0.46	52.91	0.88
JD_R3_CK_E_NLL_Cl	388.8	182.7	1.01	0.48	70.71	1.01
JD_R3_CK_S_NLN_Cl_K	388.8	182.7	0.98	0.46	59.54	0.88
JD_R3_CK_E_NLN_Cl_K	388.8	182.7	1.00	0.47	54.68	0.88

JD_R3_CK_S_NNL_GQISWI	58.2	10.7	1.03	0.19	-53.75	1.02
JD_R3_CK_E_NNL_GQISWI	58.2	10.7	1.04	0.19	-34.89	1.08
JD_R3_CK_S_NLL_GQISWI_K	58.2	10.7	1.03	0.19	-31.22	1.26
JD_R3_CK_E_LLL_GQISWI_K	58.2	10.7	0.51	0.08	-1.24	1.78

Table 3-5: The 14 chosen scenarios for Jal el Dib Round 7
(the highlighted blue cells are the statistical indicators that indicate most accurate interpolation)
(The red box is the chosen interpolation to show the error map)

Code	Statistical Indicators					
	Avg.	σ	RSR	CV	PBIAS	RMS-S
JD_R7_Kr_S_L_Cl	546.5	327	0.89	0.53	-27.77	0.89
JD_R7_Kr_S_L_TDS	508.5	616.4	0.74	0.37	73.49	0.82
JD_R7_Kr_S_L_GQI	81.9	4.1	0.76	0.04	-9.79	0.91
JD_R7_Kr_E_N_GQISWI	59.0	9.2	0.84	0.13	-20.76	0.92
JD_R7_IDW_TDS	508.5	616.4	0.90	0.45	331.77	-
JD_R7_IDW_Cl	546.5	327	1.02	0.61	433.40	-
JD_R7_CK_E_NLL_Cl_K	546.5	327	0.97	0.58	42.73	0.97
JD_R7_CK_S_LLL_Cl	546.5	327	0.93	0.56	-33.11	0.93
JD_R7_CK_S_LLL_Cl_K	546.5	327	0.89	0.53	13.86	0.86
JD_R7_CK_E_NNL_Cl_K	546.5	327	0.97	0.58	42.73	0.97
JD_R7_CK_E_LLL_Cl	546.5	327	0.96	0.57	60.72	0.89
JD_R7_CK_S_NLL_GQISWI	59.0	9.2	0.76	0.12	-2.06	1.05
JD_R7_CK_E_NLL_GQISWI	59.0	9.2	0.76	0.12	-2.06	0.98
JD_R7_CK_S_NNL_GQISWI_K	59.0	9.2	0.80	0.13	-18.12	0.92
JD_R7_CK_S_NLL_GQISWI_K	59.0	9.2	0.80	0.13	-24.94	0.92
JD_R7_CK_E_NNL_GQISWI_K	59.0	9.2	0.80	0.13	-18.34	0.89
JD_R7_CK_E_NLL_GQISWI_K	59.0	9.2	0.80	0.13	-48.20	0.89

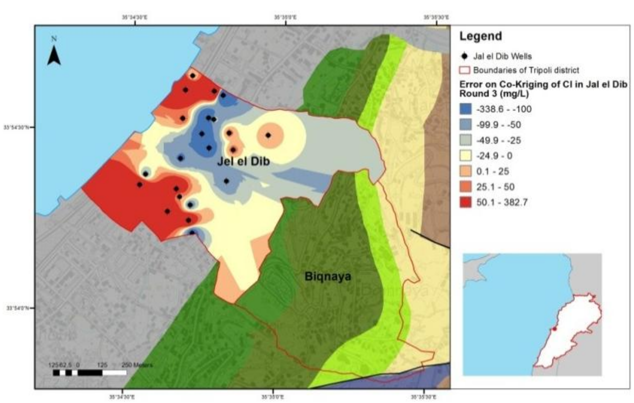

Error map in Jal el Dib round 3 using Co-kriging Exponential semivariogram for Cl

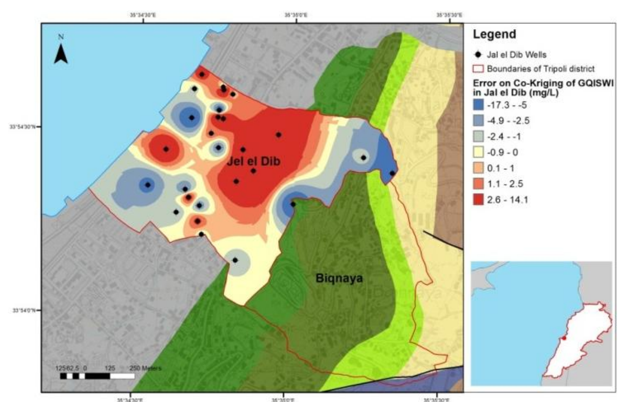

Error map in Jal el Dib round 7 using Co-kriging Spherical semivariogram for GQISWI

Figure 3-3 : Examples on error distribution of Jal el Dib

3.1 Water Quality Category Matching

Since the interest for some application is to capture the range of water quality of certain pollutants rather than the actual water quality "reading", it becomes satisfactory if interpolations or predictions captured only the water quality category, and not necessarily the exact water quality reading for a given contaminant. Thus, another method of validation is by using water quality categories (Table 3-6, and Chapter I section 3.7) for the TDS and the Chloride concentration levels.

Table 3-6: Water Quality categories and their equalivalent PP and PF ranges

Water Types	TDS range (ppm)	Cl^- range (mg/L)	DRASTIC PP ranges (Aller, et al., 1987; Marc Metni, 2002)	EPIK PF ranges (SAEFL, 1998)	EPIK PF ranges (modified)	Vulnerability
Drinking water	0-500	1-200	27-85	34 AND 34+P=4 I=3 or 4[1]	32-34	Low
Fresh Water	500-1,000	200-300	86-106	29-33	28-31	
Brackish	1,000-5,000	300-500	107-127	24-28	24-27	Moderate
Highly Brackish	5,000-15,000	500-5,000	128-148	19-23	21-23	
Saline Water	15,000-30,000	5,000-15,000	149-169	14-18	18-20	High
Sea Water	30,000-40,000	15,000-20,000	170-236	9-13	15-17	

Source: Aller, et al., 1987; Oram, et al., 2010; SAEFL, 1998; USGS, 2000; Water Quality Assosciation, 2013; WHO, 2003

[1] ONLY the locations where PF=34 AND P=4 and I=3 or 4; All these conditions should be found together for this category

Thus, for every scenario, field measured TDS (TDS-F) or Chloride levels for every well were compared with the interpolated TDS (TDS-WQA) or Chloride levels. Ideally, it is desirable to have all interpolated water quality levels for each well fall within the same category of the field measured water quality. For example, Table 3-7 summarizes the results for Kriging scenario in Jal el Dib using TDS concentration. The results show a match between the interpolated values and the measured levels. More than 77 % of the total samples were within the same water quality category (77.8%), with the remaining samples matching within one category error. Another example shows TDS measurement also for Jal el Dib using IDW interpolation with similar a percent match (74.1%).

Table 3-7: Water Quality ranges based on Chloride concentration the field measured (WQ_{Field}) versus the interpolated value (WQ_{Cl-})

WQ_{TDS} \ WQ_{Field}	Drinking water 0-500	Fresh Water 500-1,000	Brackish 1,000-5,000	Highly Brackish 5,000-15,000	Saline Water 15,000-30,000	Sea Water 30,000-40,000
Drinking water 0-500						
Fresh Water 500-1,000		3	1			
Brackish 1,000-5,000		5	18			
Highly Brackish 5,000-15,000						
Saline Water 15,000-30,000						
Sea Water 30,000-40,000						
e.g. JD_R7_CK_S_L_TDS	Match	±1	±2	±3	±4/5	Total
Number of wells	21	6	0	0	0	**27**
Percent per category	77.8	22.2	0	0	0	**100**
Cumulative Percent	77.8	100.0	100.0	100.0	100.0	**100.0**

Table 3-8: Water Quality ranges based on Chloride concentration the field measured (WQ_{Field}) versus the interpolated value (WQ_{TDS})

WQ_{TDS} \ WQ_{Field}	Drinking water 0-500	Fresh Water 500-1,000	Brackish 1,000-5,000	Highly Brackish 5,000-15,000	Saline Water 15,000-30,000	Sea Water 30,000-40,000
Drinking water 0-500						
Fresh Water 500-1,000		1				
Brackish 1,000-5,000		7	19			

Highly Brackish 5,000-15,000						
Saline Water 15,000-30,000						
Sea Water 30,000-40,000						
e.g. JD_R7_IDW_TDS	Match	±1	±2	±3	±4/5	Total
Number of wells	20	7	0	0	0	**27**
Percent per category	74.1	25.9	0	0	0	**100**
Cumulative Percent	74.1	100.0	100.0	100.0	100.0	**100.0**

The final per cent match results of 41 scenarios from three cities are summarized in three tables per interpolation method (Table 3-9,

Table 3-10,

Table 3-11). The three methodologies show comparable and similar results.

Table 3-9: Cumulative per cent match results for 10 scenarios using interpolation method Kriging (the highlighted blue cells are when the 50 percentile is crossed)

Name	Match (%)	±1 (%)	±2 (%)	±3 (%)	±4/5 (%)	Total (%)
JD_R3_Kr_E_N_Cl	59.1	77.3	100	100	100	100
JD_R3_Kr_E_L_TDS	68.2	95.5	100	100	100	100
JD_R7_Kr_S_L_Cl	44.4	92.5	100	100	100	100
JD_R7_Kr_S_L_TDS	77.8	100	100	100	100	100
BEY_R1_Kr_S_L_Cl	50.3	78.8	97	100	100	100
BEY_R1_Kr_S_L_TDS	40	93.3	100	100	100	100
TRP_R1_Kr_E_L_Cl	75	90	96.7	100	100	100
TRP_R1_Kr_E_L_TDS	68.3	100	100	100	100	100
TRP_R2_Kr_E_L_Cl	60	81.7	95	100	100	100
TRP_R2_Kr_E_L_TDS	50	98.3	100	100	100	100

CITY		PARAMETERS	
BEY	Beirut	Cl	Chloride Level (mg/L)
JD	Jal el Dib	TDS	Total Dissolved Solids (ppm)
TRP	Tripoli	GQI	Groundwater Quality Assessment
SAMPLING ROUND		GQI_{SWI}	Groundwater Quality Assessment for Seawater intrusion
R1	Round 1- Early Summer - May/June	K	Hydraulic Conductivity
R2	Round 2 - Late Summer – Sept./Oct.	TRANFORMATION	
Rx	Other Rounds	N	Normal
INTERPOLATION		L	Log
Kr	Kriging	SEMI VARIOGRAM MODEL	
IDW	Inverse Distance Weight	S	Spherical
CK	Co-Kriging	E	Exponential

Table 3-10: Cumulative per cent match results for 10 scenarios using interpolation method IDW (the highlighted blue cells are when the 50 percentile is crossed)

Name	Match (%)	±1 (%)	±2 (%)	±3 (%)	±4/5 (%)	Total (%)
JD_R3_IDW_Cl	27.3	72.8	95.5	100	100	100
JD_R3_IDW_TDS	63.6	95.4	100	100	100	100
JD_R7_IDW_TDS	74.1	100	100	100	100	100
JD_R7_IDW_Cl	44.4	81.4	100	100	100	100
BEY_R1_IDW_TDS	46.1	78.2	100	100	100	100
BEY_R1_IDW_Cl	51.5	83	93.9	100	100	100
TRP_R1_IDW_TDS	76.7	100	100	100	100	100
TRP_R1_IDW_Cl	66.7	88.4	98.4	100	100	100
TRP_R2_IDW_TDS	51.7	98.4	100	100	100	100
TRP_R2_IDW_Cl	61.7	75	95	100	100	100

Table 3-11: Cumulative per cent match results for 10 scenarios using interpolation method Co-Kriging with distance of well from shoreline, transmissivity of the tapped aquifer and well depth (the highlighted blue cells are when the 50 percentile is crossed)

Name	Match (%)	±1 (%)	±2 (%)	±3 (%)	±4/5 (%)	Total (%)
JD_R3_CK_S_NNN_Cl	27.3	72.8	95.5	100	100	100
JD_R3_CK_E_NLL_Cl	54.5	77.2	100	100	100	100
JD_R3_CK_S_NLN_Cl_K	54.5	77.2	100	100	100	100
JD_R3_CK_E_NLN_Cl_K	54.5	77.2	100	100	100	100
JD_R7_CK_E_NLL_Cl_K	48.1	85.1	100	100	100	100
JD_R7_CK_S_LLL_Cl	51.9	88.9	100	100	100	100
JD_R7_CK_S_LLL_Cl_K	51.9	85.2	100	100	100	100
JD_R7_CK_E_NNL_Cl_K	48.1	85.1	100	100	100	100
JD_R7_CK_E_LLL_Cl	55.6	81.5	100	100	100	100
BEY_R1_CK_E_LLL_Cl	46.1	78.2	94.6	100	100	100
BEY_R1_CK_S_LLL_Cl	46.1	78.2	93.4	100	100	100
BEY_R1_CK_E_LLL_Cl_K	46.7	78.8	95.2	100	100	100
BEY_R1_CK_S_LLL_Cl_K	46.7	75.8	93.4	100	100	100
TRP_R1_CK_S_LNN_Cl_K	68.3	90	98.3	100	100	100
TRP_R1_CK_S_LLN_Cl_K	68.3	90	98.3	100	100	100
TRP_R1_CK_E_LNN_Cl_K	41.7	71.7	81.7	100	100	100
TRP_R1_CK_E_LLN_Cl_K	68.3	90	98.3	100	100	100
TRP_R2_CK_S_LNN_Cl_K	73.3	81.6	96.6	100	100	100
TRP_R2_CK_S_LLN_Cl_K	71.7	81.7	96.7	100	100	100
TRP_R2_CK_E_LNN_Cl_K	71.7	85	96.7	100	100	100
TRP_R2_CK_E_LLN_Cl_K	70	85	96.7	100	100	100

In an effort to assess the robustness of the comparisons, the sensitivity of the results was tested by varying the measured water quality data by ±3 % of their original values Considering 3 percent error margin in the water quality measuring appliances, some of the field measured values could fall into one category, and with the error readjustment some would be considered under-estimated or over-estimated. Doing the 3 percent error adjustment to all the field points (Annex 5.3[7]), number of points that changed water quality class were counted and they ranged between zero percent of the measured points, to 13 percent of the measured points changed water quality class.

3.2 GQA V/S GVA

Although the groundwater vulnerability assessment (GVA) works with physical setting and varies at a geological scale, some VA methods were used to analyze non-vertical contamination of groundwater. Present-time field measured data were used to cross-check the results of the VA methods (Table 2-1) (Chachadi et al. 2001; Elewa et al. 2013; Rangel-Medina et al. 2004; Selmi 2013).

Here, we compare the groundwater quality assessment using geospatial analysis with the results of two groundwater vulnerability assessment models: DRASTIC and EPIK. It is important to

[7] Jal el Dib Round 3 for chloride 0 out of 22 (minimum) wells changed the water quality class for TDS 3 out of 22, which is the 13% (maximum), and for Round 7, 1 out of 27 sampled wells in chloride and TDS changed water quality class before and after error adjustment. In Beirut 6 out of 165 wells for chloride and 8 out of 165 wells for TDS are a class lower or a class higher than the actual measurement. In Tripoli, measuring chloride for Round 1 and Round 2, 4 out of 60 wells and 3 out of 60 wells, respectively, changed water quality class, and for TDS both rounds had 5 out of 60 wells changed its class after the readjustment.

note the fact that in such a comparison we would be comparing a dynamic system (water quality under seawater intrusion) with a static/fixed system (the outcropping geology of the aquifers).

Figure 3-4 shows the process and the interlinking of the two methodologies to produce another validation process. After conducting the matching process with the established water quality categories (Section 3.7 Chapter I) for the interpolated results, they were compared with the matching process for the vulnerability assessment results.

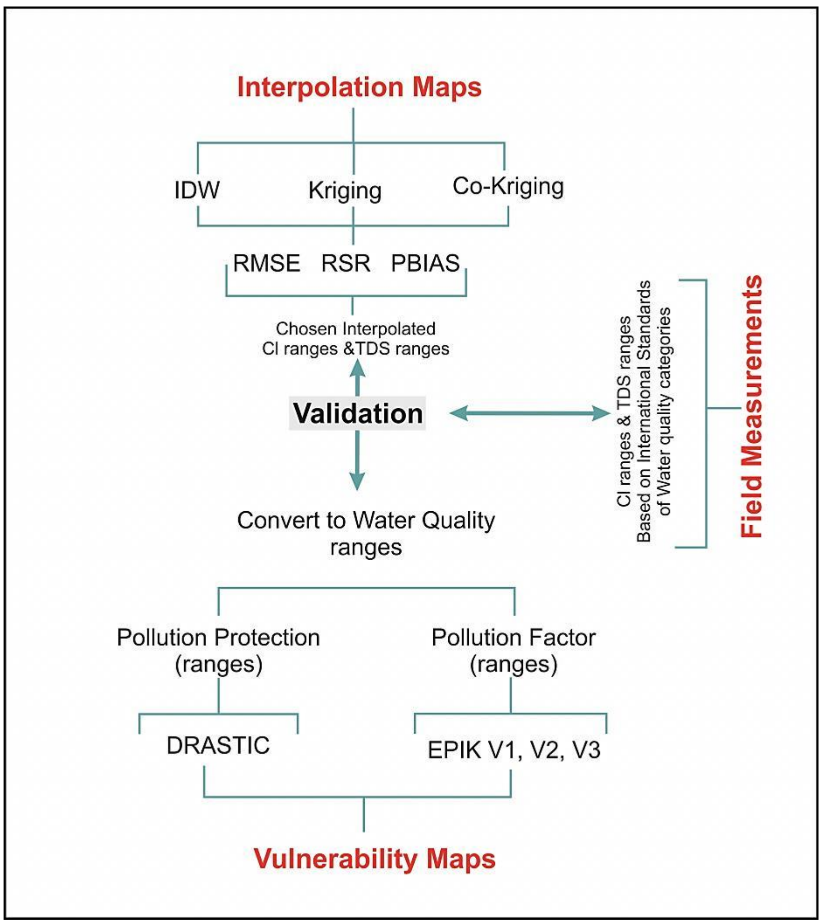

Figure 3-4: Comparing the Interpolation results with Vulnerability assessment results

Table 3-12 compares the ability of geospatial interpolation methods to that of VA methods in predicting the Chloride water quality category. DRASTIC performed better than EPIK in Jal el Dib (January, 2013), however interpolation results (Kriging and Co-Kriging) showed better percentages than both DRASTIC and EPIK. Similar results were obtained for TDS where DRASTIC and EPIK performed poorly (4.5 to 27.3%) as compared to interpolation-based results using Kriging or IDW (63.6%-68.2%).

Table 3-12: Cumulative per cent water category matching result for EPIK (EP), DRASTIC (DR) and the interpolation results (Kr, IDW, CK) for Jal el Dib Round 3 (January 2013)
(the highlighted blue are when the 50 percentile is crossed)

		Name	Match (%)	±1 (%)	±2 (%)	±3 (%)	±4/5 (%)	Total (%)
Cl^-	EPIK	JD_R3_EP1_Cl	22.7	72.7	77.2	100	100	100
		JD_R3_EP2_Cl	22.7	72.7	77.2	100	100	100
		JD_R3_EP3_Cl	18.2	72.7	77.2	100	100	100
	DR.	JD_R3_DR_Cl	45.5	68.2	100	100	100	100
	Interpolation	JD_R3_Kr_E_N_Cl	59.1	77.3	100	100	100	100
		JD_R3_IDW_Cl	27.3	72.8	95.5	100	100	100
		JD_R3_CK_S_NNN_Cl	27.3	72.8	95.5	100	100	100
		JD_R3_CK_E_NLL_Cl	54.5	77.2	100	100	100	100
		JD_R3_CK_S_NLN_Cl_K	54.5	77.2	100	100	100	100
		JD_R3_CK_E_NLN_Cl_K	54.5	77.2	100	100	100	100
TDS	EPIK	JD_R3_EP1_TDS	27.3	90.9	100	100	100	100
		JD_R3_EP2_TDS	27.3	90.9	100	100	100	100
		JD_R3_EP3_TDS	4.5	27.2	90.8	100	100	100
	DR.	JD_R3_DR_TDS	22.7	90.9	100	100	100	100
	Interp.	JD_R3_Kr_E_L_TDS	68.2	95.5	100	100	100	100
		JD_R3_IDW_TDS	63.6	95.4	100	100	100	100

CITY		PARAMETERS	
BEY	Beirut	Cl	Chloride Level (mg/L)
JD	Jal el Dib	TDS	Total Dissolved Solids (ppm)
TRP	Tripoli	GQI	Groundwater Quality Assessment
SAMPLING ROUND		GQI_{SWI}	Groundwater Quality Assessment for Seawater intrusion
R1	Round 1- Early Summer - May/June	K	Hydraulic Conductivity

R2	Round 2 - Late Summer – Sept./Oct.	TRANFORMATION	
Rx	Other Rounds	N	Normal
INTERPOLATION		L	Log
Kr	Kriging	SEMI VARIOGRAM MODEL	
IDW	Inverse Distance Weight	S	Spherical
CK	Co-Kriging	E	Exponential
VULNERABILITY ASSESSMENT (VA) METHOD			
DR	DRASTIC		
EP1	EPIK-Version 1 (urbanization low impact)		
EP2	EPIK-Version 2 (no urbanization)		
EP3	EPIK-Version 3 (urban areas high vulnerability)		

Table 3-13 shows similar conclusion for the second round for Jal el Dib (October 2013). For Chloride concentration, DRASTIC vulnerability assessment results produced better results than EPIK and relatively worse results than interpolation methods results (similar to the January round). For TDS measurements, EPIK (Version 1 and 2) performed well with comparable or better results than Kriging and IDW (unlike the January round).

Table 3-13: Cumulative percent water category matching result for EPIK (EP), DRASTIC (DR) and the interpolation results (Kr, IDW, CK) for Jal el Dib Round 7 (October 2013)
(the highlighted blue are when the 50 percentile is crossed)

		Name	Match (%)	±1 (%)	±2 (%)	±3 (%)	±4/5 (%)	Total (%)
Cl⁻	EPIK	JD_R7_EP1_Cl	22.2	100	100	100	100	100
		JD_R7_EP2_Cl	22.2	100	100	100	100	100
		JD_R7_EP3_Cl	40.7	81.4	100	100	100	100
	DR.	JD_R7_DR_Cl	14.8	77.8	88.9	100	100	100
	Interpolation	JD_R7_Kr_S_L_Cl	44.4	92.5	100	100	100	100
		JD_R7_IDW_Cl	44.4	81.4	100	100	100	100
		JD_R7_CK_E_NLL_Cl_K	48.1	85.1	100	100	100	100
		JD_R7_CK_S_LLL_Cl	51.9	88.9	100	100	100	100
		JD_R7_CK_S_LLL_Cl_K	51.9	85.2	100	100	100	100
		JD_R7_CK_E_NNL_Cl_K	48.1	85.1	100	100	100	100
		JD_R7_CK_E_LLL_Cl	55.6	81.5	100	100	100	100
TDS	EPIK	JD_R7_EP1_TDS	77.8	100	100	100	100	100
		JD_R7_EP2_TDS	77.8	100	100	100	100	100
		JD_R7_EP3_TDS	11.1	77.8	100	100	100	100
	DR.	JD_R7_DR_TDS	55.6	77.8	96.3	100	100	100
	Int erp	JD_R7_Kr_S_L_TDS	77.8	100	100	100	100	100

		JD_R7_IDW_TDS	74.1	100	100	100	100	100

In Beirut, Table 3-14 shows the results for Chloride concentrations and TDS levels. The vulnerability assessment methods produced low matching results similar to the interpolation-based models.

Table 3-14: Cumulative percent water category matching result for EPIK (EP), DRASTIC (DR) and the interpolation results (Kr, IDW, CK) for Beirut Round 1 (May, June 2013)
(the highlighted blue are when the 50 percentile is crossed)

		Name	Match (%)	±1 (%)	±2 (%)	±3 (%)	±4/5 (%)	Total (%)
Cl^-	EPIK	BEY_EP1_Cl	20	66.1	82.5	92.8	100	100
		BEY_EP2_Cl	22.4	66.6	83	93.9	100	100
		BEY_EP3_Cl	21.2	48.5	66.7	80.6	100	100
	DR.	BEY_DR_Cl	12.1	40.6	86.1	97.6	100	100
	Interpolation	BEY_R1_Kr_S_L_Cl	50.3	78.8	97	100	100	100
		BEY_R1_IDW_Cl	51.5	83	93.9	100	100	100
		BEY_R1_CK_E_LLL_Cl	46.1	78.2	94.6	100	100	100
		BEY_R1_CK_S_LLL_Cl	46.1	78.2	93.4	100	100	100
		BEY_R1_CK_E_LLL_Cl_K	46.7	78.8	95.2	100	100	100
		BEY_R1_CK_S_LLL_Cl_K	46.7	75.8	93.4	100	100	100
TDS	EPIK	BEY_EP1_TDS	23.6	64.8	84.2	98.7	100	100
		BEY_EP2_TDS	24.2	67.2	86	98.7	100	100
		BEY_EP3_TDS	10.9	37	67.3	82.5	100	100
	DR.	BEY_DR_TDS	27.3	49.1	71.5	98.2	100	100
	Interp.	BEY_R1_Kr_S_L_TDS	40	93.3	100	100	100	100
		BEY_R1_IDW_TDS	46.1	78.2	100	100	100	100

For both rounds of Tripoli EPIK and DRASTIC showed low match percentages, whereas the interpolation-based models showed a high match percentage both for Chloride and TDS levels (Table 3-15, Table 3-16).

Table 3-15: Percent water category matching result for EPIK (EP), DRASTIC (DR) and the interpolation results (Kr, IDW, CK) for Tripoli Round 1 (July 2007)
(the highlighted blue are when the 50 percentile is crossed)

		Name	Match (%)	±1 (%)	±2 (%)	±3 (%)	±4/5 (%)	Total (%)
Cl^-	EPIK	TRP_R1_EP1_Cl	16.7	30	91.7	100	100	100
		TRP_R1_EP2_Cl	16.7	30	93.3	100	100	100
		TRP_R1_EP3_Cl	10	25	40	93.3	100	100
	DR.	TRP_R1_DR_Cl	26.2	43.1	89.3	100	100	100
	Interpolation	TRP_R1_Kr_E_L_Cl	75	90	96.7	100	100	100
		TRP_R1_IDW_Cl	66.7	88.4	98.4	100	100	100
		TRP_R1_CK_S_LNN_Cl_K	68.3	90	98.3	100	100	100
		TRP_R1_CK_S_LLN_Cl_K	68.3	90	98.3	100	100	100
		TRP_R1_CK_E_LNN_Cl_K	41.7	71.7	81.7	100	100	100
		TRP_R1_CK_E_LLN_Cl_K	68.3	90	98.3	100	100	100
TDS	EPIK	TRP_R1_EP1_TDS	11.7	50	90	100	100	100
		TRP_R1_EP2_TDS	11.7	50	91.7	100	100	100
		TRP_R1_EP3_TDS	0	26.7	55	91.7	100	100
	DR.	TRP_R1_DR_TDS	8.3	55	91.7	100	100	100
	Interp.	TRP_R1_Kr_E_L_TDS	68.3	100	100	100	100	100
		TRP_R1_IDW_TDS	76.7	100	100	100	100	100

The result differences for water quality assessment (WQA) and groundwater vulnerability assessment (GVA) has not been large for the other two cities. This anomaly in Tripoli could be attributed to the relatively high vulnerability in Tripoli even though the outcropping geology is not highly vulnerable (semi-karstic).

Table 3-16: Cumulative percent water category matching result for EPIK (EP), DRASTIC (DR) and the interpolation results (Kr, IDW, CK) for Tripoli Round 2 (September 2006)
(the highlighted blue are when the 50 percentile is crossed)

		Name	Match (%)	±1 (%)	±2 (%)	±3 (%)	±4/5 (%)	Total (%)
Cl^-	EPIK	TRP_R2_EP1_Cl	8.3	25	90	100	100	100
		TRP_R2_EP2_Cl	8.3	25	91.7	100	100	100
		TRP_R2_EP3_Cl	13.3	21.6	41.6	93.3	100	100
	DR.	TRP_R2_DR_Cl	18.3	35	85	100	100	100
	Interpolation	TRP_R2_Kr_E_L_Cl	60	81.7	95	100	100	100
		TRP_R2_IDW_Cl	61.7	75	95	100	100	100

		TRP_R2_CK_S_LNN_Cl_K	73.3	81.6	96.6	100	100	100
		TRP_R2_CK_S_LLN_Cl_K	71.7	81.7	96.7	100	100	100
		TRP_R2_CK_E_LNN_Cl_K	71.7	85	96.7	100	100	100
		TRP_R2_CK_E_LLN_Cl_K	70	85	96.7	100	100	100
TDS	EPIK	TRP_R2_EP1_TDS	11.7	36.7	90	100	100	100
TDS	EPIK	TRP_R2_EP2_TDS	11.7	36.7	91.7	100	100	100
TDS	EPIK	TRP_R2_EP3_TDS	0	20	50	91.7	100	100
TDS	DR.	TRP_R2_DR_TDS	8.3	38.3	86.6	100	100	100
TDS	Interp.	TRP_R2_Kr_E_L_TDS	50	98.3	100	100	100	100
TDS	Interp.	TRP_R2_IDW_TDS	51.7	98.4	100	100	100	100

Another method to compare the two approaches (GQA, GVA) was by adding EPIK PF values as a secondary parameter when conducting Co-Kriging. One example for this exercise was conducted for the city of Beirut (Table 3-3). The results of the statistical indicators did not improve much, thus adding the PF to the Co-Kriging did not contribute to the spatial distribution of the studied parameter.

4 Concluding remarks

The correct process of producing an interpolation map is conducted by evaluating the data input, fitting a semivariogram model to it, selecting the interpolation method, and cross-validate the resulted for a final check of accuracy (Figure 1-1 and Figure 2-1). In this study, several scenarios were compared to evaluate the most suitable variogram model and interpolation method that produced relatively accurate results for groundwater quality assessment contaminated by seawater.

Leave-one-out cross validation method was utilized to generate different (four) statistical indicators for each scenario per city. Upon comparison, results showed that the ability of interpolation models to predict is not consistent. The performance of the interpolation methods (IDW, Kriging, Co-Kriging) varied, with IDW performing better in locations with relatively better groundwater quality, as opposed to Co-Kriging which performed better with lower water qualities.

A second evaluation test was conducted by dividing the water quality into categories (ranging from drinking water up to seawater), and analyzing the extent of match between the field measured value and the interpolated value. The better performance of IDW was expected, because IDW does not smooth the extreme results as Kriging or Co-Kriging do, therefore field measured value and IDW interpolated values were similar.

Finally, the performance of geospatial interpolation methods (GQA) was compared to vulnerability assessment methods in their ability to match water quality categories. The results showed better performance of interpolation methodology for groundwater contamination analysis, with significant difference between the results of GVA and GQA results. This highlights that the main purpose of the GVA is to present the data in its normal condition without the impact of urbanization, unsustainable abstraction, or seawater intrusion.

In conclusion, there is no one “best” interpolation method or a semivariogram model that fits all data, each dataset would require a prior analysis of the type and accordingly decision regarding the interpolation method and the semivariogram model would be made. Moreover, Groundwater Quality Assessment using Geospatial Analysis (GQA-GA) and Groundwater Vulnerability Assessment (GVA) both are useful depending on the required analysis. GQA-GA aims to predict locations for protection, thus it produces action plans for decision makers with regard to reversing the contamination or stopping further deterioration. On the other hand, GVA is used to project possible groundwater deterioration and to delineate groundwater protection zones for decision makers to consider, but cannot be used to delineate present water quality variations. A source of uncertainty in this comparison between GQA-GA and GVA, is in the fact that the comparison is between static vulnerability assessment models and dynamic water quality geostatistical methods.

Regarding the accuracy of the geospatial analysis of the water quality data, the lack of accurate data on well depth, and thus the tapped aquifers was a major concern. Lack of accurate information on the well drilling reduces the accuracy of the resulting geospatial distribution of the water quality parameter. Secondly, the analyzed datasets had high standard deviation, and this was also shown in the error distribution map, which shows no significant geospatial distribution.

BIBLIOGRAPHY

Abdul Basit S. (1971). *Ground water quality in Beirut and suburbs.* Master of Engineering, American University of Beirut, Beirut.

Ahmadian, S. (2013). Geostatistical Based Modelling of Variations of Groundwater Quality During 2006 to 2009 (in Tehran-Karaj Plain). *Journal of Basic and Applied Scientific Research, 3*(2s), 264-272.

Aller, L., Lehr, J. H., & Petty, R. (1987). DRASTIC: A Standardized System to Evaluate Ground Water Pollution Potential Using Hydrogeologic Settings. Worthington, Ohio: National Water Well Association.

APHA. (1998). Standard Methods for the Examination of Water and Wastewater.

Arslan, H. (2012). Spatial and temporal mapping of groundwater salinity using ordinary kriging and indicator kriging: The case of Bafra Plain, Turkey. *Agricultural Water Management, 113*, 57-63. doi: 10.1016/j.agwat.2012.06.015

Babiker, I. S., Mohamed, M. A. A., & Hiyama, T. (2006). Assessing groundwater quality using GIS. *Water Resources Management, 21*(4), 699-715. doi: 10.1007/s11269-006-9059-6

Bajjali, W. (2005). Model the effect of four artificial recharge dams on the quality of groundwater using geostatistical methods in GIS environment, Oman. *Journal of Spatial Hydrology, 5*(2), 1-15.

Barrocu, G., Muzzu, M., & Uras, G. (2006). Hydrogeology and vulnerability map (EPIK method) of the “Supramonte” karstic system, north-central Sardinia. *Environmental Geology, 51*(5), 701-706. doi: 10.1007/s00254-006-0382-2

Bohling, G. (2005a). Introduction to Geostatistics and Variogram Analysis: Kansas Geological Survey.

Bohling, G. (2005b). Kriging: Kansas Geological Survey.

Chachadi, A. G., & Lobo-Ferreira, J.-P. (2005). *Assessing Aquifer Vulnerability to seawater intrusion using GALDIT method: Part 2- GALDIT Indicators Description*. Paper presented at the The fourth Inter-Celtic Colloquium on Hydrology and Management of Water Resources, Guimaraes, Portugal.

Chachadi, A. G., & Lobo-Ferreira, J. P. (2001). Sea water intrusion Vulnerability mapping of aquifers using the GALDIT method. In TERI & European Commission DG XII (Eds.), *Coastin: a Coastal Policy Research Newsletter* (Vol. Number 4, pp. 7-9).

Chachadi, A. G., Lobo-Ferreira, J. P., Noronha, L., & S., C. B. (2002). Assessing the impact of sea-level rise on salt water intrusion in coastal aquifers using GALDIT model. In TERI & European Commission DG XII (Eds.), *Coastin: a Coastal Policy Research Newsletter* (Vol. Number 7, pp. 27-32).

Chang, N.-B. (Ed.). (2010). *Effects of Urbanization on Groundwater: An Engineering Case-Based Approach for Sustainable Development*. Virginia, USA: American Society of Civil Engineers.

Civita, M., & de Maio, M. (1997). *SINTACS Un sistema parametrico per la valutazione e la cartografia della vulnerabilità all'inquinamento Metodologia e automazione* (Vol. null).

Cooper, R. M., & Istok, J. D. (1988). Geostatistics Applied to Groundwater Contamination. I: Methodology. *Journal of Environmental Engineering, 114*, 270-299.

Delbari, M., Motlagh, M. B., Kiani, M., & Amiri, M. (2013). Investigating spatio-temporal variability of groundwater quality parameters using geostatistics and GIS. *International Research Journal of Applied and Basic Sciences, 4*(10), 3623-3632.

Doerfliger, N. (1996). *Advances in karst groundwater protection strategy using artificial tracer test analysis on a multiattribute vulnerability mapping (EPIK method).* PhD, University of Neuchatel, Neuchatel, Switzerland.

Doerfliger, N., Jeannin, P.-Y., & Zwahlen, F. (1999). Water vulnerability assessment in karst environments: a new method of defining protection areas using a multi-attribute approach and GIS tools (EPIK method). *Environmental Geology, 39*(2), 165-176.

Doerfliger, N., & Zwahlen, F. (1998). *Practical guide: groundwater vulnerability mapping in karstic regions (EPIK)* (Vol. null).

El-Fadel, M., Rachid, G., Alameddine, I., & Najm, M. A. (2014). *Saltware Intrusion in karst aquifers along the Eastern Mediterranean.* Paper presented at the 23rd Salt water Intrusion Meeting, Husum, Germany.

El-Fadel, M., Tomaszkiewicz, M., Adra, Y., Sadek, S., & Abou Najm, M. (2014). GIS-Based Assessment for the Development of a Groundwater Quality Index Towards Sustainable Aquifer Management. *Water Resources Management, 28*(11), 3471-3487. doi: 10.1007/s11269-014-0683-2

Elewa, H. H., Shohaib, R. E., Qaddah, A. A., & Nousir, A. M. (2013). Determining groundwater protection zones for the Quaternary aquifer of northeastern Nile Delta using GIS-based vulnerbaility mapping. *Environmental Earth Sciences, 68*, 313-331. doi: 10.1007/s12665-012-1740-x

ESRI. (2008). Introduction to Modeling Spatial Processes Using Geostatistical Analyst. In K. Krivoruchko (Ed.).

Fetter, C. W. (2001). *Applied hydrogeology* (4th ed.). Upper Saddle River, N.J.: Prentice Hall.

Fijani, E., Nadiri, A. A., Asghari Moghaddam, A., Tsai, F. T. C., & Dixon, B. (2013). Optimization of DRASTIC method by supervised committee machine artificial intelligence to assess groundwater vulnerability for Maragheh–Bonab plain aquifer, Iran. *Journal of Hydrology, 503*, 89-100. doi: 10.1016/j.jhydrol.2013.08.038

Focazio, M., Reilly, T., Rupert, M., & Helsel, D. (2002). Assessing Ground-water Vulnerability to Contamination: Providing Scientifically Defensible Information for Decision Makers: USGS.

Foster, S., & Hirata, R. (1988). *Groundwater pollution risk assessment: a methodology using available data. WHO-PAHO-CEPIS Technical report* (Vol. null).

Gogu, R. C., & Dassargues, A. (2000). Current trends and future challenges in groundwater vulnerability assessment using overlay and index methods. *Environmental Geology, 39*(6), 549-559.

Gogu, R. C., & Dassargues, A. (2000). Sensitivity analysis for the EPIK method of vulnerability assessment in a small karstic aquifer, southern Belgium. *Hydrogeology Journal, 8*(3), 337-345.

Gogu, R. C., Hallet, V., & Dassargues, A. (2003). Comparison of aquifer vulnerability assessment techniques. Application to the Neblon river basin (Begium). *Environmental Geology, 44*, 881-892. doi: 10.1007/s00254-003-0842-x

Goldscheider, N. (2005). Karst groundwater vulnerbaility mapping: application of a new method in the Swabian Alb, Germany. *Hydrogeology Journal, 13*(4), 555-564.

Howard, K. W. F. (2002). Urban Groundwater Issues—An Introduction. In K. F. Howard & R. Israfilov (Eds.), *Current Problems of Hydrogeology in Urban Areas, Urban Agglomerates and Industrial Centres* (Vol. 8, pp. 1-15): Springer Netherlands.

Hu, J. J. (1995). *Methods of generating Surface in Environmental GIS applications.* Paper presented at the Esri International User Conference, Palm Springs, California.

IPCC. (2007). Climate Change 2007: Impacts, Adaptation and Vulnerability. In Contribution of Working Group II to the Fourth Assessment Report of the IPCC, M. L. Parry, O. F. Canziani, P. J. O. Palutikof, P. J. v. d. Linden & C. E. Hanson (Eds.), (pp. 976). Cambridge, UK: Campridge University Press.

IPCC. (2013). Climate Change (IPCC 5): The physical science basis. In Contribution of Working Group I to the Fifth Assessment Report of the IPCC, T. F. Stocker, D. Qin, G.-K. Plattner, m. M. B. Tignor, S. K. allen, j. Boschung, A. Nauels, YuXia, V. Bex & P. M. Midgley (Eds.), (pp. 1535). Cambrige, Unite Kingdom and New York, USA.

Jamrah, A., Al-Futaisi, A., Rajmohan, N., & Al-Yaroubi, S. (2008). Assessment of groundwater vulnerability in the coastal region of Oman using DRASTIC index method in GIS environment. *Environmental Monitoring and Assessment, 147*(1-3), 125-138. doi: 10.1007/s10661-007-0104-6

Jiménez-Madrid, A., Martínez-Navarrete, C., & Carrasco-Cantos, F. (2010). Groundwater Risk Intensity Assessment. Application to Carbonate Aquifers of the Western Mediterranean (Southern Spain). *Geodinamica Acta, 23*(1-3), 101-111. doi: 10.3166/ga.23.101-111

Kallioras, A., Pliakas, F., Skias, S., & Gkiougkis, I. (2011). Groundwater vulnerability assessment at SW Rhodope aquifer system in NE Greece. In N. Lambrakis, G. Stournaras & K. Katsanou (Eds.), *Advances in the Research of Aquiatic Environment*. New York: Springer.

Khan, M. M. A., Umar, R., & Lateh, H. (2010). Assessment of aquifer vulnerability in parts of Indo Gangetic plain, India. *International Journal of the Physical Sciences, 5*(11), 1711-1720.

Khayat, Z. (2001). *Groundwater Conditions in the Koura-Zgharta Miocene Limestone Aquifer*. Master of Science, American University of Beirut, Beirut.

Kura, N. U., Ramli, M. F., Ibrahim, S., Sulaiman, W. N., & Aris, A. Z. (2014). An integrated assessment of seawater intrusion in a small tropical island using geophysical, geochemical, and geostatistical techniques. *Environmental science and pollution research international*. doi: 10.1007/s11356-014-2598-0

Loáiciga, H. A., Pingel, T. J., & Garcia, E. S. (2012). Sea Water Intrusion by Sea-Level Rise: Scenarios for the 21st Century. *Ground Water, 50*(1), 37-47. doi: 10.1111/j.1745-6584.2011.00800.x

Lobo-Ferreira, J.-P., Chachadi, A. G., Diamantino, C., & Henriques, M. J. (2005). *Assessing Aquifer Vulnerability to seawater intrusion using GALDIT method: Part 1- Application to the Portuguese Aquifer of Monte Gordo*. Paper presented at the The fourth Inter-Celtic Colloquium on Hydrology and Management of Water Resources, Guimaraes, Portugal.

Magiera, P. (2000). Methoden zur Abschatzung der Verschmutzungsempfind-lichkeit des Grundwassers (Methods for Assessment of Pollution Groundwater Vulnerability). *Grundwasser, 3*.

Marín, A. I., Dörfliger, N., & Andreo, B. (2010). Comparative Application of Two Methods (COP and PaPRIKa) for Groundwater Vulnerability Mapping in the Lez Karst System (Montpellier, South France). In B. Andreo, F. Carrasco, J. J. Durán & J. W. LaMoreaux (Eds.), *Advances in Research in Karst Media* (pp. 329-334): Springer Berlin Heidelberg.

Mary River Catchment Coordinating Committee. (2013). Water Quality Standards.

Metni, M. (2002). *Groundwater in Lebanon: a Vulnerbaility assessment appraoch towards protection.* Master of Science, American University of Beirut, Beirut.

Metni, M., El-Fadel, M., Sadek, S., Kayal, R., & El-Khoury, D. L. (2004). Groundwater Resources in Lebanon: A Vulnerability Assessment. *Water Resources Development, 20*(4), 475-491.

Milnes, E. (2011). Process-based groundwater salinisation risk assessment methodology: Application to the Akrotiri Aquifer (Southern Cyprus). *Journal of Hydrology, 399*, 29-47. doi: 10.1016/j.jhydrol.2010.12.032

Moujabber, M. E., Samra, B. B., Darwish, T., & Atallah, T. (2006). Comparison of Different Indicators for Groundwater Contamination by Seawater Intrusion on the Lebanese Coast. *Water Resources Management, 20*(2), 161-180. doi: 10.1007/s11269-006-7376-4

Murgulet, D., & Tick, G. (2007). The extent of saltwater intrusion in southern Baldwin County, Alabama. *Environmental Geology, 55*(6), 1235-1245. doi: 10.1007/s00254-007-1068-0

Mutua, F., & Kuria, D. (2012). A comparison of spatial rainfall estimation techniques: A case study of Nyando River Basin Kenya. *Journal of Agriculture, Science and Technology, 14*(2), 149-165.

Najib, S., Grozavu, A., Mehdi, K., Breaban, I.-G., Guessir, H., & Boutayeb, K. (2012). Application of the Method GALDIT for the cartography of Groundwater Vulnerability; Aquifer of Chaouia Coast (Morocco). *scientific Annals of "Alaxandru Ioan Cuza"University of IASI, LVIII*(II-c).

Nas, B., & Berktay, A. (2010). Groundwater quality mapping in urban groundwater using GIS. [Research Support, Non-U.S. Gov't]. *Environmental Monitoring and Assessment, 160*(1-4), 215-227. doi: 10.1007/s10661-008-0689-4

Oram, B., Halsor, S., & Redmond, B. (2010). Water Quality: Your Private Well: What do the Results Mean? : Wilkes University.

Ozler, H. M. (2003). hydrochemistry and salt-water intrusion in the Van aquifer, east Turkey. *Environmental Geology, 43*, 759-775.

Panagopoulos, G. P., Antonakos, A. K., & Lambrakls, N. J. (2006). Optimization of the DRASTIC method for groundwater vulnerability assessment via the use of simple statistical methods and GIS. *Hydrogeology Journal, 14*, 894-911. doi: 10.1007/s10040-005-0008-x

Panteleit, B., Hamer, K., Kringel, R., Kessels, W., & Schulz, H. D. (2010). Geochemical processes in the saltwater–freshwater transition zone: comparing results of a sand tank experiment with field data. *Environmental Earth Sciences, 62*(1), 77-91. doi: 10.1007/s12665-010-0499-1

Pera, S., & Valcarce, R. M. (2009). Groundwater vulnerability assessment in La Habana city area, Cuba *Applied Research partnership with developing and transition countries*: Institute of Earth Sciences, Canobbio; Politecnico Jose Antonio Echeveria, La Habana.

Polemio, M., Casarano, D., & Linoni, P. P. (2009). Karstic aquifer vulnerability assessment methods and results at a test site (Apulia, southern Italy). *Natural Hazards and Earth System Sciences, 9*, 1461-1470.

Pulido-Leboeuf, P., Pulido-Bosch, A., Calvache, M. L., Vallejos, Á., & Andreu, J. M. (2003). Strontium, SO42−/Cl− and Mg2+/Ca2+ ratios as tracers for the evolution of seawater into coastal aquifers: the example of Castell de Ferro aquifer (SE Spain). *Comptes Rendus Geoscience, 335*(14), 1039-1048. doi: 10.1016/j.crte.2003.08.004

Rangel-Medina, M., S., R.-M., M., M.-M., & Castillo-Gurrola, J. (2004). Estimation of vulnerbaility to saline intrusion. *Geofisica Internacional, 43*(4), 611-621.

Ranjan, P., Kazama, S., & Sawamoto, M. (2006). Effects of climate change on coastal fresh groundwater resources. *Global Environmental Change, 16*(4), 388-399. doi: http://dx.doi.org/10.1016/j.gloenvcha.2006.03.006

Saadeh, M. (2008). *Influence of Overexploitation and Seawater Intrusion on the Quality of Groundwater in Greater Beirut.* PhD, Alischen Aachen University, Aachen.

SAEFL. (1998). Annex 3: groundwater Vulnerbaility Mapping in Karst Areas - The EPIK Method *Guideline for Groundwater vulnerbaility Mapping and Risk Assessment for the Susceptibility of Groundwater Resources to Contamination*: Technical Cooperation Project Management, Protection and Sustainable Use of Groundwater and Soil Resources in the Arab Region.

Sajil Kumar, P. J., Elango, L., & James, E. J. (2013). Assessment of hydrochemistry and groundwater quality in the coastal area of South Chennai, India. *Arabian Journal of Geosciences*. doi: 10.1007/s12517-013-0940-3

Sajil Kumar, P. J., Jeghathambal, P., & James, E. J. (2011). Multivariate and Geostatistical Analysis of Groundwater Quality in Palar River Basin. *International Journal of Geology, 5*(4), 108-119.

Salemi, E., Colombani, N., Aschonitis, V., & Mastrocicco, M. (2011). Assessment of specific vulnerbaility to nitrates using LOS indices in the Ferrara Province, Italy. In N. Lambrakis, G. Stournaras & K. Katsanou (Eds.), *Advances in the Research of Aquiatic Environment*. New York: Springer.

Selmi, A. (2013). *Water Management and Modelling of a Coastal Aquifer - Case Study (Gaza Strip).* Doctor of Philosphy in Earth Sciences, University of Milan Bicocca.

Sener, E., & Davraz, A. (2012). Assessment of groundwater vulnerability based on a modified DRASTIC model, GIS and an analytic hierarchy process (AHP) method: the case of Egirdir Lake basin (Isparta, Turkey). *Hydrogeology Journal, 21*(3), 701-714. doi: 10.1007/s10040-012-0947-y

Sheikhy Narany, T., Ramli, M. F., Aris, A. Z., Sulaiman, W. N., Juahir, H., & Fakharian, K. (2014). Identification of the hydrogeochemical processes in groundwater using classic integrated geochemical methods and geostatistical techniques, in amol-babol plain, iran. *TheScientificWorldJournal, 2014*, 419058. doi: 10.1155/2014/419058

Shirazi, S. M., imran, H. M., & Akib, S. (2012). GIS-based DRASTIC method for groundwater vulnerbaility assessment: a review. *Journal of Risk Research, 15*(8), 991-1011. doi: 10.1080/13669877.2012.686053

Smith, T. E. (2014). Continuous Spatial Data Analysis. from ESE 502-Penn Engineering http://www.seas.upenn.edu/~ese502/NOTEBOOK/Part_II/4_Variograms.pdf

Tomaszkiewicz, M., Abou Najm, M., & El-Fadel, M. (2014). Development of a groundwater quality index for seawater intrusion in coastal aquifers. *Environmental Modelling & Software, 57*, 13-26. doi: 10.1016/j.envsoft.2014.03.010

Tomaszkiewicz, M., Najm, M. A., & El-Fadel, M. (2013). Development of a Groundwater Quality Index for Seawater Intrusion in Coastal Aquifers (In-press). *Journal of Environmental Modelling and Software*.

UNESCO, WHO, & UNEP. (1996). Water Quality Assessments - A Guide to Use of Biota, Sediments and Water in Environmental Monitoring (second edition). In D. Chapman (Ed.).

United States Environmental Protection Agency. (2003). Drinking Water Advisory: Consumer Acceptability Advice and Health Effects Analysis on Sodium. Washington D.C.: Health and Ecological Criteria Division.

USGS. (2000). Is Seawater Intrusion Affecting Ground Water on Lopez Island, Washington?

Vengosh, A., & Rosenthal, E. (1994). Saline groundwater in Israel: its bearing on the water crisis in the country. *Journal of Hydrology, 156*, 389-430.

Vlaicu, M., & Munteanu, C.-M. (2008). *Karst Groundwaters Vulnerbaility Assessment Methods.* Paper presented at the "Emile Racovitza" Institute of Speology, Bucharest.

Voigt, H.-J., Heinkele, T., Jahnke, C., & Wolter, R. (2004). Characterization of groundwater vulnerbaility to fulfill requirements of the water framework directive of the European Union. *Geoffisca International, 43*(4), 567-574.

Vorosmarty, C. J., Green, P., Salisbury, J., & Lammers, R. B. (2000). Global Water Resources: Vulnerability from Climate Change and Population Growth. *Science, 289*, 284-288.

Voudouris, K., Mandilaras, D., & Antonakos, A. (2004). *Methods to Define the Areal Distribution of the Salt Intrusion: Examples from South Greece.* Paper presented at the 18th SWIM, Cartagena, Spain.

Walthall, C. L., J. Hatfield, P. Backlund, L. Lengnick, E. Marshall, M. Walsh, S. Adkins, M. Aillery, E.A. Ainsworth, , C. Ammann, C. J. A., I. Bartomeus, L.H. Baumgard, F. Booker, B. Bradley, D.M. Blumenthal, J. Bunce, K. Burkey, , S.M. Dabney, J. A. D., J. Dukes, A. Funk, K. Garrett, M. Glenn, D.A. Grantz, D. Goodrich, S. Hu, R.C. Izaurralde, , R.A.C. Jones, S.-H. K., A.D.B. Leaky, K. Lewers, T.L. Mader, A. McClung, J. Morgan, D.J. Muth, M. Nearing, D.M. , Oosterhuis, D. O., C. Parmesan, W.T. Pettigrew, W. Polley, R. Rader, C. Rice, M. Rivington, E. Rosskopf, W.A. Salas, , & L.E. Sollenberger, R. S., C. Stöckle, E.S. Takle, D. Timlin, J.W. White, R. Winfree, L. Wright-Morton, L.H. Ziska. (2012). Climate Change and Agriculture in the United States: Effects and Adaptation *USDA Technical Bulleting 1935* (pp. 186). Washington, DC.

Water Quality Assosciation. (Ed.) (2013). Water Quality Assosiation.

Werner, A. D., Ward, J. D., Morgan, L. K., Simmons, C. T., Robinson, N. I., & Teubner, M. D. (2012). Vulnerability Indicators of Sea Water Intrusion. *Ground Water, 50*(1), 48-58. doi: 10.1111/j.1745-6584.2011.00817.x

WHO. (2003). Chloride in Drinking-water *Background document for development of WHO Guidelines for Drinking-water Quality*.

WHO. (2004). Health risks from drinking demineralised water. In F. Kozisek (Ed.), *Rolling revision of the WHO Guidelines for drinking-water quality*. Geneva.

WHO. (2009). Bromide in drinking-water *Background document for development of WHO Guidelines for Drinking-water Quality*.

WHO. (2011). Hardness in Drinking-water *Background document for development of WHO Guidelines for Drinking-water Quality*.

Ziary, Y., & Safari, H. (2007). *To Compare Two Interpolation Methods: IDW, KRIGING for Providing Properties (Area) Surface Interpolation Map Land Price. District 5, Municipality of Tehran area 1.* Paper presented at the The XXX FIG Working Week and General Assembly : Strategic Integration of Surveying Services, Hong Kong.

5 Annexes

5.1 Annex 1: Detailed explanation on the definitions of EPIK components for the three versions

Process:

1. Produce each subcategory of EPIK as a separate shapefile (it is sometimes required to convert ratsers into polygons), the raster files would have the Cell size=50.
2. The shapefiles per category would be merged (added up) into one shapefile per parameter (4 shapefiles)
3. Reconvert all the shapefiles into raster, to be able to use the raster calculator, that is when the weights would be given per parameter per rank of each sub-category.
4. In case of overlays, the larger Weight gets the priority over the overlay areas
5. For Slope: Interpolation -> topo to raster (50 cell size)
6. Surface -> slope
7. The Int function is the Map Algebra

Parameter		Weight Rank
Epikarst – V1		3
E1	Fractures, developed faults, current/paleo channels/Rivers, flood plains Buffer (500m) around faults Buffer 500m around Rivers	2
E2	Karst outcropping formations	3
E3	The rest of the area, where karstic morphology absent	4

Protective Cover		1
P1	No protective cover (rest of the area)	1
P2	Zones of coast + quaternary cover Dynamic buffer around the coast reaching the eleveation of 100m asl	2
P3	Zones close to water channels 500m buffer around rivers	3
P4	Aquicludes + urban areas except the coast	4
Infiltration[8]		3
I1	Slopes greater than 10% in Karstic area	2
I2	Slopes less than 25% around the coast which is the area between zero m asl and 100 m asl	3
I3	Rest of the area (includes the urbanization)	4
Karst network development		2
K1	Well-developed karst formation (C4, C5, e, J, m2 + Fault buffers) excluding urbanization	1
K2	Poorly developed karst or aquifers (C1, C2, Q, ncg, ml, p) excluding urbanization	2
K3	Rest of the area (bc, bj, bm, bp, C3) + urban areas	3

Parameter		Weight Rank
Epikarst - V2		3
E1	Fractures, developed faults, current/paleo channels/Rivers, flood plains Buffer (500m) around faults Buffer 500m around Rivers	2
E2	Karst outcropping formations	3
E3	The rest of the area, where karstic morphology absent	4
Protective Cover		1
P1	No protective cover (rest of the area	1
P2	Zones of coast + quaternary cover Dynamic buffer around the coast from zero m asl to 100 m asl	2

[8] Slope is calculated from the topographic calculated from the contour of 50m interval. The slope produced first should be converted to non-float raster by using “INT” function in the Map Calculator, then it is a raster which you can convert to polygon, otherwise, the slope file is not converted to polygon to be able to extract or divide and integrate into the categories required.

INT: converts input floating-point values to integer values through truncation

Truncation: removing some of the decimals

P3	Zones close to water channels 500m buffer around rivers	3
P4	Aquicludes	4
Infiltration		3
I1	Slopes greater than 10% in Karstic area	2
I2	Slopes less than 25% around the coast up to 100m asl	3
I3	rest of the area	4
Karst network development		2
K1	Well-developed karst formation (C4, C5, e, J, m2 + Fault buffers) excluding urbanization	1
K2	Poorly developed karst or aquifers (C1, C2, Q, ncg, ml, p) excluding urbanization	2
K3	Rest of the area (bc, bj, bm, bp, C3)	3

Parameter		Weight Rank
Epikarst – V3		3
E1	Fractures, developed faults, current/paleo channels/Rivers, flood plains Buffer (500m) around faults Buffer 500m around Rivers	2
E2	Karst outcropping formations	3
E3	The rest of the area, where karstic morphology absent	4
Protective Cover		1
P1	No protective cover (rest of the area)+urban areas	1
P2	Zones of coast + quaternary cover Dynamic buffer around the coast from zero m asl to 100m asl	2
P3	Zones close to water channels 500m buffer around rivers	3
P4	Aquicludes	4
Infiltration		3
I1	Slopes greater than 10% in Karstic area + coastal urban areas (within the coastal buffer that Is from zero meter asl and 100m asl)	2
I2	Slopes less than 25% around the coast	3
I3	Slopes greater than 25% on aquiclude + rest of the area	4
Karst network development		2
K1	Well-developed karst formation (C4, C5, e, J, m2 + Fault buffers) including coastal urbanization	1
K2	Poorly developed karst or aquifers (C1, C2, Q, ncg, ml, p) excluding urbanization	2
K3	Rest of the area (bc, bj, bm, bp, C3)	3

5.2 Annex 2: DRASTIC ranges for field measured water quality parameters Matching with Metni, (2002) DRASTIC Pollution Protection (PP) ranges

Table 5-1: Field measured Chloride levels (WQ_{Field}) matching with Metni, 2002 DRASTIC Pollution Protection (PP) ranges ($WQ_{DRASTIC}$) for Round 1 Beirut for Chloride

$WQ_{DRASTIC}$ \ WQ_{Field}	Drinking water 1-200	Fresh Water 200-300	Brackish 300-500	Highly Brackish 500-5,000	Saline Water 5,000-15,000	Sea Water 15,000-20,000
Drinking water 27-85						
Fresh Water 86-106	29	20	8	35	10	
Brackish 107-127		1		2		
Highly Brackish 128-148	6		1			
Saline Water 149-169						
Sea Water 170-236		4	3	40	6	
e.g. BEY_R1_DR_Cl	Match	±1	±2	±3	±4/5	Total
Number of wells	20	47	75	19	4	165
Percent per category	12.1	28.5	45.5	11.5	2.4	100.0
Cumulative Percent	12.1	40.6	86.1	97.6	100.0	100.0

Table 5-2: Field measured Chloride levels (WQ_{Field}) matching with Metni, 2002 DRASTIC Pollution Protection (PP) ranges ($WQ_{DRASTIC}$) for Round 1 Beirut for TDS

$WQ_{DRASTIC}$ \ WQ_{Field}	Drinking water 0-500	Fresh Water 500-1,000	Brackish 1,000-5,000	Highly Brackish 5,000-15,000	Saline Water 15,000-30,000	Sea Water 30,000-40,000
Drinking water 27-85						
Fresh Water 86-106	5	43	26	22	6	
Brackish 107-127		1	2			
Highly Brackish 128-148	2	5				
Saline Water 149-169						
Sea Water 170-236	1	2	36	10	4	
BEY_R1_DR_TDS	Match	±1	±2	±3	±4/5	Total

Number of wells	45	36	37	44	3	165
Percent per category	27.3	21.8	22.4	26.7	1.8	100.0
Cumulative Percent	27.3	49.1	71.5	98.2	100	100.0

Table 5-3: Field measured Chloride levels (WQ_{Field}) matching with Metni, 2002 DRASTIC Pollution Protection (PP) ranges ($WQ_{DRASTIC}$) for Round 3 Jal el Dib for Chloride

WQ_{Field} / $WQ_{DRASTIC}$	Drinking water 1-200	Fresh Water 200-300	Brackish 300-500	Highly Brackish 500-5,000	Saline Water 5,000-15,000	Sea Water 15,000-20,000
Drinking water 27-85	1		3			
Fresh Water 86-106						
Brackish 107-127	4	1	9	4		
Highly Brackish 128-148						
Saline Water 149-169						
Sea Water 170-236						
JD_R3_DR_Cl	Match	±1	±2	±3	±4/5	Total
Number of wells	10	5	7	0	0	22
Percent per category	45.5	22.7	31.8	0.0	0.0	100.0
Cumulative Percent	45.5	68.2	100	100	100	100

Table 5-4: Field measured Chloride levels (WQ_{Field}) matching with Metni, 2002 DRASTIC Pollution Protection (PP) ranges ($WQ_{DRASTIC}$) for Round 3 Jal el Dib for TDS

WQ_{Field} / $WQ_{DRASTIC}$	Drinking water 0-500	Fresh Water 500-1,000	Brackish 1,000-5,000	Highly Brackish 5,000-15,000	Saline Water 15,000-30,000	Sea Water 30,000-40,000
Drinking water 27-85		4				
Fresh Water 86-106						
Brackish 107-127	2	11	5			
Highly Brackish 128-148						
Saline Water 149-169						
Sea Water 170-236						
JD_R3_DR_TDS	Match	±1	±2	±3	±4/5	Total
Number of wells	45	36	37	44	3	165
Percent per category	27.3	21.8	22.4	26.7	1.8	100.0

Cumulative Percent	22.7	90.9	100	100	100	100

Table 5-5: Field measured Chloride levels (WQ_{Field}) matching with Metni, 2002 DRASTIC Pollution Protection (PP) ranges ($WQ_{DRASTIC}$) for Round 7 Jal el Dib for Chloride

$WQ_{DRASTIC}$ \ WQ_{Field}	Drinking water 1-200	Fresh Water 200-300	Brackish 300-500	Highly Brackish 500-5,000	Saline Water 5,000-15,000	Sea Water 15,000-20,000
Drinking water 27-85		2	2	3		
Fresh Water 86-106	1					
Brackish 107-127		4	4	10		
Highly Brackish 128-148						
Saline Water 149-169			1			
Sea Water 170-236						

JD_R3_DR_Cl	Match	±1	±2	±3	±4/5	Total
Number of wells	4	17	3	3	0	27
Percent per category	14.8	63.0	11.1	11.1	0.0	100.0
Cumulative Percent	14.8	77.8	88.9	100	100	100

Table 5-6: Field measured Chloride levels (WQ_{Field}) matching with Metni, 2002 DRASTIC Pollution Protection (PP) ranges ($WQ_{DRASTIC}$) for Round 7 Jal el Dib for TDS

$WQ_{DRASTIC}$ \ WQ_{Field}	Drinking water 0-500	Fresh Water 500-1,000	Brackish 1,000-5,000	Highly Brackish 5,000-15,000	Saline Water 15,000-30,000	Sea Water 30,000-40,000
Drinking water 27-85		2	5			
Fresh Water 86-106		1				
Brackish 107-127		4	14			
Highly Brackish 128-148						
Saline Water 149-169		1				
Sea Water 170-236						

JD_R7_DR_TDS	Match	±1	±2	±3	±4/5	Total
Number of wells	15	6	5	1	0	27
Percent per category	55.6	22.2	18.5	3.7	0.0	100.0
Cumulative Percent	55.6	77.8	96.3	100	100	100

Table 5-7: Field measured Chloride levels (WQ_{Field}) matching with Metni, 2002 DRASTIC Pollution Protection (PP) ranges ($WQ_{DRASTIC}$) for Round 1 Tripoli for Chloride

$WQ_{DRASTIC}$ \ WQ_{Field}	Drinking water 1-200	Fresh Water 200-300	Brackish 300-500	Highly Brackish 500-5,000	Saline Water 5,000-15,000	Sea Water 15,000-20,000
Drinking water 27-85		2	5			
Fresh Water 86-106		1				
Brackish 107-127		4	14			
Highly Brackish 128-148						
Saline Water 149-169		1				
Sea Water 170-236						

JD_R3_DR_Cl	Match	±1	±2	±3	±4/5	Total
Number of wells	17	11	30	7	0	65
Percent per category	26.2	16.9	46.2	10.7	0	100
Cumulative Percent	26.2	43.1	89.3	100	100	100

Table 5-8: Field measured Chloride levels (WQ_{Field}) matching with Metni, 2002 DRASTIC Pollution Protection (PP) ranges ($WQ_{DRASTIC}$) for Round 1 Tripoli for TDS

$WQ_{DRASTIC}$ \ WQ_{Field}	Drinking water 0-500	Fresh Water 500-1,000	Brackish 1,000-5,000	Highly Brackish 5,000-15,000	Saline Water 15,000-30,000	Sea Water 30,000-40,000
Drinking water 27-85		2	5			
Fresh Water 86-106		1				
Brackish 107-127		4	14			
Highly Brackish 128-148						
Saline Water 149-169		1				
Sea Water 170-236						

TRP_R1_DR_TDS	Match	±1	±2	±3	±4/5	Total
Number of wells	5	28	22	5	0	60
Percent per category	8.3	46.7	36.7	8.3	0.0	100.0
Cumulative Percent	8.3	55	91.7	100	100	100

Table 5-9: Field measured Chloride levels (WQ_{Field}) matching with Metni, 2002 DRASTIC Pollution Protection (PP) ranges ($WQ_{DRASTIC}$) for Round 2 Tripoli for Chloride

$WQ_{DRASTIC}$ \ WQ_{Field}	Drinking water 1-200	Fresh Water 200-300	Brackish 300-500	Highly Brackish 500-5,000	Saline Water 5,000-15,000	Sea Water 15,000-20,000
Drinking water 27-85	4					
Fresh Water 86-106	5					
Brackish 107-127	30		4	3		
Highly Brackish 128-148	9		2	3		
Saline Water 149-169						
Sea Water 170-236						

TRP_R2_DR_Cl	Match	±1	±2	±3	±4/5	Total
Number of wells	11	10	30	9	0	60
Percent per category	18.3	16.7	50.0	15.0	0.0	100.0
Cumulative Percent	18.3	35	85	100	100	100

Table 5-10: Field measured Chloride levels (WQ_{Field}) matching with Metni, 2002 DRASTIC Pollution Protection (PP) ranges ($WQ_{DRASTIC}$) for Round 2 Tripoli for TDS

$WQ_{DRASTIC}$ \ WQ_{Field}	Drinking water 0-500	Fresh Water 500-1,000	Brackish 1,000-5,000	Highly Brackish 5,000-15,000	Saline Water 15,000-30,000	Sea Water 30,000-40,000
Drinking water 27-85	1	3				
Fresh Water 86-106	3	1	1			
Brackish 107-127	26	8	3			
Highly Brackish 128-148	8	3	3			
Saline Water 149-169						
Sea Water 170-236						

TRP_R1_DR_TDS	Match	±1	±2	±3	±4/5	Total
Number of wells	5	18	29	8	0	60
Percent per category	8.3	30.0	48.3	13.3	0.0	100.0
Cumulative Percent	8.3	38.3	86.6	100	100	100

5.3 Annex 3: Error of 3% calculated for field measured (Cl & TDS)

5.3.1 Jal el Dib

Table 5-11: Jal el Dib R3 Chloride measurements with the ±3% error margin

Cl (mg/L)	+3%	-3%
102.1	105.2	99.0
113.0	116.4	109.6
128.0	131.8	124.2
153.0	157.6	148.4
153.5	158.1	148.9
220.5	227.1	213.9
284.0	292.5	275.5
356.0	366.7	345.3
389.0	400.7	377.3
391.0	402.7	379.3
407.0	419.2	394.8
409.0	421.3	396.7
421.0	433.6	408.4
424.5	437.2	411.8
432.0	445.0	419.0
447.0	460.4	433.6
450.0	463.5	436.5
461.0	474.8	447.2
484.0	498.5	469.5
564.0	580.9	547.1
574.0	591.2	556.8
717.5	739.0	696.0
756.5	779.2	733.8

Table 5-12: Jal el Dib R3 TDS measurements with the ±3% error margin

TDS (ppm)	+3%	-3%
427.0	439.8	414.2
430.0	442.9	417.1
509.0	524.3	493.7
545.0	561.4	528.7
577.0	594.3	559.7

TDS (ppm)	+3%	-3%
689.0	709.7	668.3
821.0	845.6	796.4
826.0	850.8	801.2
848.0	873.4	822.6
849.0	874.5	823.5
856.0	881.7	830.3
892.0	918.8	865.2
915.0	942.5	887.6
937.0	965.1	908.9
951.0	979.5	922.5
960.0	988.8	931.2
979.0	1,008.4	949.6
987.0	1,016.6	957.4
1,320.0	1,359.6	1,280.4
1,410.0	1,452.3	1,367.7
1,640.0	1,689.2	1,590.8
1,900.0	1,957.0	1,843.0
4,400.0	4,532.0	4,268.0

Table 5-13: Jal el Dib R7 Chloride measurements with the ±3% error margin

Cl^-	+3%	-3%
180	185.4	174.6
230	236.9	223.1
235	242.05	227.95
255	262.65	247.35
285	293.55	276.45
285	293.55	276.45
290	298.7	281.3
320	329.6	310.4
320	329.6	310.4
335	345.05	324.95
375	386.25	363.75
420	432.6	407.4
420	432.6	407.4
480	494.4	465.6
515	530.45	499.55
530	545.9	514.1
560	576.8	543.2

Cl^-	+3%	-3%
595	612.85	577.15
610	628.3	591.7
710	731.3	688.7
720	741.6	698.4
735	757.05	712.95
815	839.45	790.55
880	906.4	853.6
945	973.35	916.65
1040	1071.2	1008.8
1670	1720.1	1619.9

Table 5-14: Jal el Dib R7 TDS measurements with the ±3% error margin

TDS	+3%	-3%
659.2	678.976	639.424
659.2	678.976	639.424
691.8	712.554	671.046
699.2	720.176	678.224
816.7	841.201	792.199
863.3	889.199	837.401
866.2	892.186	840.214
879.3	905.679	852.921
1024.8	1055.544	994.056
1047.6	1079.028	1016.172
1103.2	1136.296	1070.104
1114.6	1148.038	1081.162
1114.6	1148.038	1081.162
1155.8	1190.474	1121.126
1195.4	1231.262	1159.538
1260.2	1298.006	1222.394
1264.5	1302.435	1226.565
1355.6	1396.268	1314.932
1397.5	1439.425	1355.575
1479.6	1523.988	1435.212
1900.9	1957.927	1843.873
1955.2	2013.856	1896.544
1955.2	2013.856	1896.544
2103.8	2166.914	2040.686
2451.7	2525.251	2378.149
2478.3	2552.649	2403.951

TDS	+3%	-3%
3485.7	3590.271	3381.129

5.3.2 Beirut

Table 5-15: Beirut R1 Cl^- measurements with the ±3% error margin

Cl^-	+3%	-3%
100	103	97
100	103	97
100	103	97
110	113.3	106.7
115	118.45	111.55
115	118.45	111.55
115	118.45	111.55
127	130.81	123.19
135	139.05	130.95
135	139.05	130.95
135	139.05	130.95
135	139.05	130.95
145	149.35	140.65
150	154.5	145.5
150	154.5	145.5
155	159.65	150.35
155	159.65	150.35
155	159.65	150.35
160	164.8	155.2
160	164.8	155.2
160	164.8	155.2
160	164.8	155.2
160	164.8	155.2
160	164.8	155.2
165	169.95	160.05
165	169.95	160.05
165	169.95	160.05
165	169.95	160.05
170	175.1	164.9
175	180.25	169.75
180	185.4	174.6
185	190.55	179.45
185	190.55	179.45

Cl^-	+3%	-3%
190	195.7	184.3
190	195.7	184.3
205	211.15	198.85
215	221.45	208.55
215	221.45	208.55
216	222.48	209.52
220	226.6	213.4
225	231.75	218.25
225	231.75	218.25
230	236.9	223.1
245	252.35	237.65
250	257.5	242.5
250	257.5	242.5
250	257.5	242.5
255	262.65	247.35
255	262.65	247.35
255	262.65	247.35
260	267.8	252.2
265	272.95	257.05
265	272.95	257.05
280	288.4	271.6
280	288.4	271.6
280	288.4	271.6
285	293.55	276.45
285	293.55	276.45
290	298.7	281.3
290	298.7	281.3
325	334.75	315.25
370	381.1	358.9
400	412	388
400	412	388
400	412	388
410	422.3	397.7
430	442.9	417.1
465	478.95	451.05
485	499.55	470.45
485	499.55	470.45
485	499.55	470.45
490	504.7	475.3
505	520.15	489.85

Cl^-	+3%	-3%
505	520.15	489.85
510	525.3	494.7
590	607.7	572.3
590	607.7	572.3
595	612.85	577.15
615	633.45	596.55
615	633.45	596.55
620	638.6	601.4
625	643.75	606.25
685	705.55	664.45
765	787.95	742.05
895	921.85	868.15
910	937.3	882.7
930	957.9	902.1
935	963.05	906.95
940	968.2	911.8
945	973.35	916.65
965	993.95	936.05
995	1024.85	965.15
1010	1040.3	979.7
1090	1122.7	1057.3
1115	1148.45	1081.55
1125	1158.75	1091.25
1220	1256.6	1183.4
1240	1277.2	1202.8
1259	1296.77	1221.23
1350	1390.5	1309.5
1355	1395.65	1314.35
1385	1426.55	1343.45
1390	1431.7	1348.3
1420	1462.6	1377.4
1435	1478.05	1391.95
1460	1503.8	1416.2
1530	1575.9	1484.1
1570	1617.1	1522.9
1585	1632.55	1537.45
1610	1658.3	1561.7
1625	1673.75	1576.25
1640	1689.2	1590.8
1670	1720.1	1619.9

Cl^-	+3%	-3%
1670	1720.1	1619.9
1685	1735.55	1634.45
1740	1792.2	1687.8
1760	1812.8	1707.2
1820	1874.6	1765.4
1900	1957	1843
1915	1972.45	1857.55
1930	1987.9	1872.1
2160	2224.8	2095.2
2190	2255.7	2124.3
2225	2291.75	2158.25
2225	2291.75	2158.25
2260	2327.8	2192.2
2340	2410.2	2269.8
2360	2430.8	2289.2
2550	2626.5	2473.5
2625	2703.75	2546.25
2685	2765.55	2604.45
2765	2847.95	2682.05
2785	2868.55	2701.45
2815	2899.45	2730.55
3015	3105.45	2924.55
3140	3234.2	3045.8
3240	3337.2	3142.8
3345	3445.35	3244.65
3355	3455.65	3254.35
3475	3579.25	3370.75
3490	3594.7	3385.3
3735	3847.05	3622.95
3768	3881.04	3654.96
4010	4130.3	3889.7
4540	4676.2	4403.8
4555	4691.65	4418.35
4595	4732.85	4457.15
4665	4804.95	4525.05
4925	5072.75	4777.25
5275	5433.25	5116.75
5910	6087.3	5732.7
6115	6298.45	5931.55
7040	7251.2	6828.8

Cl⁻	+3%	-3%
7240	7457.2	7022.8
7265	7482.95	7047.05
7720	7951.6	7488.4
8000	8240	7760
8890	9156.7	8623.3
8900	9167	8633
10655	10974.65	10335.35
11240	11577.2	10902.8
12565	12941.95	12188.05
13080	13472.4	12687.6
13575	13982.25	13167.75
15000	15450	14550

Table 5-16: Beirut R1 TDS measurements with the ±3% error margin

TDS	+3%	-3%
398.6	410.5	386.6
401.7	413.7	389.6
415.6	428.1	403.1
423.3	436.0	410.6
449.5	463.0	436.0
486.2	500.8	471.6
487.7	502.4	473.1
499.9	514.9	484.9
518.1	533.7	502.6
522.7	538.4	507.0
527.2	543.0	511.4
565.0	581.9	548.0
578.5	595.9	561.2
578.5	595.9	561.2
586.0	603.6	568.4
586.0	603.6	568.4
598.0	616.0	580.1
604.0	622.1	585.9
616.0	634.5	597.5
624.9	643.7	606.2
628.7	647.5	609.8
629.4	648.3	610.5
643.6	662.9	624.3
647.3	666.7	627.9

648.8	668.2	629.3
648.8	668.2	629.3
650.3	669.8	630.8
651.8	671.3	632.2
651.8	671.3	632.2
662.2	682.0	642.3
662.2	682.0	642.3
666.6	686.6	646.6
668.1	688.1	648.1
669.6	689.7	649.5
672.5	692.7	652.4
680.0	700.4	659.6
696.3	717.1	675.4
709.6	730.8	688.3
714.0	735.4	692.6
716.9	738.4	695.4
727.3	749.1	705.4
727.3	749.1	705.4
728.0	749.8	706.2
741.2	763.5	719.0
743.5	765.8	721.1
784.5	808.1	761.0
794.8	818.6	770.9
797.7	821.6	773.8
797.7	821.6	773.8
798.4	822.4	774.5
824.7	849.5	800.0
835.7	860.7	810.6
842.9	868.2	817.6
892.3	919.1	865.5
925.6	953.3	897.8
932.8	960.8	904.8
945.0	973.4	916.7
973.1	1,002.3	943.9
983.2	1,012.7	953.7
1,060.5	1,092.3	1,028.7
1,081.9	1,114.3	1,049.4
1,093.3	1,126.1	1,060.5
1,160.0	1,194.8	1,125.2
1,258.8	1,296.6	1,221.1
1,306.6	1,345.8	1,267.4

1,328.3	1,368.2	1,288.5
1,359.8	1,400.6	1,319.0
1,361.2	1,402.0	1,320.4
1,370.3	1,411.4	1,329.2
1,467.1	1,511.1	1,423.1
1,517.0	1,562.5	1,471.5
1,723.6	1,775.3	1,671.9
1,764.6	1,817.6	1,711.7
1,778.3	1,831.6	1,725.0
1,805.6	1,859.8	1,751.4
1,846.5	1,901.9	1,791.1
1,860.1	1,915.9	1,804.3
1,873.7	1,929.9	1,817.5
1,887.3	1,943.9	1,830.7
1,914.5	1,971.9	1,857.1
1,995.8	2,055.7	1,936.0
2,009.4	2,069.6	1,949.1
2,036.4	2,097.5	1,975.3
2,076.9	2,139.2	2,014.6
2,117.3	2,180.8	2,053.8
2,157.7	2,222.4	2,092.9
2,265.0	2,332.9	2,197.0
2,571.2	2,648.3	2,494.0
2,571.2	2,648.3	2,494.0
2,624.1	2,702.8	2,545.4
2,663.7	2,743.6	2,583.8
2,703.3	2,784.4	2,622.2
2,703.3	2,784.4	2,622.2
2,756.0	2,838.7	2,673.3
2,808.7	2,892.9	2,724.4
2,913.6	3,001.1	2,826.2
2,979.0	3,068.4	2,889.6
2,992.2	3,082.0	2,902.4
3,265.7	3,363.7	3,167.8
3,317.6	3,417.1	3,218.1
3,382.4	3,483.8	3,280.9
3,395.3	3,497.2	3,293.4
3,434.1	3,537.1	3,331.1
3,601.7	3,709.8	3,493.7
3,614.6	3,723.1	3,506.2
3,666.1	3,776.0	3,556.1

3,768.8	3,881.8	3,655.7
3,768.8	3,881.8	3,655.7
3,807.2	3,921.4	3,693.0
3,922.4	4,040.0	3,804.7
3,947.9	4,066.3	3,829.5
3,999.0	4,118.9	3,879.0
4,050.0	4,171.5	3,928.5
4,113.7	4,237.1	3,990.2
4,228.1	4,354.9	4,101.2
4,228.1	4,354.9	4,101.2
4,405.5	4,537.7	4,273.4
4,582.4	4,719.9	4,444.9
4,695.8	4,836.6	4,554.9
4,808.9	4,953.2	4,664.7
4,808.9	4,953.2	4,664.7
4,946.9	5,095.3	4,798.5
4,997.0	5,146.9	4,847.1
5,084.6	5,237.1	4,932.1
5,097.1	5,250.0	4,944.2
5,246.9	5,404.3	5,089.5
5,383.9	5,545.4	5,222.4
5,383.9	5,545.4	5,222.4
5,681.8	5,852.3	5,511.3
5,768.4	5,941.5	5,595.4
5,780.8	5,954.2	5,607.4
5,892.0	6,068.8	5,715.2
5,892.0	6,068.8	5,715.2
6,163.1	6,348.0	5,978.2
6,200.0	6,386.0	6,014.0
6,384.2	6,575.7	6,192.6
6,726.8	6,928.6	6,525.0
6,970.6	7,179.7	6,761.5
7,140.8	7,355.0	6,926.6
7,262.2	7,480.1	7,044.3
7,322.8	7,542.5	7,103.1
7,407.6	7,629.9	7,185.4
8,251.4	8,498.9	8,003.8
8,335.3	8,585.4	8,085.3
8,395.3	8,647.1	8,143.4
8,574.8	8,832.1	8,317.6
8,837.6	9,102.8	8,572.5

8,861.5	9,127.3	8,595.6
9,373.1	9,654.3	9,091.9
10,929.7	11,257.6	10,601.8
11,794.0	12,147.8	11,440.1
11,875.4	12,231.7	11,519.2
12,084.7	12,447.3	11,722.2
12,235.7	12,602.8	11,868.6
14,173.1	14,598.3	13,748.0
15,201.7	15,657.8	14,745.7
16,337.7	16,827.8	15,847.6
17,016.1	17,526.6	16,505.6
19,149.7	19,724.2	18,575.2
20,041.9	20,643.2	19,440.7
20,264.5	20,872.4	19,656.5
21,041.7	21,673.0	20,410.5
21,484.8	22,129.3	20,840.2
23,798.5	24,512.5	23,084.5
28,263.1	29,111.0	27,415.2

5.3.3 Tripoli

Table 5-17: Tripoli R1 Cl^- measurements with the ±3% error margin

Cl^-	3%	-3%
29	29.87	28.13
58	59.74	56.26
70	72.1	67.9
80	82.4	77.6
80	82.4	77.6
80	82.4	77.6
80	82.4	77.6
80	82.4	77.6
90	92.7	87.3
90	92.7	87.3
90	92.7	87.3
90	92.7	87.3
90	92.7	87.3
100	103	97
100	103	97

Cl^-	3%	-3%
100	103	97
100	103	97
100	103	97
100	103	97
110	113.3	106.7
110	113.3	106.7
110	113.3	106.7
110	113.3	106.7
110	113.3	106.7
110	113.3	106.7
110	113.3	106.7
110	113.3	106.7
110	113.3	106.7
120	123.6	116.4
120	123.6	116.4
120	123.6	116.4
120	123.6	116.4
120	123.6	116.4
120	123.6	116.4
120	123.6	116.4
130	133.9	126.1
130	133.9	126.1
130	133.9	126.1
150	154.5	145.5
170	175.1	164.9
180	185.4	174.6
200	206	194
200	206	194
210	216.3	203.7
220	226.6	213.4
280	288.4	271.6
300	309	291
320	329.6	310.4
330	339.9	320.1
330	339.9	320.1
360	370.8	349.2
390	401.7	378.3
410	422.3	397.7
410	422.3	397.7
410	422.3	397.7

Cl^-	3%	-3%
470	484.1	455.9
490	504.7	475.3
780	803.4	756.6
950	978.5	921.5
1610	1658.3	1561.7

Table 5-18: Tripoli R1 TDS measurements with the ±3% error margin

TDS	3%	-3%
209	215.27	202.73
210	216.3	203.7
218	224.54	211.46
228	234.84	221.16
241	248.23	233.77
244	251.32	236.68
251	258.53	243.47
259	266.77	251.23
264	271.92	256.08
271	279.13	262.87
275	283.25	266.75
301	310.03	291.97
328	337.84	318.16
336	346.08	325.92
343	353.29	332.71
352	362.56	341.44
365	375.95	354.05
393	404.79	381.21
394	405.82	382.18
400	412	388
403	415.09	390.91
409	421.27	396.73
429	441.87	416.13
434	447.02	420.98
440	453.2	426.8
442	455.26	428.74
468	482.04	453.96
477	491.31	462.69
490	504.7	475.3
490	504.7	475.3
496	510.88	481.12

TDS	3%	-3%
511	526.33	495.67
512	527.36	496.64
525	540.75	509.25
533	548.99	517.01
540	556.2	523.8
540	556.2	523.8
546	562.38	529.62
564	580.92	547.08
566	582.98	549.02
585	602.55	567.45
601	619.03	582.97
631	649.93	612.07
674	694.22	653.78
700	721	679
746	768.38	723.62
750	772.5	727.5
786	809.58	762.42
820	844.6	795.4
874	900.22	847.78
885	911.55	858.45
908	935.24	880.76
946	974.38	917.62
1350	1390.5	1309.5
1360	1400.8	1319.2
1490	1534.7	1445.3
1500	1545	1455
1500	1545	1455
2130	2193.9	2066.1
3420	3522.6	3317.4

Table 5-19: Tripoli R2 Cl^- measurements with the ±3% error margin

Cl^-	3%	-3%
33	33.99	32.01
36	37.08	34.92
40	41.2	38.8
43	44.29	41.71
50	51.5	48.5
50	51.5	48.5
53	54.59	51.41

Cl^-	3%	-3%
54	55.62	52.38
55	56.65	53.35
57	58.71	55.29
57	58.71	55.29
58	59.74	56.26
60	61.8	58.2
60	61.8	58.2
63	64.89	61.11
63	64.89	61.11
64	65.92	62.08
65	66.95	63.05
66	67.98	64.02
66	67.98	64.02
67	69.01	64.99
69	71.07	66.93
70	72.1	67.9
70	72.1	67.9
72	74.16	69.84
74	76.22	71.78
79	81.37	76.63
80	82.4	77.6
82	84.46	79.54
84	86.52	81.48
85	87.55	82.45
92	94.76	89.24
94	96.82	91.18
97	99.91	94.09
100	103	97
104	107.12	100.88
115	118.45	111.55
116	119.48	112.52
126	129.78	122.22
130	133.9	126.1
152	156.56	147.44
154	158.62	149.38
159	163.77	154.23
160	164.8	155.2
162	166.86	157.14
195	200.85	189.15
224	230.72	217.28

Cl^-	3%	-3%
304	313.12	294.88
308	317.24	298.76
310	319.3	300.7
350	360.5	339.5
420	432.6	407.4
468	482.04	453.96
550	566.5	533.5
580	597.4	562.6
600	618	582
750	772.5	727.5
1180	1215.4	1144.6
1600	1648	1552
1950	2008.5	1891.5

Table 5-20: Tripoli R2 TDS measurements with the ±3% error margin

TDS	3%	-3%
270	278.1	261.9
274	282.22	265.78
285	293.55	276.45
288	296.64	279.36
288	296.64	279.36
291	299.73	282.27
337	347.11	326.89
344	354.32	333.68
345	355.35	334.65
349	359.47	338.53
360	370.8	349.2
377	388.31	365.69
380	391.4	368.6
381	392.43	369.57
400	412	388
404	416.12	391.88
406	418.18	393.82
408	420.24	395.76
408	420.24	395.76
412	424.36	399.64
412	424.36	399.64
415	427.45	402.55
422	434.66	409.34

TDS	3%	-3%
437	450.11	423.89
444	457.32	430.68
449	462.47	435.53
453	466.59	439.41
454	467.62	440.38
456	469.68	442.32
459	472.77	445.23
462	475.86	448.14
466	479.98	452.02
469	483.07	454.93
476	490.28	461.72
484	498.52	469.48
486	500.58	471.42
490	504.7	475.3
499	513.97	484.03
511	526.33	495.67
520	535.6	504.4
521	536.63	505.37
541	557.23	524.77
545	561.35	528.65
584	601.52	566.48
658	677.74	638.26
663	682.89	643.11
742	764.26	719.74
750	772.5	727.5
752	774.56	729.44
867	893.01	840.99
965	993.95	936.05
980	1009.4	950.6
992	1021.76	962.24
1040	1071.2	1008.8
1050	1081.5	1018.5
1250	1287.5	1212.5
1980	2039.4	1920.6
2210	2276.3	2143.7
2750	2832.5	2667.5
3460	3563.8	3356.2

5.4 Annex 4: EPIK ranges for field measured water quality parameters matching with the Protection Factor (PF) ranges of three versions of EPIK

5.4.1 EPIK Version 1

Table 5-21: Field measurements (WQ_{Field}) matching with EPIK Protection Factor (WQ_{EPIK}) ranges Version 1 produced by this study for Round 1 Beirut for Chloride

WQ_{EPIK} \ WQ_{Field}	Drinking water 1-200	Fresh Water 200-300	Brackish 300-500	Highly Brackish 500-5,000	Saline Water 5,000-15,000	Sea Water 15,000-20,000
Drinking water 27-85						
Fresh Water 86-106	8	3	3			
Brackish 107-127	7	7	2	36	10	
Highly Brackish 128-148	8	6	3	23	1	
Saline Water 149-169	12	9	4	18	5	
Sea Water 170-236						
BEY_R1_EP1_Cl	Match	±1	±2	±3	±4/5	Total
Number of wells	33	76	27	17	12	165
Percent per category	20	46.1	16.4	10.3	7.2	100
Cumulative Percent	20	66.1	82.5	92.8	100	100

Table 5-22: Field measurements (WQ_{Field}) matching with EPIK Protection Factor (WQ_{EPIK}) ranges Version 1 produced by this study for Round 1 Beirut for TDS

WQ_{EPIK} \ WQ_{Field}	Drinking water 0-500	Fresh Water 500-1,000	Brackish 1,000-5,000	Highly Brackish 5,000-15,000	Saline Water 15,000-30,000	Sea Water 30,000-40,000
Drinking water 27-85						
Fresh Water 86-106		8	6			
Brackish 107-127	2	12	24	18	6	
Highly Brackish	4	11	21	4	1	

128-148						
Saline Water 149-169	2	20	13	10	3	
Sea Water 170-236						
BEY_R1_EP1_TDS	Match	±1	±2	±3	±4/5	Total
Number of wells	39	68	32	24	2	165
Percent per category	23.6	41.2	19.4	14.5	1.3	100.0
Cumulative Percent	23.6	64.8	84.2	98.7	100	100

Table 5-23: Field measurements (WQ_{Field}) matching with EPIK Protection Factor (WQ_{EPIK}) ranges Version 1 produced by this study for Round 3 Jal el Dib for Chloride

WQ_{Field} / WQ_{EPIK}	Drinking water 1-200	Fresh Water 200-300	Brackish 300-500	Highly Brackish 500-5,000	Saline Water 5,000-15,000	Sea Water 15,000-20,000
Drinking water 27-85						
Fresh Water 86-106						
Brackish 107-127			1			
Highly Brackish 128-148	5	1	11	4		
Saline Water 149-169						
Sea Water 170-236						
BEY_R1_EP1_Cl	Match	±1	±2	±3	±4/5	Total
Number of wells	5	11	1	5	0	22
Percent per category	22.7	50	4.5	22.8	0	100
Cumulative Percent	22.7	72.7	77.2	100	100	100

Table 5-24: Field measurements (WQ_{Field}) matching with EPIK Protection Factor (WQ_{EPIK}) ranges Version 1 produced by this study for Round 3 Jal el Dib for TDS

WQ_{Field} / WQ_{EPIK}	Drinking water 0-500	Fresh Water 500-1,000	Brackish 1,000-5,000	Highly Brackish 5,000-15,000	Saline Water 15,000-30,000	Sea Water 30,000-40,000
Drinking water 27-85						
Fresh Water 86-106		1				

Brackish 107-127	2	14	5			
Highly Brackish 128-148						
Saline Water 149-169						
Sea Water 170-236						
JD_R3_EP1_TDS	Match	±1	±2	±3	±4/5	Total
Number of wells	6	14	2	0	0	22
Percent per category	27.3	63.6	9.1	0	0	100
Cumulative Percent	27.3	90.9	100	100	100	100

Table 5-25: Field measurements (WQ_{Field}) matching with EPIK Protection Factor (WQ_{EPIK}) ranges Version 1 produced by this study for Round 7 Jal el Dib for Chloride

WQ_{Field} / WQ_{EPIK}	Drinking water 1-200	Fresh Water 200-300	Brackish 300-500	Highly Brackish 500-5,000	Saline Water 5,000-15,000	Sea Water 15,000-20,000
Drinking water 27-85						
Fresh Water 86-106	1	1	2			
Brackish 107-127		5	5	13		
Highly Brackish 128-148						
Saline Water 149-169						
Sea Water 170-236						
JD_R7_EP1_Cl	Match	±1	±2	±3	±4/5	Total
Number of wells	6	21	0	0	0	27
Percent per category	22.2	77.8	0	0	0	100
Cumulative Percent	22.2	100	100	100	100	100

Table 5-26: Field measurements (WQ_{Field}) matching with EPIK Protection Factor (WQ_{EPIK}) ranges Version 1 produced by this study for Round 7 Jal el Dib for TDS

WQ_{Field} / WQ_{EPIK}	Drinking water 0-500	Fresh Water 500-1,000	Brackish 1,000-5,000	Highly Brackish 5,000-15,000	Saline Water 15,000-30,000	Sea Water 30,000-40,000
Drinking water 27-85						

Fresh Water 86-106		3	1			
Brackish 107-127		5	18			
Highly Brackish 128-148						
Saline Water 149-169						
Sea Water 170-236						
JD_R7_EP1_TDS	Match	±1	±2	±3	±4/5	Total
Number of wells	21	6	0	0	0	27
Percent per category	77.8	22.2	0.0	0.0	0.0	100.0
Cumulative Percent	77.8	100	100	100	100	100

Table 5-27: Field measurements (WQ_{Field}) matching with EPIK Protection Factor (WQ_{EPIK}) ranges Version 1 produced by this study for Round 1 Tripoli for Chloride

WQField / WQEPIK	Drinking water 1-200	Fresh Water 200-300	Brackish 300-500	Highly Brackish 500-5,000	Saline Water 5,000-15,000	Sea Water 15,000-20,000
Drinking water 27-85						
Fresh Water 86-106	1					
Brackish 107-127	37	4	10	3		
Highly Brackish 128-148	5					
Saline Water 149-169						
Sea Water 170-236						
TRP_R1_EP1_Cl	Match	±1	±2	±3	±4/5	Total
Number of wells	10	8	37	5	0	60
Percent per category	16.7	13.3	61.7	8.3	0.0	100.0
Cumulative Percent	16.7	30	91.7	100	100	100

Table 5-28: Field measurements (WQ_{Field}) matching with EPIK Protection Factor (WQ_{EPIK}) ranges Version 1 produced by this study for Round 1 Tripoli for TDS

WQField / WQEPIK	Drinking water 0-500	Fresh Water 500-1,000	Brackish 1,000-5,000	Highly Brackish 5,000-15,000	Saline Water 15,000-30,000	Sea Water 30,000-40,000

Drinking water 27-85						
Fresh Water 86-106	1					
Brackish 107-127	24	22	7			
Highly Brackish 128-148	6					
Saline Water 149-169						
Sea Water 170-236						
TRP_R1_EP1_TDS	Match	±1	±2	±3	±4/5	Total
Number of wells	7	23	24	6	0	60
Percent per category	11.7	38.3	40.0	10.0	0.0	100.0
Cumulative Percent	11.7	50	90	100	100	100

Table 5-29: Field measurements (WQ_{Field}) matching with EPIK Protection Factor (WQ_{EPIK}) ranges Version 1 produced by this study for Round 2 Tripoli for Chloride

WQ_{Field} / WQ_{EPIK}	Drinking water 1-200	Fresh Water 200-300	Brackish 300-500	Highly Brackish 500-5,000	Saline Water 5,000-15,000	Sea Water 15,000-20,000
Drinking water 27-85						
Fresh Water 86-106	1					
Brackish 107-127	39	1	5	7		
Highly Brackish 128-148	6		1			
Saline Water 149-169						
Sea Water 170-236						
TRP_R2_EP1_Cl	Match	±1	±2	±3	±4/5	Total
Number of wells	5	10	39	6	0	60
Percent per category	8.3	16.7	65.0	10.0	0.0	100.0
Cumulative Percent	8.3	25	90	100	100	100

Table 5-30: Field measurements (WQ_{Field}) matching with EPIK Protection Factor (WQ_{EPIK}) ranges Version 1 produced by this study for Round 2 Tripoli for TDS

WQ_{Field} / WQ_{EPIK}	Drinking water	Fresh Water	Brackish 1,000-	Highly Brackish	Saline Water	Sea Water 30,000-

	0-500	500-1,000	5,000	5,000-15,000	15,000-30,000	40,000
Drinking water 27-85						
Fresh Water 86-106	1					
Brackish 107-127	31	14	7			
Highly Brackish 128-148	6	1				
Saline Water 149-169						
Sea Water 170-236						
TRP_R2_EP1_TDS	Match	±1	±2	±3	±4/5	Total
Number of wells	7	15	32	6	0	60
Percent per category	11.7	25.0	53.3	10.0	0.0	100.0
Cumulative Percent	11.7	36.7	90	100	100	100

5.4.2 EPIK Version 2

Table 5-31: Field measurements (WQ_{Field}) matching with EPIK Protection Factor (WQ_{EPIK}) ranges Version 2 produced by this study for Round 1 Beirut for Chloride

WQ_{Field} / WQ_{EPIK}	Drinking water 1-200	Fresh Water 200-300	Brackish 300-500	Highly Brackish 500-5,000	Saline Water 5,000-15,000	Sea Water 15,000-20,000
Drinking water 27-85						
Fresh Water 86-106	8	3	3			
Brackish 107-127	8	7	4	37	11	
Highly Brackish 128-148	9	6	3	26	1	
Saline Water 149-169	10	9	2	14	4	
Sea Water 170-236						
BEY_R1_EP2_Cl	Match	±1	±2	±3	±4/5	Total
Number of wells	37	73	27	18	10	165
Percent per category	22.4	44.2	16.4	10.9	6.1	100.0
Cumulative Percent	22.4	66.6	83	93.9	100	100

Table 5-32: Field measurements (WQ_{Field}) matching with EPIK Protection Factor (WQ_{EPIK}) ranges Version 2 produced by this study for Round 1 Beirut for TDS

WQ_{EPIK} \ WQ_{Field}	Drinking water 0-500	Fresh Water 500-1,000	Brackish 1,000-5,000	Highly Brackish 5,000-15,000	Saline Water 15,000-30,000	Sea Water 30,000-40,000
Drinking water 27-85						
Fresh Water 86-106		8	6			
Brackish 107-127	2	14	25	19	7	
Highly Brackish 128-148	4	12	23	5	1	
Saline Water 149-169	2	17	10	8	2	
Sea Water 170-236						
BEY_R1_EP2_TDS	Match	±1	±2	±3	±4/5	Total
Number of wells	40	71	31	21	2	165
Percent per category	24.2	43.0	18.8	12.7	1.3	100.0
Cumulative Percent	24.2	67.2	86	98.7	100	100

Table 5-33: Field measurements (WQ_{Field}) matching with EPIK Protection Factor (WQ_{EPIK}) ranges Version 2 produced by this study for Round 3 Jal el Dib for Chloride

WQ_{EPIK} \ WQ_{Field}	Drinking water 1-200	Fresh Water 200-300	Brackish 300-500	Highly Brackish 500-5,000	Saline Water 5,000-15,000	Sea Water 15,000-20,000
Drinking water 27-85						
Fresh Water 86-106						
Brackish 107-127			1			
Highly Brackish 128-148	5	1	11	4		
Saline Water 149-169						
Sea Water 170-236						
JD_R3_EP2_Cl	Match	±1	±2	±3	±4/5	Total
Number of wells	5	11	1	5	0	22
Percent per category	22.7	50	4.5	22.8	0	100.0
Cumulative Percent	22.7	72.7	77.2	100	100	100

Table 5-34: Field measurements (WQ_{Field}) matching with EPIK Protection Factor (WQ_{EPIK}) ranges Version 2 produced by this study for Round 3 Jal el Dib for TDS

WQ_{EPIK} \ WQ_{Field}	Drinking water 0-500	Fresh Water 500-1,000	Brackish 1,000-5,000	Highly Brackish 5,000-15,000	Saline Water 15,000-30,000	Sea Water 30,000-40,000
Drinking water 27-85						
Fresh Water 86-106		1				
Brackish 107-127	2	14	5			
Highly Brackish 128-148						
Saline Water 149-169						
Sea Water 170-236						
JD_R3_EP2_TDS	Match	±1	±2	±3	±4/5	Total
Number of wells	6	14	2	0	0	22
Percent per category	27.3	63.6	9.1	0	0	100
Cumulative Percent	27.3	90.9	100	100	100	100

Table 5-35: Field measurements (WQ_{Field}) matching with EPIK Protection Factor (WQ_{EPIK}) ranges Version 2 produced by this study for Round 7 Jal el Dib for Chloride

WQ_{EPIK} \ WQ_{Field}	Drinking water 1-200	Fresh Water 200-300	Brackish 300-500	Highly Brackish 500-5,000	Saline Water 5,000-15,000	Sea Water 15,000-20,000
Drinking water 27-85						
Fresh Water 86-106	1	1	2			
Brackish 107-127		5	5	13		
Highly Brackish 128-148						
Saline Water 149-169						
Sea Water 170-236						
JD_R7_EP2_Cl	Match	±1	±2	±3	±4/5	Total
Number of wells	6	21	0	0	0	27
Percent per category	22.2	77.8	0	0	0	100

Cumulative Percent	22.2	100	100	100	100	100

Table 5-36: Field measurements (WQ_{Field}) matching with EPIK Protection Factor (WQ_{EPIK}) ranges Version 2 produced by this study for Round 7 Jal el Dib for TDS

WQ_{Field} / WQ_{EPIK}	Drinking water 0-500	Fresh Water 500-1,000	Brackish 1,000-5,000	Highly Brackish 5,000-15,000	Saline Water 15,000-30,000	Sea Water 30,000-40,000
Drinking water 27-85						
Fresh Water 86-106		3	1			
Brackish 107-127		5	18			
Highly Brackish 128-148						
Saline Water 149-169						
Sea Water 170-236						
JD_R7_EP2_TDS	Match	±1	±2	±3	±4/5	Total
Number of wells	21	6	0	0	0	27
Percent per category	77.8	22.2	0	0	0	100
Cumulative Percent	77.8	100	100	100	100	100

Table 5-37: Field measurements (WQ_{Field}) matching with EPIK Protection Factor (WQ_{EPIK}) ranges Version 2 produced by this study for Round 1 Tripoli for Chloride

WQ_{Field} / WQ_{EPIK}	Drinking water 1-200	Fresh Water 200-300	Brackish 300-500	Highly Brackish 500-5,000	Saline Water 5,000-15,000	Sea Water 15,000-20,000
Drinking water 27-85						
Fresh Water 86-106	1					
Brackish 107-127	38	4	10	3		
Highly Brackish 128-148	4					
Saline Water 149-169						
Sea Water 170-236						
TRP_R1_EP2_Cl	Match	±1	±2	±3	±4/5	Total
Number of wells	10	8	38	4	0	60

Percent per category	16.7	13.3	63.3	6.7	0	100
Cumulative Percent	16.7	30	93.3	100	100	100

Table 5-38: Field measurements (WQ_{Field}) matching with EPIK Protection Factor (WQ_{EPIK}) ranges Version 2 produced by this study for Round 1 Tripoli for TDS

WQ_{EPIK} \ WQ_{Field}	Drinking water 0-500	Fresh Water 500-1,000	Brackish 1,000-5,000	Highly Brackish 5,000-15,000	Saline Water 15,000-30,000	Sea Water 30,000-40,000
Drinking water 27-85						
Fresh Water 86-106	1					
Brackish 107-127	25	22	7			
Highly Brackish 128-148	5					
Saline Water 149-169						
Sea Water 170-236						
TRP_R1_EP2_TDS	Match	±1	±2	±3	±4/5	Total
Number of wells	7	23	25	5	0	60
Percent per category	11.7	38.3	41.7	8.3	0	100
Cumulative Percent	11.7	50	91.7	100	100	100

Table 5-39: Field measurements (WQ_{Field}) matching with EPIK Protection Factor (WQ_{EPIK}) ranges Version 2 produced by this study for Round 2 Tripoli for Chloride

WQ_{EPIK} \ WQ_{Field}	Drinking water 1-200	Fresh Water 200-300	Brackish 300-500	Highly Brackish 500-5,000	Saline Water 5,000-15,000	Sea Water 15,000-20,000
Drinking water 27-85						
Fresh Water 86-106	1					
Brackish 107-127	40	1	5	7		
Highly Brackish 128-148	5		1			
Saline Water 149-169						
Sea Water 170-236						
TRP_R2_EP2_Cl	Match	±1	±2	±3	±4/5	Total

Number of wells	5	10	40	5	0	60
Percent per category	8.3	16.7	66.7	8.3	0	100
Cumulative Percent	8.3	25	91.7	100	100	100

Table 5-40: Field measurements (WQ_{Field}) matching with EPIK Protection Factor (WQ_{EPIK}) ranges Version 2 produced by this study for Round 2 Tripoli for TDS

WQ_{Field} / WQ_{EPIK}	Drinking water 0-500	Fresh Water 500-1,000	Brackish 1,000-5,000	Highly Brackish 5,000-15,000	Saline Water 15,000-30,000	Sea Water 30,000-40,000
Drinking water 27-85						
Fresh Water 86-106	1					
Brackish 107-127	32	14	7			
Highly Brackish 128-148	5	1				
Saline Water 149-169						
Sea Water 170-236						
TRP_R2_EP2_TDS	Match	±1	±2	±3	±4/5	Total
Number of wells	7	15	33	5	0	60
Percent per category	11.7	25	55	8.3	0	100
Cumulative Percent	11.7	36.7	91.7	100	100	100

5.4.3 EPIK Version 3

Table 5-41: Field measurements (WQ_{Field}) matching with EPIK Protection Factor (WQ_{EPIK}) ranges Version 3 produced by this study for Round 1 Beirut for Chloride

WQ_{Field} / WQ_{EPIK}	Drinking water 1-200	Fresh Water 200-300	Brackish 300-500	Highly Brackish 500-5,000	Saline Water 5,000-15,000	Sea Water 15,000-20,000
Drinking water 27-85						
Fresh Water 86-106						
Brackish 107-127						
Highly Brackish 128-148	14	9	5	34	10	
Saline Water 149-169	8	5	3	25	1	

Sea Water 170-236	13	11	4	18	5	
BEY_R1_EP3_Cl	Match	±1	±2	±3	±4/5	Total
Number of wells	35	45	30	23	32	165
Percent per category	21.2	27.3	18.2	13.9	19.4	100
Cumulative Percent	21.2	48.5	66.7	80.6	100	100

Table 5-42: Field measurements (WQ_{Field}) matching with EPIK Protection Factor (WQ_{EPIK}) ranges Version 3 produced by this study for Round 1 Beirut for TDS

WQ_{Field} / WQ_{EPIK}	Drinking water 0-500	Fresh Water 500-1,000	Brackish 1,000-5,000	Highly Brackish 5,000-15,000	Saline Water 15,000-30,000	Sea Water 30,000-40,000
Drinking water 27-85						
Fresh Water 86-106						
Brackish 107-127						
Highly Brackish 128-148	2	18	29	17	6	
Saline Water 149-169	4	10	22	5	1	
Sea Water 170-236	2	23	13	10	3	
BEY_R1_EP3_TDS	Match	±1	±2	±3	±4/5	Total
Number of wells	18	43	50	25	29	165
Percent per category	10.9	26.1	30.3	15.2	17.5	100
Cumulative Percent	10.9	37	67.3	82.5	100	100

Table 5-43: Field measurements (WQ_{Field}) matching with EPIK Protection Factor (WQ_{EPIK}) ranges Version 3 produced by this study for Round 3 Jal el Dib for Chloride

WQ_{Field} / WQ_{EPIK}	Drinking water 1-200	Fresh Water 200-300	Brackish 300-500	Highly Brackish 500-5,000	Saline Water 5,000-15,000	Sea Water 15,000-20,000
Drinking water 27-85						

Fresh Water 86-106						
Brackish 107-127			1	1		
Highly Brackish 128-148	5	1	11	3		
Saline Water 149-169						
Sea Water 170-236						
JD_R3_EP3_Cl	Match	±1	±2	±3	±4/5	Total
Number of wells	4	12	1	5	0	22
Percent per category	18.2	54.5	4.5	22.8	0	100
Cumulative Percent	18.2	72.7	77.2	100	100	100

Table 5-44: Field measurements (WQ_{Field}) matching with EPIK Protection Factor (WQ_{EPIK}) ranges Version 3 produced by this study for Round 3 Jal el Dib for TDS

WQ_{Field} / WQ_{EPIK}	Drinking water 0-500	Fresh Water 500-1,000	Brackish 1,000-5,000	Highly Brackish 5,000-15,000	Saline Water 15,000-30,000	Sea Water 30,000-40,000
Drinking water 27-85						
Fresh Water 86-106						
Brackish 107-127		1	1			
Highly Brackish 128-148	2	14	4			
Saline Water 149-169						
Sea Water 170-236						
JD_R3_EP3_TDS	Match	±1	±2	±3	±4/5	Total
Number of wells	1	5	14	2	0	22
Percent per category	4.5	22.7	63.6	9.2	0	100
Cumulative Percent	4.5	27.2	90.8	100	100	100

Table 5-45: Field measurements (WQ_{Field}) matching with EPIK Protection Factor (WQ_{EPIK}) ranges Version 3 produced by this study for Round 7 Jal el Dib for Chloride

WQ_{Field}	Drinking	Fresh	Brackish	Highly	Saline	Sea Water

WQEPIK	water 1-200	Water 200-300	300-500	Brackish 500-5,000	Water 5,000-15,000	15,000-20,000
Drinking water 27-85						
Fresh Water 86-106	1					
Brackish 107-127		1		2		
Highly Brackish 128-148		5	7	11		
Saline Water 149-169						
Sea Water 170-236						
JD_R7_EP3_Cl	Match	±1	±2	±3	±4/5	Total
Number of wells	11	11	5	0	0	27
Percent per category	40.7	40.7	18.6	0	0	100
Cumulative Percent	40.7	81.4	100	100	100	100

Table 5-46: Field measurements (WQ_{Field}) matching with EPIK Protection Factor (WQ_{EPIK}) ranges Version 3 produced by this study for Round 7 Jal el Dib for TDS

WQField / WQEPIK	Drinking water 0-500	Fresh Water 500-1,000	Brackish 1,000-5,000	Highly Brackish 5,000-15,000	Saline Water 15,000-30,000	Sea Water 30,000-40,000
Drinking water 27-85						
Fresh Water 86-106		1				
Brackish 107-127		1	2			
Highly Brackish 128-148		6	17			
Saline Water 149-169						
Sea Water 170-236						
JD_R7_EP3_TDS	Match	±1	±2	±3	±4/5	Total
Number of wells	3	18	6	0	0	27
Percent per category	11.1	66.7	22.2	0	0	100
Cumulative Percent	11.1	77.8	100	100	100	100

Table 5-47: Field measurements (WQ_{Field}) matching with EPIK Protection Factor (WQ_{EPIK}) ranges Version 3 produced by this study for Round 1 Tripoli for Chloride

WQ_{EPIK} \ WQ_{Field}	Drinking water 1-200	Fresh Water 200-300	Brackish 300-500	Highly Brackish 500-5,000	Saline Water 5,000-15,000	Sea Water 15,000-20,000
Drinking water 27-85						
Fresh Water 86-106	1					
Brackish 107-127	7	2	3			
Highly Brackish 128-148	31	2	6	3		
Saline Water 149-169	2					
Sea Water 170-236	2		1			
TRP_R1_EP3_Cl	Match	±1	±2	±3	±4/5	Total
Number of wells	6	9	9	32	4	60
Percent per category	10	15	15	53.3	6.7	100
Cumulative Percent	10	25	40	93.3	100	100

Table 5-48: Field measurements (WQ_{Field}) matching with EPIK Protection Factor (WQ_{EPIK}) ranges Version 3 produced by this study for Round 1 Tripoli for TDS

WQ_{EPIK} \ WQ_{Field}	Drinking water 0-500	Fresh Water 500-1,000	Brackish 1,000-5,000	Highly Brackish 5,000-15,000	Saline Water 15,000-30,000	Sea Water 30,000-40,000
Drinking water 27-85						
Fresh Water 86-106	1					
Brackish 107-127	4	8				
Highly Brackish 128-148	22	13	7			
Saline Water 149-169	2					
Sea Water 170-236	2	1				
TRP_R1_EP3_TDS	Match	±1	±2	±3	±4/5	Total
Number of wells	0	16	17	22	5	60
Percent per category	0	26.7	28.3	36.7	8.3	100
Cumulative Percent	0	26.7	55	91.7	100	100

Table 5-49: Field measurements (WQ_{Field}) matching with EPIK Protection Factor (WQ_{EPIK}) ranges Version 3 produced by this study for Round 2 Tripoli Tripoli for Chloride

WQ_{EPIK} \ WQ_{Field}	Drinking water 1-200	Fresh Water 200-300	Brackish 300-500	Highly Brackish 500-5,000	Saline Water 5,000-15,000	Sea Water 15,000-20,000
Drinking water 27-85						
Fresh Water 86-106	1					
Brackish 107-127	11		1			
Highly Brackish 128-148	30	1	4	7		
Saline Water 149-169	2					
Sea Water 170-236	2		1			
TRP_R2_EP3_Cl	Match	±1	±2	±3	±4/5	Total
Number of wells	8	5	12	31	4	60
Percent per category	13.3	8.3	20	51.7	6.7	100
Cumulative Percent	13.3	21.6	41.6	93.3	100	100

Table 5-50: Field measurements (WQ_{Field}) matching with EPIK Protection Factor (WQ_{EPIK}) ranges Version 3 produced by this study for Round 2 Tripoli for TDS

WQ_{EPIK} \ WQ_{Field}	Drinking water 0-500	Fresh Water 500-1,000	Brackish 1,000-5,000	Highly Brackish 5,000-15,000	Saline Water 15,000-30,000	Sea Water 30,000-40,000
Drinking water 27-85						
Fresh Water 86-106	1					
Brackish 107-127	8	4				
Highly Brackish 128-148	25	10	7			
Saline Water 149-169	2					
Sea Water 170-236	2	1				
TRP_R2_EP3_TDS	Match	±1	±2	±3	±4/5	Total
Number of wells	0	12	18	25	5	60
Percent per category	0	20	30	41.7	8.3	100

Cumulative Percent	0	20	50	91.7	100	100

5.5 Annex 5: Validation of water quality assessment interpolation methods

The main disadvantage of water quality assessment interpolation methods is in the process of interpolation itself. An estimation of an unknown value is produced based on the neighboring known points by different mathematical formulas which include many assumptions. In order to validate the extent of accuracy of the conducted interpolations "Leave-one-out" cross-validation technique was used for all the sampled wells. After this cross-validation technique, the percentage of error is calculated using the produced difference between the interpolated value and the field-measured value along with other statistical indicators that would assess the accuracy of the interpolation technique used.

For this study, after conducting the 78 scenarios per city, the results and maps are first checked visually, later using Leave-one-out cross-validation method 4 statistical indicators RSR, CV, PBIAS, and RMS- (Ahmadian, 2013; Delbari, et al., 2013; Nas & Berktay, 2010).

RMSE-observations standard deviation of data ratio (RSR): the lower the value, the more accurate the prediction (interpolation)

$$RSR = \frac{RMSE}{\sigma} = \sqrt{\frac{\sum_{i=1}^{N}(So_i - Ss_i)^2}{\sum_{i=1}^{N}(So_i - \bar{S}o)^2}}$$

Where So_i is the field measured parameter, and Ss_i is the interpolated value for that point, N is number of sampled wells, and $\bar{S}o$ is the mean of the measured parameter and σ is the standard deviation of the measured points.

Coefficient of variation (CV): is the Root Mean Square value divided by the average of the measured data, the lower the value the better the performance of the model or the interpolation.

$$CV = \frac{RMS}{\overline{So}}$$

Per cent bias (PBIAS): It is the Percent BIAS. Calculated "sum of the error (difference between measured and predicted)x100/average of data without transformation" The optimal value of PBIAS is 0. Positive values indicate the model‘s tendency to underestimate, and negative values indicate that the model has a tendency to overestimate.

$$PBIAS = \frac{\sum_{i=1}^{N}(So_i - Ss_i) \times 100}{\sum_{i=1}^{N}(So_i)}$$

Root-Mean-Square Standardized (RMS Standardized): It is the Root Mean square divided by the standard Error. The root mean square standardized error should be close to 1 if the prediction standard errors are valid. If the root mean square standardized error is greater than 1, you are underestimating the variability in your predictions. If the root mean square standardized error is less than 1, you are overestimating the variability in your predictions.

$$RMS - S = \sqrt{\frac{\sum_{i=1}^{N}[{(\bar{S}s_i - Ss_i)}/{\bar{\sigma}s_i}]^2}{N}}$$

5.6 Annex 6: Multi-Contaminant quality indicator

Table 5-51: calculations of GQI

$CI = \frac{X' - X}{X' + X}$	**CI**= concentration index, value between -1 and 1 **X'**= the measured concentration **X**= WHO standard value
$R = 0.5 \times CI^2 + 4.5 \times CI + 5$	**R**= rank of vulnerability with min=1 and max=10 **CI**= -1 R=1 **CI**=0 R=5 **CI**=1 R=10
$GQI = 100 - \frac{R_1 w_1 + R_2 w_2 + \cdots + R_n w_n}{N}$	GQI value between 1 and 100. 1 low quality index, 100 high quality index color codes: red for low quality index, light blue for high quality index w, stands for the relative weight of the parameter N is the total number of parameters used in the suitability analyses.
$w = R + 2$	Weighting the parameters that have higher impact on the health

Source: Babiker, et al., 2006

Table 5-52: WHO standards

Parameters (Unit)	WHO standard
Cl (mg/L)	200
Ca (mg/L)	300
Mg (mg/L)	300
pH	6.5-8.5
EC (uS)	0-800
TDS (ppm)	600
Nitrates (mg/L)	50
Sulfates (mg/L)	250
Na (mg/L)	200
K (mg/L)	300
Br (mg/L)	8.5
Alkalinity CO_3 (mg/L CO_3)	100
Alkalinity HCO_3 (mg/L CO_3)	350

Source: Foster & Hirata, 1988; Mary River Catchment Coordinating Committee, 2013; UNESCO et al., 1996; United States Environmental Protection Agency, 2003; Water Quality Assosciation, 2013; WHO, 2004, 2009, 2011

Groundwater Quality index for Sea Water intrusion (GQI_{SWI}): The concept of this method is similar to GQI; however, it has been produced specifically for sea water intrusion. The formulas differ (**Error! Reference source not found.**). The calculated GQI_{SWI} values ould be plotted versus the produced GQI, to estimate the salinity level as a percent; the higher the index, the lower the salinity percentage.

Table 5-53: Calculation of GQISWI

$f_{sea} = \frac{m_{Cl,sample} - m_{Cl,fresh}}{m_{Cl,sea} - m_{Cl,fresh}}$
$GQI_{cation} = \begin{cases} (1 - \%(Na^{+} + K^{+}))x50 \;\; if \%Ca^{2+} < 50\% \\ (1 - \%Mg^{2+})x50 \; if \; \%Ca^{2+} \geq 50\% \end{cases}$
$GQI_{cation} = \begin{cases} \left(1 + \%\left(CO_{3}{}^{2+} + HCO_{3}{}^{-}\right)\right)x50 \;\; if \%Cl^{-} < 50\% \\ (\%SO_{4}{}^{2-})x50 \; if \; \%Cl^{-} \geq 50\% \end{cases}$
$GQI_{cation} = \begin{cases} \left(\frac{20,000 - EC}{20,000 - 200}\right) \;\; if \; 200 \leq EC \leq 20,000 \\ 0 \; if \; EC > 20,000 \end{cases}$
$GQI_{SWI} = \frac{GQI_{cation} + GQI_{anion} + GQI_{EC}}{2}$

5.7 Annex 7: Semivariogram Models

The Spherical model is the most widely used model; it assumes a correlation that reaches to zero value at extremely large distances. The exponential model assumes that the correlation between two points at larger distances asymptotically reaches zero (Bohling, 2005a; Delbari, et al., 2013; Smith, 2014). The formulas and the graphical representation of each of these models are shown in Figure 5-1 and Figure 5-2.

Spherical variogram model
$$\begin{cases} c\,(1.5\left(\frac{h}{a}\right) - 0.5\,(\frac{h}{a})^3) \text{ if } h \leq a \\ \text{c otherwise} \end{cases}$$

Exponential variogram model $g(h) = (1 - \exp(\frac{-3h}{a}))$

Gaussian Variogram Model $g(h) = (1 - \exp\left(\frac{-3h^2}{a^2}\right))$

Figure 5-1: Formulas for different variogram models

Where *g(h)* is the function of the model *c* is the nugget effect, *h* is the lag distance, *a* is the range of influence.

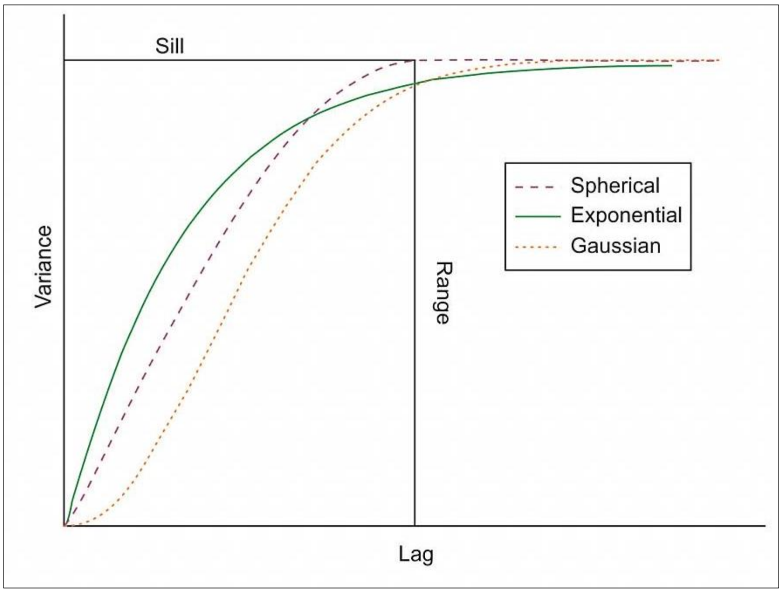

Figure 5-2: General representations of variograms of the three models (Delbari, et al., 2013; Smith, 2014)

5.8 Annex 8: Interpolation Methods

5.8.1 Inverse Distance Weight

IDW is an interpolation method in which the influence of one point on another decreases with the increasing distance between them.

$$Z_o = \frac{\sum_{i=1}^{N} Z_i d_1^{-n}}{\sum_{i=1}^{N} d_i^{-n}}$$

Where Z_o = the estimation value of variable z in point *i*; Z_i = sample value in point *i*; d_i = the distance of sample point to estimated point and N = A coefficient that determines weigh based on a distance.

Although IDW was proven to be less accurate than kriging, it is considered the simplest and most straight-forward interpolation method and it has been widely used in the reviewed references, therefore for this study IDW was chosen as one of the interpolation methods (Bajjali, 2005; Hu, 1995; Kura, et al., 2014; Mutua & Kuria, 2012; Ziary & Safari, 2007). In

ArcGIS Geostatistical Analyst tool, the default settings for the number of neighbouring points that has effect on a chosen point varies with the input data, whereas the power value is fixed for all datasets, and it is 2[9]. For this study, the default settings for number of neighbours and power values are used.

5.8.2 Kriging interpolation

Kriging is a method of interpolation that assumes that two points close to each are more similar to each other than with those that are further. It is an interpolation method which smoothens out the peaks of the dataset, it reduces the data-clustering affect by reducing the weight of points within a specific cluster (Bohling, 2005b; Sajil Kumar, et al., 2011). It is commonly used in hydrological and environmental parameter interpolation and with the rise ArcGIS use Kriging has become even more popular (Kura, et al., 2014 Stein 1999 and Yamamoto 2000 as cited in Nas & Berktay, 2010 and Table 2-1). The advantage of this method is that it is flexible with the required input, on the other hand, the disadvantage of Kriging that it does not prioritize the measuring points but smoothens the whole surface (Delbari, et al., 2013; Kura, et al., 2014; Nas & Berktay, 2010).

$$\hat{Z}(S_0) = \sum_{i=1}^{N} \lambda_i Z(S_i)$$

[9] The weights that are used in relation to the distance between two points in IDW, is raised to a value (power), it could control the extent of weight per point over a certain distance. Which is the power, when the value is 2 (Inverse Distance squared Weighted interpolation). For more flexible and accurate power value, the RMSPE (root mean square prediction error) should be the lowest

Where $Z(S_i)$ is the measured value at the *i*th location, λ_i = an unknown weight for the measured value at the *i*th location, S_0= the prediction location and N= the number of measured values.

ArcGIS has the default setting for this interpolation method, with anisotropy as False, Stable semivariogram model, and default calculated setting of nugget and Lag which varies depending on the dataset. For this study, the variogram model and the isotropy were altered, but the nugget and lag values were kept default varying with the dataset.

5.8.3 Co-Kriging

In previous work which applied all interpolation methods and compared the results, stated that co-kriging produced the best results for cross-validation test (Ahmadian, 2013; Arslan, 2012). **Co-Kriging** is a multi-variable interpolation method (Ahmadian, 2013). There would be a one main variable to which the other variables are cross-correlated. In this method the ESDA should be done for all variables, and evaluate the link between the co-variants the primary, if there is no link, than the method would be autocorrelation of the primary variable and the result would be similar to Ordinary Kriging, thus no improvements in the interpolation results.

$$Z^*(x_0) = \sum_{i=1} \lambda_{1i} Z_1(x_i) + \sum_{j=1} \lambda_{2j}\, Z_2(x_j)$$

Where x_0 is the variant and λ_{1i} is the principle measuring parameter and λ_{2j} are supplementary parameters. For this study, several variations (variables/ semivariograms/transformation) of Co-Kriging method are used and it would be based on the validation exercises that the improvement of the results would be evaluated. The principle measurement for this study was the Chloride Concentration and GQI_{swi} (when available), and the covariants well depth, hydraulic conductivity and distance to shoreline.

5.9 Annex 9: List of all 380 scenarios conducted and validated

The 380 scenarios are listed in with a coding system that is shown in Table 5-54 showing the code name of each scenario, and the relevant codes for each interpolation and vulnerability assessment methodology, semivariogram model, transformation and city in addition to the parameters analyzed are shown in Table 5-55.

Table 5-54: List of all the Interpolation scenarios conducted for this study (Total of 380) with their respective names in the agreed codes

PARAMETER	INTERPOLATION	SEMIVARIOGRAM	TRANFORMATION	JAL EL DIB ROUND 3	JAL EL DIB ROUND 7	BEIRUT ROUND 1	TRIPOLI ROUND 1	TRIPOLI ROUND 2
Cl	Kriging	Spherical	No Transformation	JD_R3_Kr_S_N_Cl	JD_R7_Kr_S_N_Cl	BEY_R1_Kr_S_N_Cl	TRP_R1_Kr_S_N_Cl	TRP_R2_Kr_S_N_Cl
	Kriging	Spherical	Log Transformation	JD_R3_Kr_S_L_Cl	JD_R7_Kr_S_L_Cl	BEY_R1_Kr_S_L_Cl	TRP_R1_Kr_S_L_Cl	TRP_R2_Kr_S_L_Cl
	Kriging	Exponential	No Transformation	JD_R3_Kr_E_N_Cl	JD_R7_Kr_E_N_Cl	BEY_R1_Kr_E_N_Cl	TRP_R1_Kr_E_N_Cl	TRP_R2_Kr_E_N_Cl
	Kriging	Exponential	Log Transformation	JD_R3_Kr_E_L_Cl	JD_R7_Kr_E_L_Cl	BEY_R1_Kr_E_L_Cl	TRP_R1_Kr_E_L_Cl	TRP_R2_Kr_E_L_Cl
	IDW	-	-	JD_R3_IDW_Cl	JD_R7_IDW_Cl	BEY_R1_IDW_Cl	TRP_R1_IDW_Cl	TRP_R2_IDW_Cl
TDS	Kriging	Spherical	No Transformation	JD_R3_Kr_S_N_TDS	JD_R7_Kr_S_N_TDS	BEY_R1_Kr_S_N_TDS	TRP_R1_Kr_S_N_TDS	TRP_R2_Kr_S_N_TDS
	Kriging	Spherical	Log Transformation	JD_R3_Kr_S_L_TDS	JD_R7_Kr_S_L_TDS	BEY_R1_Kr_S_L_TDS	TRP_R1_Kr_S_L_TDS	TRP_R2_Kr_S_L_TDS
	Kriging	Exponential	No Transformation	JD_R3_Kr_E_N_TDS	JD_R7_Kr_E_N_TDS	BEY_R1_Kr_E_N_TDS	TRP_R1_Kr_E_N_TDS	TRP_R2_Kr_E_N_TDS
	Kriging	Exponential	Log Transformation	JD_R3_Kr_E_L_TDS	JD_R7_Kr_E_L_TDS	BEY_R1_Kr_E_L_TDS	TRP_R1_Kr_E_L_TDS	TRP_R2_Kr_E_L_TDS
	IDW	-	-	JD_R3_IDW_TDS	JD_R7_IDW_TDS	BEY_R1_IDW_TDS	TRP_R1_IDW_TDS	TRP_R2_IDW_TDS
GQI	Kriging	Spherical	No Transformation	JD_R3_Kr_S_N_GQI	JD_R7_Kr_S_N_GQI	BEY_R1_Kr_S_N_GQI	TRP_R1_Kr_S_N_GQI	TRP_R2_Kr_S_N_GQI
	Kriging	Spherical	Log Transformation	JD_R3_Kr_S_L_GQI	JD_R7_Kr_S_L_GQI	BEY_R1_Kr_S_L_GQI	TRP_R1_Kr_S_L_GQI	TRP_R2_Kr_S_L_GQI
	Kriging	Exponential	No Transformation	JD_R3_Kr_E_N_GQI	JD_R7_Kr_E_N_GQI	BEY_R1_Kr_E_N_GQI	TRP_R1_Kr_E_N_GQI	TRP_R2_Kr_E_N_GQI
	Kriging	Exponential	Log Transformation	JD_R3_Kr_E_L_GQI	JD_R7_Kr_E_L_GQI	BEY_R1_Kr_E_L_GQI	TRP_R1_Kr_E_L_GQI	TRP_R2_Kr_E_L_GQI
	IDW	-	-	JD_R3_IDW_GQI	JD_R7_IDW_GQI	BEY_R1_IDW_GQI	TRP_R1_IDW_GQI	TRP_R2_IDW_GQI
GQISWI	Kriging	Spherical	No Transformation	JD_R3_Kr_S_N_GQISWI	JD_R7_Kr_S_N_GQISWI	BEY_R1_Kr_S_N_GQISWI	TRP_R1_Kr_S_N_GQISWI	TRP_R2_Kr_S_N_GQISWI
	Kriging	Spherical	Log Transformation	JD_R3_Kr_S_L_GQISWI	JD_R7_Kr_S_L_GQISWI	BEY_R1_Kr_S_L_GQISWI	TRP_R1_Kr_S_L_GQISWI	TRP_R2_Kr_S_L_GQISWI
	Kriging	Exponential	No Transformation	JD_R3_Kr_E_N_GQISWI	JD_R7_Kr_E_N_GQISWI	BEY_R1_Kr_E_N_GQISWI	TRP_R1_Kr_E_N_GQISWI	TRP_R2_Kr_E_N_GQISWI
	Kriging	Exponential	Log Transformation	JD_R3_Kr_E_L_GQISWI	JD_R7_Kr_E_L_GQISWI	BEY_R1_Kr_E_L_GQISWI	TRP_R1_Kr_E_L_GQISWI	TRP_R2_Kr_E_L_GQISWI
	IDW	-	-	JD_R3_IDW_GQISWI	JD_R7_IDW_GQISWI	BEY_R1_IDW_GQISWI	TRP_R1_IDW_GQISWI	TRP_R2_IDW_GQISWI
Cl	Co-Kriging	Spherical	No Transformation	JD_R3_CK_S_NNN_Cl	JD_R7_CK_S_NNN_Cl	BEY_R1_CK_S_NNN_Cl	TRP_R1_CK_S_NNN_Cl	TRP_R2_CK_S_NNN_Cl
Well Depth			No Transformation					
Distance from Coast			No Transformation					
Cl	Co-Kriging	Spherical	No Transformation	JD_R3_CK_S_NLN_Cl	JD_R7_CK_S_NLN_Cl	BEY_R1_CK_S_NLN_Cl	TRP_R1_CK_S_NLN_Cl	TRP_R2_CK_S_NLN_Cl
Well Depth			Log Transformation					
Distance from Coast			No Transformation					
Cl	Co-Kriging	Spherical	Log Transformation	JD_R3_CK_S_LNN_Cl	JD_R7_CK_S_LNN_Cl	BEY_R1_CK_S_LNN_Cl	TRP_R1_CK_S_LNN_Cl	TRP_R2_CK_S_LNN_Cl
Well Depth			No Transformation					
Distance from Coast			No Transformation					
Cl	Co-Kriging	Spherical	Log Transformation	JD_R3_CK_S_LLN_Cl	JD_R7_CK_S_LLN_Cl	BEY_R1_CK_S_LLN_Cl	TRP_R1_CK_S_LLN_Cl	TRP_R2_CK_S_LLN_Cl
Well Depth			Log Transformation					
Distance from Coast			No Transformation					
Cl	Co-Kriging	Spherical	No Transformation	JD_R3_CK_S_NNL_Cl	JD_R7_CK_S_NNL_Cl	BEY_R1_CK_S_NNL_Cl	TRP_R1_CK_S_NNL_Cl	TRP_R2_CK_S_NNL_Cl
Well Depth			No Transformation					
Distance from Coast			Log Transformation					
Cl	Co-Kriging	Spherical	No Transformation	JD_R3_CK_S_NLL_Cl	JD_R7_CK_S_NLL_Cl	BEY_R1_CK_S_NLL_Cl	TRP_R1_CK_S_NLL_Cl	TRP_R2_CK_S_NLL_Cl
Well Depth			Log Transformation					
Distance from Coast			Log Transformation					
Cl	Co-Kriging	Spherical	Log Transformation	JD_R3_CK_S_LLL_Cl	JD_R7_CK_S_LLL_Cl	BEY_R1_CK_S_LLL_Cl	TRP_R1_CK_S_LLL_Cl	TRP_R2_CK_S_LLL_Cl
Well Depth			Log Transformation					
Distance from Coast			Log Transformation					
Cl	Co-Kriging	Exponential	No Transformation	JD_R3_CK_E_NNN_Cl	JD_R7_CK_E_NNN_Cl	BEY_R1_CK_E_NNN_Cl	TRP_R1_CK_E_NNN_Cl	TRP_R2_CK_E_NNN_Cl
Well Depth			No Transformation					

Distance from Coast			No Transformation					
Cl	Co-Kriging	Exponential	No Transformation	JD_R3_CK_E_NLN_Cl	JD_R7_CK_E_NLN_Cl	BEY_R1_CK_E_NLN_Cl	TRP_R1_CK_E_NLN_Cl	TRP_R2_CK_E_NLN_Cl
Well Depth			Log Transformation					
Distance from Coast			No Transformation					
Cl	Co-Kriging	Exponential	Log Transformation	JD_R3_CK_E_LNN_Cl	JD_R7_CK_E_LNN_Cl	BEY_R1_CK_E_LNN_Cl	TRP_R1_CK_E_LNN_Cl	TRP_R2_CK_E_LNN_Cl
Well Depth			No Transformation					
Distance from Coast			No Transformation					
Cl	Co-Kriging	Exponential	Log Transformation	JD_R3_CK_E_LLN_Cl	JD_R7_CK_E_LLN_Cl	BEY_R1_CK_E_LLN_Cl	TRP_R1_CK_E_LLN_Cl	TRP_R2_CK_E_LLN_Cl
Well Depth			Log Transformation					
Distance from Coast			No Transformation					
Cl	Co-Kriging	Exponential	No Transformation	JD_R3_CK_E_NNL_Cl	JD_R7_CK_E_NNL_Cl	BEY_R1_CK_E_NNL_Cl	TRP_R1_CK_E_NNL_Cl	TRP_R2_CK_E_NNL_Cl
Well Depth			No Transformation					
Distance from Coast			Log Transformation					
Cl	Co-Kriging	Exponential	No Transformation	JD_R3_CK_E_NLL_Cl	JD_R7_CK_E_NLL_Cl	BEY_R1_CK_E_NLL_Cl	TRP_R1_CK_E_NLL_Cl	TRP_R2_CK_E_NLL_Cl
Well Depth			Log Transformation					
Distance from Coast			Log Transformation					
Cl	Co-Kriging	Exponential	Log Transformation	JD_R3_CK_E_LLL_Cl	JD_R7_CK_E_LLL_Cl	BEY_R1_CK_E_LLL_Cl	TRP_R1_CK_E_LLL_Cl	TRP_R2_CK_E_LLL_Cl
Well Depth			Log Transformation					
Distance from Coast			Log Transformation					
Cl	Co-Kriging	Spherical	No Transformation	JD_R3_CK_S_NNN_Cl_K	JD_R7_CK_S_NNN_Cl_K	BEY_R1_CK_S_NNN_Cl_K	TRP_R1_CK_S_NNN_Cl_K	TRP_R2_CK_S_NNN_Cl_K
Hydraulic Conductivity			No Transformation					
Distance from Coast			No Transformation					
Cl	Co-Kriging	Spherical	No Transformation	JD_R3_CK_S_NLN_Cl_K	JD_R7_CK_S_NLN_Cl_K	BEY_R1_CK_S_NLN_Cl_K	TRP_R1_CK_S_NLN_Cl_K	TRP_R2_CK_S_NLN_Cl_K
Hydraulic Conductivity			Log Transformation					
Distance from Coast			No Transformation					
Cl	Co-Kriging	Spherical	Log Transformation	JD_R3_CK_S_LNN_Cl_K	JD_R7_CK_S_LNN_Cl_K	BEY_R1_CK_S_LNN_Cl_K	TRP_R1_CK_S_LNN_Cl_K	TRP_R2_CK_S_LNN_Cl_K
Hydraulic Conductivity			No Transformation					
Distance from Coast			No Transformation					
Cl	Co-Kriging	Spherical	Log Transformation	JD_R3_CK_S_LLN_Cl_K	JD_R7_CK_S_LLN_Cl_K	BEY_R1_CK_S_LLN_Cl_K	TRP_R1_CK_S_LLN_Cl_K	TRP_R2_CK_S_LLN_Cl_K
Hydraulic Conductivity			Log Transformation					
Distance from Coast			No Transformation					
Cl	Co-Kriging	Spherical	No Transformation	JD_R3_CK_S_NNL_Cl_K	JD_R7_CK_S_NNL_Cl_K	BEY_R1_CK_S_NNL_Cl_K	TRP_R1_CK_S_NNL_Cl_K	TRP_R2_CK_S_NNL_Cl_K
Hydraulic Conductivity			No Transformation					
Distance from Coast			Log Transformation					
Cl	Co-Kriging	Spherical	No Transformation	JD_R3_CK_S_NLL_Cl_K	JD_R7_CK_S_NLL_Cl_K	BEY_R1_CK_S_NLL_Cl_K	TRP_R1_CK_S_NLL_Cl_K	TRP_R2_CK_S_NLL_Cl_K
Hydraulic Conductivity			Log Transformation					
Distance from Coast			Log Transformation					
Cl	Co-Kriging	Spherical	Log Transformation	JD_R3_CK_S_LLL_Cl_K	JD_R7_CK_S_LLL_Cl_K	BEY_R1_CK_S_LLL_Cl_K	TRP_R1_CK_S_LLL_Cl_K	TRP_R2_CK_S_LLL_Cl_K
Hydraulic Conductivity			Log Transformation					
Distance from Coast			Log Transformation					
Cl	Co-Kriging	Exponential	No Transformation	JD_R3_CK_E_NNN_Cl_K	JD_R7_CK_E_NNN_Cl_K	BEY_R1_CK_E_NNN_Cl_K	TRP_R1_CK_E_NNN_Cl_K	TRP_R2_CK_E_NNN_Cl_K
Hydraulic Conductivity			No Transformation					
Distance from Coast			No Transformation					
Cl	Co-Kriging	Exponential	No Transformation	JD_R3_CK_E_NLN_Cl_K	JD_R7_CK_E_NLN_Cl_K	BEY_R1_CK_E_NLN_Cl_K	TRP_R1_CK_E_NLN_Cl_K	TRP_R2_CK_E_NLN_Cl_K
Hydraulic Conductivity			Log Transformation					
Distance from Coast			No Transformation					
Cl	Co-Kriging	Exponential	Log Transformation	JD_R3_CK_E_LNN_Cl_K	JD_R7_CK_E_LNN_Cl_K	BEY_R1_CK_E_LNN_Cl_K	TRP_R1_CK_E_LNN_Cl_K	TRP_R2_CK_E_LNN_Cl_K
Hydraulic Conductivity			No Transformation					
Distance from Coast			No Transformation					
Cl	Co-Kriging	Exponential	Log Transformation	JD_R3_CK_E_LLN_Cl_K	JD_R7_CK_E_LLN_Cl_K	BEY_R1_CK_E_LLN_Cl_K	TRP_R1_CK_E_LLN_Cl_K	TRP_R2_CK_E_LLN_Cl_K
Hydraulic Conductivity			Log Transformation					
Distance from Coast			No Transformation					
Cl	Co-Kriging	Exponential	No Transformation	JD_R3_CK_E_NNL_Cl_K	JD_R7_CK_E_NNL_Cl_K	BEY_R1_CK_E_NNL_Cl_K	TRP_R1_CK_E_NNL_Cl_K	TRP_R2_CK_E_NNL_Cl_K
Hydraulic Conductivity			No Transformation					
Distance from Coast			Log Transformation					
Cl	Co-Kriging	Exponential	No Transformation	JD_R3_CK_E_NLL_Cl_K	JD_R7_CK_E_NLL_Cl_K	BEY_R1_CK_E_NLL_Cl_K	TRP_R1_CK_E_NLL_Cl_K	TRP_R2_CK_E_NLL_Cl_K
Hydraulic Conductivity			Log Transformation					

Distance from Coast			Log Transformation					
Cl	Co-Kriging	Exponential	Log Transformation	JD_R3_CK_E_LLL_Cl_K	JD_R7_CK_E_LLL_Cl_K	BEY_R1_CK_E_LLL_Cl_K	TRP_R1_CK_E_LLL_Cl_K	TRP_R2_CK_E_LLL_Cl_K
Hydraulic Conductivity			Log Transformation					
Distance from Coast			Log Transformation					
GQISWI	Co-Kriging	Spherical	No Transformation	JD_R3_CK_S_NNN_GQISWI	JD_R7_CK_S_NNN_GQISWI	BEY_R1_CK_S_NNN_GQISWI	TRP_R1_CK_S_NNN_GQISWI	TRP_R2_CK_S_NNN_GQISWI
Well Depth			No Transformation					
Distance from Coast			No Transformation					
GQISWI	Co-Kriging	Spherical	No Transformation	JD_R3_CK_S_NLN_GQISWI	JD_R7_CK_S_NLN_GQISWI	BEY_R1_CK_S_NLN_GQISWI	TRP_R1_CK_S_NLN_GQISWI	TRP_R2_CK_S_NLN_GQISWI
Well Depth			Log Transformation					
Distance from Coast			No Transformation					
GQISWI	Co-Kriging	Spherical	Log Transformation	JD_R3_CK_S_LNN_GQISWI	JD_R7_CK_S_LNN_GQISWI	BEY_R1_CK_S_LNN_GQISWI	TRP_R1_CK_S_LNN_GQISWI	TRP_R2_CK_S_LNN_GQISWI
Well Depth			No Transformation					
Distance from Coast			No Transformation					
GQISWI	Co-Kriging	Spherical	Log Transformation	JD_R3_CK_S_LLN_GQISWI	JD_R7_CK_S_LLN_GQISWI	BEY_R1_CK_S_LLN_GQISWI	TRP_R1_CK_S_LLN_GQISWI	TRP_R2_CK_S_LLN_GQISWI
Well Depth			Log Transformation					
Distance from Coast			No Transformation					
GQISWI	Co-Kriging	Spherical	No Transformation	JD_R3_CK_S_NNL_GQISWI	JD_R7_CK_S_NNL_GQISWI	BEY_R1_CK_S_NNL_GQISWI	TRP_R1_CK_S_NNL_GQISWI	TRP_R2_CK_S_NNL_GQISWI
Well Depth			No Transformation					
Distance from Coast			Log Transformation					
GQISWI	Co-Kriging	Spherical	No Transformation	JD_R3_CK_S_NLL_GQISWI	JD_R7_CK_S_NLL_GQISWI	BEY_R1_CK_S_NLL_GQISWI	TRP_R1_CK_S_NLL_GQISWI	TRP_R2_CK_S_NLL_GQISWI
Well Depth			Log Transformation					
Distance from Coast			Log Transformation					
GQISWI	Co-Kriging	Spherical	Log Transformation	JD_R3_CK_S_LLL_GQISWI	JD_R7_CK_S_LLL_GQISWI	BEY_R1_CK_S_LLL_GQISWI	TRP_R1_CK_S_LLL_GQISWI	TRP_R2_CK_S_LLL_GQISWI
Well Depth			Log Transformation					
Distance from Coast			Log Transformation					
GQISWI	Co-Kriging	Exponential	No Transformation	JD_R3_CK_E_NNN_GQISWI	JD_R7_CK_E_NNN_GQISWI	BEY_R1_CK_E_NNN_GQISWI	TRP_R1_CK_E_NNN_GQISWI	TRP_R2_CK_E_NNN_GQISWI
Well Depth			No Transformation					
Distance from Coast			No Transformation					
GQISWI	Co-Kriging	Exponential	No Transformation	JD_R3_CK_E_NLN_GQISWI	JD_R7_CK_E_NLN_GQISWI	BEY_R1_CK_E_NLN_GQISWI	TRP_R1_CK_E_NLN_GQISWI	TRP_R2_CK_E_NLN_GQISWI
Well Depth			Log Transformation					
Distance from Coast			No Transformation					
GQISWI	Co-Kriging	Exponential	Log Transformation	JD_R3_CK_E_LNN_GQISWI	JD_R7_CK_E_LNN_GQISWI	BEY_R1_CK_E_LNN_GQISWI	TRP_R1_CK_E_LNN_GQISWI	TRP_R2_CK_E_LNN_GQISWI
Well Depth			No Transformation					
Distance from Coast			No Transformation					
GQISWI	Co-Kriging	Exponential	Log Transformation	JD_R3_CK_E_LLN_GQISWI	JD_R7_CK_E_LLN_GQISWI	BEY_R1_CK_E_LLN_GQISWI	TRP_R1_CK_E_LLN_GQISWI	TRP_R2_CK_E_LLN_GQISWI
Well Depth			Log Transformation					
Distance from Coast			No Transformation					
GQISWI	Co-Kriging	Exponential	No Transformation	JD_R3_CK_E_NNL_GQISWI	JD_R7_CK_E_NNL_GQISWI	BEY_R1_CK_E_NNL_GQISWI	TRP_R1_CK_E_NNL_GQISWI	TRP_R2_CK_E_NNL_GQISWI
Well Depth			No Transformation					
Distance from Coast			Log Transformation					
GQISWI	Co-Kriging	Exponential	No Transformation	JD_R3_CK_E_NLL_GQISWI	JD_R7_CK_E_NLL_GQISWI	BEY_R1_CK_E_NLL_GQISWI	TRP_R1_CK_E_NLL_GQISWI	TRP_R2_CK_E_NLL_GQISWI
Well Depth			Log Transformation					
Distance from Coast			Log Transformation					
GQISWI	Co-Kriging	Exponential	Log Transformation	JD_R3_CK_E_LLL_GQISWI	JD_R7_CK_E_LLL_GQISWI	BEY_R1_CK_E_LLL_GQISWI	TRP_R1_CK_E_LLL_GQISWI	TRP_R2_CK_E_LLL_GQISWI
Well Depth			Log Transformation					
Distance from Coast			Log Transformation					
GQISWI	Co-Kriging	Spherical	No Transformation	JD_R3_CK_S_NNN_GQISWIK	JD_R7_CK_S_NNN_GQISWIK	BEY_R1_CK_S_NNN_GQISWIK	TRP_R1_CK_S_NNN_GQISWIK	TRP_R2_CK_S_NNN_GQISWIK
Hydraulic Conductivity			No Transformation					
Distance from Coast			No Transformation					
GQISWI	Co-Kriging	Spherical	No Transformation	JD_R3_CK_S_NLN_GQISWIK	JD_R7_CK_S_NLN_GQISWIK	BEY_R1_CK_S_NLN_GQISWIK	TRP_R1_CK_S_NLN_GQISWIK	TRP_R2_CK_S_NLN_GQISWIK
Hydraulic Conductivity			Log Transformation					
Distance from Coast			No Transformation					
GQISWI	Co-Kriging	Spherical	Log Transformation	JD_R3_CK_S_LNN_GQISWIK	JD_R7_CK_S_LNN_GQISWIK	BEY_R1_CK_S_LNN_GQISWIK	TRP_R1_CK_S_LNN_GQISWIK	TRP_R2_CK_S_LNN_GQISWIK
Hydraulic Conductivity			No Transformation					
Distance from Coast			No Transformation					
GQISWI	Co-Kriging	Spherical	Log Transformation	JD_R3_CK_S_LLN_GQISWIK	JD_R7_CK_S_LLN_GQISWIK	BEY_R1_CK_S_LLN_GQISWIK	TRP_R1_CK_S_LLN_GQISWIK	TRP_R2_CK_S_LLN_GQISWIK
Hydraulic Conductivity			Log Transformation					

Distance from Coast			No Transformation					
GQISWI	Co-Kriging	Spherical	No Transformation	JD_R3_CK_S_NNL_GQISWIK	JD_R7_CK_S_NNL_GQISWIK	BEY_R1_CK_S_NNL_GQISWIK	TRP_R1_CK_S_NNL_GQISWIK	TRP_R2_CK_S_NNL_GQISWIK
Hydraulic Conductivity			No Transformation					
Distance from Coast			Log Transformation					
GQISWI	Co-Kriging	Spherical	No Transformation	JD_R3_CK_S_NLL_GQISWIK	JD_R7_CK_S_NLL_GQISWIK	BEY_R1_CK_S_NLL_GQISWIK	TRP_R1_CK_S_NLL_GQISWIK	TRP_R2_CK_S_NLL_GQISWIK
Hydraulic Conductivity			Log Transformation					
Distance from Coast			Log Transformation					
GQISWI	Co-Kriging	Spherical	Log Transformation	JD_R3_CK_S_LLL_GQISWIK	JD_R7_CK_S_LLL_GQISWIK	BEY_R1_CK_S_LLL_GQISWIK	TRP_R1_CK_S_LLL_GQISWIK	TRP_R2_CK_S_LLL_GQISWIK
Hydraulic Conductivity			Log Transformation					
Distance from Coast			Log Transformation					
GQISWI	Co-Kriging	Exponential	No Transformation	JD_R3_CK_E_NNN_GQISWIK	JD_R7_CK_E_NNN_GQISWIK	BEY_R1_CK_E_NNN_GQISWIK	TRP_R1_CK_E_NNN_GQISWIK	TRP_R2_CK_E_NNN_GQISWIK
Hydraulic Conductivity			No Transformation					
Distance from Coast			No Transformation					
GQISWI	Co-Kriging	Exponential	No Transformation	JD_R3_CK_E_NLN_GQISWIK	JD_R7_CK_E_NLN_GQISWIK	BEY_R1_CK_E_NLN_GQISWIK	TRP_R1_CK_E_NLN_GQISWIK	TRP_R2_CK_E_NLN_GQISWIK
Hydraulic Conductivity			Log Transformation					
Distance from Coast			No Transformation					
GQISWI	Co-Kriging	Exponential	Log Transformation	JD_R3_CK_E_LNN_GQISWIK	JD_R7_CK_E_LNN_GQISWIK	BEY_R1_CK_E_LNN_GQISWIK	TRP_R1_CK_E_LNN_GQISWIK	TRP_R2_CK_E_LNN_GQISWIK
Hydraulic Conductivity			No Transformation					
Distance from Coast			No Transformation					
GQISWI	Co-Kriging	Exponential	Log Transformation	JD_R3_CK_E_LLN_GQISWIK	JD_R7_CK_E_LLN_GQISWIK	BEY_R1_CK_E_LLN_GQISWIK	TRP_R1_CK_E_LLN_GQISWIK	TRP_R2_CK_E_LLN_GQISWIK
Hydraulic Conductivity			Log Transformation					
Distance from Coast			No Transformation					
GQISWI	Co-Kriging	Exponential	No Transformation	JD_R3_CK_E_NNL_GQISWIK	JD_R7_CK_E_NNL_GQISWIK	BEY_R1_CK_E_NNL_GQISWIK	TRP_R1_CK_E_NNL_GQISWIK	TRP_R2_CK_E_NNL_GQISWIK
Hydraulic Conductivity			No Transformation					
Distance from Coast			Log Transformation					
GQISWI	Co-Kriging	Exponential	No Transformation	JD_R3_CK_E_NLL_GQISWIK	JD_R7_CK_E_NLL_GQISWIK	BEY_R1_CK_E_NLL_GQISWIK	TRP_R1_CK_E_NLL_GQISWIK	TRP_R2_CK_E_NLL_GQISWIK
Hydraulic Conductivity			Log Transformation					
Distance from Coast			Log Transformation					
GQISWI	Co-Kriging	Exponential	Log Transformation	JD_R3_CK_E_LLL_GQISWIK	JD_R7_CK_E_LLL_GQISWIK	BEY_R1_CK_E_LLL_GQISWIK	TRP_R1_CK_E_LLL_GQISWIK	TRP_R2_CK_E_LLL_GQISWIK
Hydraulic Conductivity			Log Transformation					
Distance from Coast			Log Transformation					

Table 5-55: Coding system for the Interpolation and Vulnerability Assessment Analysis

City	Jal el Dib	JD
	Beirut	BEY
	Tripoli	TRP
Round	Round 1- Early Summer - May/June	R1
	Round 2 - Late Summer - September/October	R2
	Other Rounds	Rx
Method	Kriging	Kr
	IDW	IDW
	Co-Kriging	CK
Variogram Model	Spherical	S
	Exponential	E
Transformation	No Tranformation	N
	Log Transformation	L
Parameters	Chloride Level	Cl
	Total Dissolved Solids	TDS
	Groundwater Quality Index	GQI
	Groundwater Quality Index for Sea Water Intrusion	GQISWI
	Water Depth	-
	Hydraulic Conductivity	K
	Distance from Shoreline	-
Vulnerability Assessment Methods	EPIK Version 1	EP1
	EPIK Version 2	EP2
	EPIK Version 3	EP3
	DRASTIC	DR

5.10 Annex 10: Results of Leave one Out Validation

Table 5-56 : All interpolation scenarios conducted for Jal el Dib Round 3 (January 2013) wells (Blue highlight are the ones performed the best)

Code	Statistical Indicators					
	Avg.	σ	RSR	CV	PBIAS	RMS-S
JD_R3_Kr_S_N_Cl	388.8	182.7	1.01	0.47	58.27	1.02
JD_R3_Kr_S_L_Cl			1.05	0.49	101.74	0.77
JD_R3_Kr_E_N_Cl			1.01	0.47	69.41	1.00
JD_R3_Kr_E_L_Cl			1.05	0.50	97.75	0.76
JD_R3_IDW_Cl			1.23	0.57	80.53	-
JD_R3_Kr_S_N_TDS	1090.0	825.5	0.95	0.72	44.06	0.98
JD_R3_Kr_S_L_TDS			0.84	0.63	-63.95	1.21
JD_R3_Kr_E_N_TDS			0.94	0.71	29.15	0.97
JD_R3_Kr_E_L_TDS			0.88	0.66	-58.04	1.51
JD_R3_IDW_TDS			0.94	0.71	147.93	-
JD_R3_Kr_S_N_GQI	83.1	3.2	1.11	0.04	-2.27	1.04
JD_R3_Kr_S_L_GQI			0.94	0.04	-2.27	1.04
JD_R3_Kr_E_N_GQI			0.94	0.04	-2.70	1.00
JD_R3_Kr_E_L_GQI			0.96	0.04	-2.57	1.01
JD_R3_IDW_GQI			1.07	0.04	-9.72	-
JD_R3_Kr_S_N_GQISWI	58.2	10.7	0.89	0.18	-29.93	1.01
JD_R3_Kr_S_L_GQISWI			1.01	0.19	-39.13	1.12
JD_R3_Kr_E_N_GQISWI			0.99	0.19	-6.84	1.03
JD_R3_Kr_E_L_GQISWI			1.03	0.19	-11.03	1.10
JD_R3_IDW_GQISWI			1.07	0.20	-70.53	-
JD_R3_CK_S_NNN_Cl	388.8	182.7	0.99	0.46	52.91	0.88
JD_R3_CK_S_NLN_Cl			0.99	0.40	52.96	0.04
JD_R3_CK_S_LNN_Cl			1.36	0.64	2.69	2.58
JD_R3_CK_S_LLN_Cl			1.36	0.64	0.43	2.59
JD_R3_CK_S_NNL_Cl			1.02	0.48	58.23	1.03
JD_R3_CK_S_NLL_Cl			1.02	0.48	60.32	1.03
JD_R3_CK_S_LLL_Cl			1.01	0.48	229.20	0.57
JD_R3_CK_E_NNN_Cl			1.01	0.47	48.21	0.89
JD_R3_CK_E_NLN_Cl			1.01	0.47	48.64	0.89
JD_R3_CK_E_LNN_Cl			1.33	0.47	36.59	1.93
JD_R3_CK_E_LLN_Cl			1.33	0.63	33.03	1.96
JD_R3_CK_E_NNL_Cl			1.02	0.48	71.08	1.01
JD_R3_CK_E_NLL_Cl			1.01	0.48	70.71	1.01
JD_R3_CK_E_LLL_Cl			1.32	0.62	63.94	1.66
JD_R3_CK_S_NNN_Cl_K	388.8	182.7	ERROR 1			
JD_R3_CK_S_NLN_Cl_K			0.98	0.46	59.54	0.88
JD_R3_CK_S_LNN_Cl_K			ERROR 1			
JD_R3_CK_S_LLN_Cl_K			1.35	0.63	5.83	2.50
JD_R3_CK_S_NNL_Cl_K			ERROR 1			
JD_R3_CK_S_NLL_Cl_K			1.02	0.48	100.89	1.09
JD_R3_CK_S_LLL_Cl_K			0.98	0.46	187.15	0.57

Code	Statistical Indicators					
	Avg.	σ	RSR	CV	PBIAS	RMS-S
JD_R3_CK_E_NNN_Cl_K			ERROR 1			
JD_R3_CK_E_NLN_Cl_K			1.00	0.47	54.68	0.88
JD_R3_CK_E_LNN_Cl_K			ERROR 1			
JD_R3_CK_E_LLN_Cl_K			1.33	0.62	28.92	2.47
JD_R3_CK_E_NNL_Cl_K			ERROR 1			
JD_R3_CK_E_NLL_Cl_K			1.01	0.48	105.80	1.07
JD_R3_CK_E_LLL_Cl_K			1.02	0.48	262.35	0.59
JD_R3_CK_S_NNN_GQISWI	58.2	10.7	1.19	0.22	-0.64	1.93
JD_R3_CK_S_NLN_GQISWI			1.19	0.22	-0.09	1.95
JD_R3_CK_S_LNN_GQISWI			1.19	0.22	-2.43	1.95
JD_R3_CK_S_LLN_GQISWI			1.19	0.22	-2.47	1.95
JD_R3_CK_S_NNL_GQISWI			1.03	0.19	-53.75	1.02
JD_R3_CK_S_NLL_GQISWI			1.03	0.19	-21.57	1.08
JD_R3_CK_S_LLL_GQISWI			1.17	0.22	-3.82	1.83
JD_R3_CK_E_NNN_GQISWI			1.14	0.21	-4.28	1.56
JD_R3_CK_E_NLN_GQISWI			1.13	0.21	-6.78	1.58
JD_R3_CK_E_LNN_GQISWI			1.13	0.21	-6.78	1.58
JD_R3_CK_E_LLN_GQISWI			1.13	0.21	-6.51	1.58
JD_R3_CK_E_NNL_GQISWI			1.04	0.19	-34.89	1.08
JD_R3_CK_E_NLL_GQISWI			1.11	0.21	-10.32	1.47
JD_R3_CK_E_LLL_GQISWI			1.04	0.19	-25.92	1.40
JD_R3_CK_S_NNN_GQISWI_K	58.2	10.7	ERROR 1			
JD_R3_CK_S_NLN_GQISWI_K			1.19	0.22	-3.12	1.93
JD_R3_CK_S_LNN_GQISWI_K			ERROR 1			
JD_R3_CK_S_LLN_GQISWI_K			1.19	0.22	-7.18	1.94
JD_R3_CK_S_NNL_GQISWI_K			ERROR 1			
JD_R3_CK_S_NLL_GQISWI_K			1.03	0.19	-31.22	1.26
JD_R3_CK_S_LLL_GQISWI_K			1.18	0.22	34.44	2.26
JD_R3_CK_E_NNN_GQISWI_K			ERROR 1			
JD_R3_CK_E_NLN_GQISWI_K			1.15	0.21	-15.91	1.78
JD_R3_CK_E_LNN_GQISWI_K			ERROR 1			
JD_R3_CK_E_LLN_GQISWI_K			1.10	0.20	19.90	1.88
JD_R3_CK_E_NNL_GQISWI_K			ERROR 1			
JD_R3_CK_E_NLL_GQISWI_K			1.01	0.19	-28.58	1.27
JD_R3_CK_E_LLL_GQISWI_K			0.51	0.08	-1.24	1.78

ERROR 1: The method cannot be optimized for this dataset - In this case the Hydraulic Conductivity has only value (sampled wells are tapping one aquifer) and without Log transformation on the dataset of Hydraulic Conductivity the software cannot find optimum parameters for this set of data.

Table 5-57: All interpolation scenarios conducted for Jal el Dib Round 7 (September 2013) wells (Blue highlight are the ones performed the best)

Code	Statistical Indicators					
	Avg.	σ	RSR	CV	PBIAS	RMS-S

Code	Statistical Indicators					
	Avg.	σ	RSR	CV	PBIAS	RMS-S
JD_R7_Kr_S_NCl	546.5	327.0	0.97	0.58	86.02	0.98
JD_R7_Kr_S_L_Cl			0.89	0.53	-27.77	0.89
JD_R7_Kr_E_NCl			0.96	0.58	23.06	0.95
JD_R7_Kr_E_L_Cl			0.89	0.53	-26.86	0.88
JD_R7_IDW_Cl			1.02	0.61	433.40	-
JD_R7_Kr_S_N_TDS	508.5	616.4	0.75	0.37	74.11	0.84
JD_R7_Kr_S_L_TDS			0.74	0.37	73.49	0.82
JD_R7_Kr_E_N_TDS			0.78	0.38	76.74	0.86
JD_R7_Kr_E_L_TDS			0.78	0.39	55.72	0.76
JD_R7_IDW_TDS			0.90	0.45	331.77	-
JD_R7_Kr_S_N_GQI	81.9	4.1	0.76	0.04	-9.95	0.90
JD_R7_Kr_S_L_GQI			0.76	0.04	-9.79	0.91
JD_R7_Kr_E_N_GQI			0.87	0.04	-8.55	0.91
JD_R7_Kr_E_L_GQI			0.97	0.05	0.26	0.98
JD_R7_IDW_GQI			0.85	0.04	0.85	-
JD_R7_Kr_S_N_GQISWI	59.0	9.2	0.84	0.13	-19.96	7.73
JD_R7_Kr_S_L_GQISWI			1.00	0.16	-3.28	1.12
JD_R7_Kr_E_N_GQISWI			0.84	0.13	-20.76	0.92
JD_R7_Kr_E_L_GQISWI			0.96	0.15	-13.86	1.03
JD_R7_IDW_GQISWI			0.85	0.10	-35.74	-
JD_R7_CK_S_NNNCl	546.5	327.0	1.00	0.60	-27.05	0.78
JD_R7_CK_S_NLNCl			1.00	0.60	-27.05	0.78
JD_R7_CK_S_LNNCl			1.04	0.62	142.13	2.39
JD_R7_CK_S_LLNCl			1.04	0.62	147.93	2.39
JD_R7_CK_S_NNL_Cl			0.98	0.59	91.14	0.99
JD_R7_CK_S_NLL_Cl			0.98	0.59	86.44	0.99
JD_R7_CK_S_LLL_Cl			0.93	0.56	-33.11	0.93
JD_R7_CK_E_NNNCl			1.00	0.60	-27.05	0.78
JD_R7_CK_E_NLNCl			1.00	0.60	-27.05	0.78
JD_R7_CK_E_LNNCl			1.01	0.61	165.87	1.97
JD_R7_CK_E_LLNCl			1.02	0.61	170.31	1.98
JD_R7_CK_E_NNL_Cl			1.00	0.60	-27.05	0.96
JD_R7_CK_E_NLL_Cl			0.97	0.58	44.89	0.97
JD_R7_CK_E_LLL_Cl			0.96	0.57	60.72	0.89
JD_R7_CK_S_NNN_Cl_K	546.5	327.0	1.00	0.60	-27.05	0.78
JD_R7_CK_S_NLN_Cl_K			1.00	0.60	-27.05	0.78
JD_R7_CK_S_LNN_Cl_K			1.05	0.63	149.34	2.39
JD_R7_CK_S_LLN_Cl_K			1.05	0.63	149.22	2.39
JD_R7_CK_S_NNL_Cl_K			0.98	0.59	86.46	0.99
JD_R7_CK_S_NLL_Cl_K			0.98	0.59	86.46	0.99
JD_R7_CK_S_LLL_Cl_K			0.89	0.53	13.86	0.86
JD_R7_CK_E_NNN_Cl_K			1.00	0.60	-27.05	0.78
JD_R7_CK_E_NLN_Cl_K			1.00	0.60	-27.05	0.78
JD_R7_CK_E_LNN_Cl_K			1.02	0.61	169.41	1.97
JD_R7_CK_E_LLN_Cl_K			1.02	0.61	169.41	1.97
JD_R7_CK_E_NNL_Cl_K			0.97	0.58	42.73	0.97
JD_R7_CK_E_NLL_Cl_K			0.97	0.58	42.73	0.97
JD_R7_CK_E_LLL_Cl_K			1.01	0.60	175.67	1.85
JD_R7_CK_S_NNN_GQISWI	59.0	9.2	0.82	0.13	-48.15	2.19
JD_R7_CK_S_NLN_GQISWI			0.85	0.13	-49.89	2.21

Code	Statistical Indicators					
	Avg.	σ	RSR	CV	PBIAS	RMS-S
JD_R7_CK_S_LNN_GQISWI			0.82	0.13	-48.88	2.38
JD_R7_CK_S_LLN_GQISWI			0.83	0.13	-47.75	1.80
JD_R7_CK_S_NNL_GQISWI			0.86	0.14	-50.08	1.82
JD_R7_CK_S_NLL_GQISWI			0.76	0.12	-2.06	1.05
JD_R7_CK_S_LLL_GQISWI			0.83	0.13	-41.80	0.89
JD_R7_CK_E_NNN_GQISWI			0.82	0.13	-48.52	1.98
JD_R7_CK_E_NLN_GQISWI			0.85	0.13	-51.03	2.40
JD_R7_CK_E_LNN_GQISWI			0.86	0.13	-45.95	2.28
JD_R7_CK_E_LLN_GQISWI			0.86	0.13	-50.97	2.00
JD_R7_CK_E_NNL_GQISWI			0.84	0.13	-46.81	1.83
JD_R7_CK_E_NLL_GQISWI			0.76	0.12	-2.06	0.98
JD_R7_CK_E_LLL_GQISWI			0.85	0.13	-56.13	1.87
JD_R7_CK_S_NNN_GQISWI_K			0.84	0.13	-48.11	2.20
JD_R7_CK_S_NLN_GQISWI_K			0.84	0.13	-48.11	2.20
JD_R7_CK_S_LNN_GQISWI_K			0.84	0.13	-48.95	2.38
JD_R7_CK_S_LLN_GQISWI_K			0.84	0.13	-49.15	2.38
JD_R7_CK_S_NNL_GQISWI_K			0.80	0.13	-18.12	0.92
JD_R7_CK_S_NLL_GQISWI_K			0.80	0.13	-24.94	0.92
JD_R7_CK_S_LLL_GQISWI_K			0.85	0.13	-50.90	2.36
JD_R7_CK_E_NNN_GQISWI_K			0.85	0.13	-47.58	1.80
JD_R7_CK_E_NLN_GQISWI_K			0.85	0.13	-47.58	1.80
JD_R7_CK_E_LNN_GQISWI_K			0.84	0.13	-48.37	1.98
JD_R7_CK_E_LLN_GQISWI_K			0.84	0.13	-48.37	1.98
JD_R7_CK_E_NNL_GQISWI_K			0.80	0.13	-18.34	0.89
JD_R7_CK_E_NLL_GQISWI_K			0.80	0.13	-48.20	0.89
JD_R7_CK_E_LLL_GQISWI_K	59.0	9.2	0.85	0.13	-48.53	1.96

Table 5-58: All interpolation scenarios conducted for Beirut Round 1(May June 2013) wells (Blue highlight are the ones performed the best)

Code	Statistical Indicators					
	Avg.	σ	RSR	CV	PBIAS	RMS-S
BEY_R1_Kr_S_N_Cl			0.99	1.47	230.38	0.92
BEY_R1_Kr_S_L_Cl			0.94	1.39	-256.87	1.88
BEY_R1_Kr_E_N_Cl			1.00	1.49	225.99	0.93
BEY_R1_Kr_E_L_Cl			0.98	1.46	33.31	1.85
BEY_R1_IDW_Cl	1,898.2	2,828.3	0.98	1.46	48.84	-
BEY_R1_Kr_S_N_TDS			0.96	1.21	-168.41	0.95
BEY_R1_Kr_S_L_TDS			0.89	1.11	75.45	1.69
BEY_R1_Kr_E_N_TDS			0.94	1.18	-74.13	0.89
BEY_R1_Kr_E_L_TDS			0.91	1.14	-203.84	2.06
BEY_R1_IDW_TDS	4,061.9	5,102.7	0.94	1.18	-97.76	-
BEY_R1_CK_S_NNN_Cl	1,898.2	2,828.	0.98	1.46	-743.49	0.94

Code	Statistical Indicators					
	Avg.	σ	RSR	CV	PBIAS	RMS-S
BEY_R1_CK_S_NLN_Cl			0.97	1.45	-631.72	0.93
BEY_R1_CK_S_LNN_Cl			0.97	1.44	-2,975.11	6.37
BEY_R1_CK_S_LLN_Cl			1.00	1.50	-2,962.28	6.28
BEY_R1_CK_S_NNL_Cl			0.99	1.47	96.78	0.92
BEY_R1_CK_S_NLL_Cl			0.99	1.47	135.75	0.92
BEY_R1_CK_S_LLL_Cl			0.95	1.41	-161.47	2.04
BEY_R1_CK_E_NNN_Cl			3.03	4.52	-4,600.01	4.36
BEY_R1_CK_E_NLN_Cl			4.02	5.99	-4,299.54	14.65
BEY_R1_CK_E_LNN_Cl			1.01	1.51	-2,703.74	5.42
BEY_R1_CK_E_LLN_Cl			1.02	1.52	-2,576.15	5.21
BEY_R1_CK_E_NNL_Cl			15.73	23.44	28,629.90	66.27
BEY_R1_CK_E_NLL_Cl			1.01	1.51	482.72	0.95
BEY_R1_CK_E_LLL_Cl			0.92	1.38	-34.24	1.93
BEY_R1_CK_S_NNN_Cl_K	1,898.2	2,828.3	0.94	1.40	-34.24	0.91
BEY_R1_CK_S_NLN_Cl_K			0.95	1.42	-433.98	0.92
BEY_R1_CK_S_LNN_Cl_K			1.01	1.50	-2,937.32	6.42
BEY_R1_CK_S_LLN_Cl_K			1.01	1.51	-2,938.12	6.43
BEY_R1_CK_S_NNL_Cl_K			1.01	1.51	-2,938.12	6.43
BEY_R1_CK_S_NLL_Cl_K			1.00	1.49	89.89	0.94
BEY_R1_CK_S_LLL_Cl_K			0.93	1.39	685.17	1.55
BEY_R1_CK_E_NNN_Cl_K			2.81	4.18	-3,301.47	10.48
BEY_R1_CK_E_NLN_Cl_K			3.16	4.70	-3,418.91	11.84
BEY_R1_CK_E_LNN_Cl_K			1.02	1.52	-2,713.21	5.66
BEY_R1_CK_E_LLN_Cl_K			6.77	10.08	11,085.80	28.40
BEY_R1_CK_E_NNL_Cl_K			6.77	10.08	11,085.80	28.40
BEY_R1_CK_E_NLL_Cl_K			6.77	10.08	11,085.80	28.40
BEY_R1_CK_E_LLL_Cl_K			0.96	1.43	-234.93	2.16

Table 5-59: All interpolation scenarios conducted for Tripoli Round 1 (July 2007) wells (Blue highlight are the ones performed the best)

Code	Statistical Indicators					
	Avg.	σ	RSR	CV	PBIAS	RMS-S
TRP_R1_Kr_S_N_Cl	216.6	249.8	0.90	1.04	-114.36	0.86
TRP_R1_Kr_S_L_Cl			0.91	1.05	-370.06	1.14

Code	Statistical Indicators					
	Avg.	σ	RSR	CV	PBIAS	RMS-S
TRP_R1_Kr_E_N_Cl			0.89	1.03	-132.01	0.84
TRP_R1_Kr_E_L_Cl			0.88	1.02	-434.64	1.03
TRP_R1_IDW_Cl			0.88	1.02	-494.18	-
TRP_R1_Kr_S_N_TDS			0.77	0.63	-305.99	0.86
TRP_R1_Kr_S_L_TDS			0.71	0.59	-179.05	1.04
TRP_R1_Kr_E_N_TDS			0.74	0.61	-137.80	0.80
TRP_R1_Kr_E_L_TDS			0.70	0.58	-86.27	1.03
TRP_R1_IDW_TDS	639.2	528.94	0.76	0.63	-353.54	-
TRP_R1_CK_S_NNN_Cl_K			0.84	0.97	-48.07	1.07
TRP_R1_CK_S_NLN_Cl_K			0.84	0.97	-48.07	1.07
TRP_R1_CK_S_LNN_Cl_K			0.80	0.92	-605.56	3.42
TRP_R1_CK_S_LLN_Cl_K			0.80	0.92	-605.56	3.42
TRP_R1_CK_S_NNL_Cl_K			1.05	1.21	769.23	1.35
TRP_R1_CK_S_NLL_Cl_K			1.05	1.21	694.57	1.25
TRP_R1_CK_S_LLL_Cl_K			0.87	1.00	-155.49	1.62
TRP_R1_CK_E_NNN_Cl_K			1.75	2.01	831.92	3.36
TRP_R1_CK_E_NLN_Cl_K			1.75	2.01	931.92	3.36
TRP_R1_CK_E_LNN_Cl_K			0.80	0.92	931.92	2.77
TRP_R1_CK_E_LLN_Cl_K			0.80	0.92	-589.80	2.76
TRP_R1_CK_E_NNL_Cl_K			1.01	1.17	453.18	1.15
TRP_R1_CK_E_NLL_Cl_K			1.00	1.15	444.53	1.21
TRP_R1_CK_E_LLL_Cl_K	216.60	249.80	0.98	1.13	104.73	2.61

Table 5-60: All interpolation scenarios conducted for Tripoli Round 2 (September 2006) wells (Blue highlight are the ones performed the best)

Code	Statistical Indicators					
	Avg.	σ	RSR	CV	PBIAS	RMS-S
TRP_R2_Kr_S_N_Cl			0.99	1.58	-868.26	0.80
TRP_R2_Kr_S_L_Cl			0.97	1.54	-607.16	1.34
TRP_R2_Kr_E_N_Cl			0.98	1.56	-328.40	0.78
TRP_R2_Kr_E_L_Cl			0.93	1.48	-348.22	1.51
TRP_R2_IDW_Cl	224.6	357.8	1.00	1.59	-571.71	-
TRP_R2_Kr_S_N_TDS			0.94	0.93	-286.47	549.86
TRP_R2_Kr_S_L_TDS			0.93	0.82	-375.94	1.35
TRP_R2_Kr_E_N_TDS			0.94	0.83	-124.13	0.82
TRP_R2_Kr_E_L_TDS			0.90	0.80	-177.99	1.26
TRP_R2_IDW_TDS	639.2	528.9	0.97	0.86	-440.05	-
TRP_R2_CK_S_NNN_Cl_K			0.97	1.55	-101.16	0.99
TRP_R2_CK_S_NLN_Cl_K	224.6	357.8	0.97	1.55	-101.16	0.99

Code	Statistical Indicators					
	Avg.	**σ**	**RSR**	**CV**	**PBIAS**	**RMS-S**
TRP_R2_CK_S_LNN_Cl_K			0.95	1.51	-1512.12	7.75
TRP_R2_CK_S_LLN_Cl_K			0.95	1.51	-1512.12	7.75
TRP_R2_CK_S_NNL_Cl_K			7.49	11.94	-548.59	22.59
TRP_R2_CK_S_NLL_Cl_K			7.49	11.94	-548.59	22.59
TRP_R2_CK_S_LLL_Cl_K			1.13	1.80	-239.99	2.00
TRP_R2_CK_E_NNN_Cl_K			0.98	1.56	-47.86	1.04
TRP_R2_CK_E_NLN_Cl_K			0.98	1.56	-47.86	1.04
TRP_R2_CK_E_LNN_Cl_K			0.95	1.51	-1491.03	7.75
TRP_R2_CK_E_LLN_Cl_K			0.93	1.48	-1491.03	6.00
TRP_R2_CK_E_NNL_Cl_K			1.27	2.03	1156.82	1.27
TRP_R2_CK_E_NLL_Cl_K			0.98	1.56	-48.02	0.82
TRP_R2_CK_E_LLL_Cl_K			11.28	2.05	-281.29	3.12